

December 2019

Dynamic Vehicular Trajectory Optimization for Bottleneck Mitigation and Safety Improvement

Wenqing Chen
University of Wisconsin-Milwaukee

Follow this and additional works at: <https://dc.uwm.edu/etd>



Part of the [Civil Engineering Commons](#), and the [Industrial Engineering Commons](#)

Recommended Citation

Chen, Wenqing, "Dynamic Vehicular Trajectory Optimization for Bottleneck Mitigation and Safety Improvement" (2019). *Theses and Dissertations*. 2294.
<https://dc.uwm.edu/etd/2294>

This Dissertation is brought to you for free and open access by UWM Digital Commons. It has been accepted for inclusion in Theses and Dissertations by an authorized administrator of UWM Digital Commons. For more information, please contact open-access@uwm.edu.

DYNAMIC VEHICULAR TRAJECTORY OPTIMIZATION
FOR BOTTLENECK MITIGATION AND SAFETY
IMPROVEMENT

by

Wenqing Chen

A Dissertation Submitted in
Partial Fulfillment of the
Requirements for the Degree of

Doctor of Philosophy

in Engineering

at

The University of Wisconsin-Milwaukee

December 2019

ABSTRACT

DYNAMIC VEHICULAR TRAJECTORY OPTIMIZATION FOR BOTTLENECK MITIGATION AND SAFETY IMPROVEMENT

by

Wenqing Chen

The University of Wisconsin-Milwaukee, 2019
Under the Supervision of Professor Jie Yu

Traffic bottleneck is defined as a disruption of traffic flow through a freeway or an arterial, which can be divided as two categories: stationary bottleneck and moving bottleneck. The stationary bottleneck is mainly formed by the lane drops in the multi-lane roadways, while the moving bottleneck are due to the very slowing moving vehicles which disrupt the traffic flow. Traffic bottlenecks not only impact the mobility, but also potentially cause safety issues.

Traditional strategies for eliminating bottlenecks mainly focus on expanding supply including road widening, green interval lengthening and optimization of intersection channelization. In addition, a few macroscopic methods are also made to optimize the traffic demand such as routing optimization, but these studies have some drawbacks due to the limitations of times and methodologies.

Therefore, this research utilizes the Connected and Autonomous Vehicles (CAV) technology to develop several cooperative trajectory optimization models for mitigating mobility and safety impact caused by the urban bottlenecks. The multi-phases algorithms is developed to help solve the model, where a multi-stage-based nonlinear programming procedure is developed

in the first phase to search trajectories that eliminate the conflicts in the bottleneck and minimize the travel time and the remaining ones refine the trajectories with a mixed integer linear programming to minimize idling time of vehicles, so that fuel consumption and emissions can be lowered down. Sensitivity analyses are also conducted towards those models and they imply that several indices may significantly impact the effectiveness and even cause the models lose efficacy under extreme values.

Various illustrative examples and sensitivity analyses are provided to validate the proposed models. Results indicate that (a) the model is effective to mitigate the mobility and safety impact of bottleneck under the appropriate environment; (b) the model could simultaneously optimize the trajectories of vehicles to lower down fuel consumption and emissions; (c) Some environment indices may significantly impact the models, and even cause the model to lose efficacy under extreme values. Application of the developed models under a real-world case illustrates its capability of providing informative quantitative measures to support decisions in designing, maintaining, and operating the intelligent transportation management.

© Copyright by Wenqing Chen, 2019
All Rights Reserved

TABLE OF CONTENTS

TABLE OF CONTENTS	V
LIST OF FIGURES	VIII
LIST OF TABLES	XI
ACKNOWLEDGEMENTS	XII
CHAPTER 1 INTRODUCTION	1
1.1 BACKGROUND	1
1.2 APPLICATION OF CONNECTED AND AUTOMATED VEHICLE TECHNOLOGY	5
1.3 RESEARCH OBJECTIVES	8
1.4 DISSERTATION ORGANIZATION	9
1.5 REFERENCES	11
CHAPTER 2 LITERATURE REVIEW	12
2.1 TRADITIONAL RESEARCH TOWARD BOTTLENECKS AND SAFETY RISKS	12
2.1.1 Near-side bus stops	12
2.1.2 Intersections	14
2.1.3 Dilemma zone on high-speed signalized intersections	14
2.2 BOTTLENECKS AND SAFETY RISK ELIMINATION BASED ON CAV	16
2.2.1 CAV on signalized intersection	17
2.2.2 Advanced research at unsignalized intersections	18
2.2.3 Real-time bus control	19
2.2.4 Active DZ protection	19
2.3 SUMMARY OF CRITICAL ISSUES	20
2.4 REFERENCES	21
CHAPTER 3 SINGLE VEHICLE-BASED TRAJECTORY OPTIMIZATION FOR CONNECTED AND AUTOMATED VEHICLES AT A SIGNALIZED INTERSECTION	29
3.1 INTRODUCTION	29
3.2 ILLUSTRATION OF CONTROL MODEL	33
3.2.1 Notation	33
3.2.2 Description of Control Logic	35
3.2.3 Model Formulation	37
3.3 SOLUTION ALGORITHM	40
3.3.1 A Three-phase algorithm	40
3.3.2 Minimization of average travel time	41
3.3.3 State Transfer Functions	42
3.3.4 Objective Function	44
3.3.5 Constraints	44
3.4 MILP FOR FURTHER OPTIMIZATION	45
3.4.1 Further Optimization of Vehicular Trajectories-A Linear Process	45
3.4.2 Constraints	47
3.5 AN ILLUSTRATIVE EXAMPLE	49
3.5.1 Scenarios Establishment	49

3.5.2	Evaluation of Travel Time	49
3.5.3	Evaluation of Idling Time and Speed Fluctuation	52
3.5.4	Sensitivity Analysis	54
3.6	CONCLUSIONS	55
CHAPTER 4 A PLATOON-BASED SPEED CONTROL ALGORITHM AT A SIGNALIZED INTERSECTION		57
4.1	INTRODUCTION	57
4.2	METHODOLOGY	60
4.2.1	Various speed trajectories under the same travel time	60
4.2.2	Assumptions	62
4.2.3	Acceleration/deceleration models	63
4.2.4	Car-following model	63
4.2.5	Fuel consumption model	64
4.2.6	Impact of anterior platoon and signal timing	64
4.2.7	Speed control algorithm for a fully obedient platoon	66
4.2.8	Speed control algorithm for a “mixed” platoon	70
4.3	ILLUSTRATIVE EXAMPLES	73
4.3.1	Fuel consumption rate comparison	74
4.3.2	Fuel consumption under various headways	75
4.3.3	Fuel consumption under various permutations	76
4.4	CONCLUSIONS	77
CHAPTER 5 DYNAMIC VEHICULAR SPEED CONTROL TOWARDS BOTTLE MITIGATION AND SAFETY IMPROVEMENT AT AN UNSIGNALIZED INTERSECTION		79
5.1	INTRODUCTION	79
5.1.1	Regulars and gaps at unsignalized intersections	79
5.1.2	Speed trajectories of various trajectories under the same travel time	81
5.1.3	VT-micro model	83
5.1.4	Assumptions	84
5.2	METHODOLOGIES	85
5.2.1	Impact of downstream vehicles and gaps	85
5.2.2	Speed control algorithm for the two-streams intersection	87
5.2.3	The speed control algorithm for the intersection with more than two streams	92
5.3	ILLUSTRATIVE EXAMPLES	97
5.4	CONCLUSIONS	100
CHAPTER 6 COOPERATIVE BUS-CAR TRAJECTORY OPTIMIZATION TO ELIMINATE WEAVING BOTTLENECK AROUND CURB SIDE BUS STATIONS		102
6.1	INTRODUCTION	102
6.2	TRAJECTORY OPTIMIZATION MODEL	106
6.2.1	Notation	106
6.2.2	Weaving determination	107
6.2.3	Determination of control scope	109
6.2.4	Model formulation	110
6.3	SOLUTION ALGORITHM	113

6.3.1	Phase I – Conflict elimination and total person travel time minimization	114
6.3.2	Phase II- Idling minimization	119
6.4	VALIDATION AND RESULTS	121
6.4.1	The test site	121
6.4.2	Results	123
6.4.3	Sensitivity analysis	128
6.5	CONCLUSIONS	131
CHAPTER 7 DILEMMA ZONE PROTECTION FOR SAFETY IMPROVEMENT AT AN ISOLATED SIGNALIZED INTERSECTION		133
7.1	INTRODUCTION	133
7.2	METHODOLOGY	137
7.2.1	Computation of DZ	137
7.2.2	Logic of guidance	138
7.2.3	DZ detection	139
7.2.4	Determination of guiding scope	141
7.2.5	Dynamic speed guiding model	141
7.3	SOLUTION ALGORITHM	143
7.3.1	Control of vehicular status - a multi-stage decision process	143
7.3.2	Decision variable of DP	144
7.3.3	State transfer functions of DP	144
7.3.4	Objective function of DP	145
7.3.5	Constraints of DP	145
7.4	MULTI-OBJECTIVE MIXED INTEGER LINEAR PROGRAMMING ALGORITHM	148
7.4.1	Decision variables of the MOMLIP problem	148
7.4.2	Objective function of MOMILP	149
7.4.3	Constraints of MOMILP	149
7.5	CASE STUDY	151
7.5.1	The study site	151
7.5.2	Test design	152
7.5.3	Evaluation analysis & result	153
7.5.4	Sensitivity analysis	159
7.6	CONCLUSIONS	161
CHAPTER 8 CONCLUSIONS AND FUTURE WORKS		163
8.1.1	Conclusions	163
8.1.2	Future Works	167
CURRICULUM VITAE		168

LIST OF FIGURES

FIGURE 1.1 POTENTIAL WEAVING SECTION AT A NEAR-SIDE BUS STATION.	2
FIGURE 1.2 WEAVING SECTION ON THE LINKAGE BETWEEN OFF-RAMP AND GROUND INTERSECTION.	2
FIGURE 1.3 FEATURES OF TYPES I AND II DZs.....	4
FIGURE 1.4 TRAFFIC MOVEMENTS AND REGULARS AT UNSIGNALIZED INTERSECTIONS.	5
FIGURE 1.5 ILLUSTRATION OF CONNECTIVE-VEHICLE TECHNOLOGY.....	6
FIGURE 1.6 SPEED CONTROL TO PREVENT WEAVING AT A CURB SIDE BUS STATION.....	7
FIGURE 1.7 SPEED CONTROL TO PREVENT WEAVING AT A CURB SIDE BUS STATION.....	8
FIGURE 1.8 ARCHITECTURE OF THE THESIS OUTLINE.....	9
FIGURE 3.1 TRAJECTORY OPTIMIZATION TO PREVENT CONGESTION.....	33
FIGURE 3.2 ARCHITECTURE OF THE CONTROL LOGIC.	35
FIGURE 3.3 RANGE OF RED DURATION UNDER VARIOUS INITIAL SIGNAL INFORMATION.	39
FIGURE 3.4 ARCHITECTURE OF THE THREE-PHASE ALGORITHM.	41
FIGURE 3.5 MULTI-STAGE PROCESS FOR OPTIMIZATION OF AVERAGE TRAVEL TIME.	42
FIGURE 3.6 PATTERNS OF OVER-LONG IDLING TIME AND SPEED FLUCTUATION.....	46
FIGURE 3.7 COMPARISON OF TRAVEL TIME UNDER THE CONTROL AND NON-CONTROL ENVIRONMENTS WITH VARIOUS SCENARIOS.	51
FIGURE 3.8 TRAJECTORY OF PLATOON UNDER THE CONTROL ENVIRONMENT WITH VARIOUS SCENARIOS.	51
FIGURE 3.9 TRAJECTORY OF PLATOON UNDER THE CONTROL ENVIRONMENT WITH VARIOUS SCENARIOS.	53
FIGURE 3.10 FUEL CONSUMPTION RATE FOR THE LEADING VEHICLE WITH AND WITHOUT CONTROL IN SCENARIOS 1 AND 3.....	54
FIGURE 3.11 IMPACT OF INITIAL SPEEDS ON AVERAGE TRAVEL TIME.	55
FIGURE 4.1 DYNAMIC SPEED CONTROL USING V2X.	59
FIGURE 4.2 SPEED TRAJECTORIES OF A SINGLE VEHICLE UNDER DIFFERENT SCENARIOS.	61
FIGURE 4.3 COMPARISON BETWEEN OPTIMAL SPEED AND NON-OPTIMAL SPEED TRAJECTORIES UNDER THE SAME TRAVEL TIME.	62
FIGURE 4.4 IMPACTS OF THE ANTERIOR PLATOON AND THE SIGNAL LIGHT.....	66
FIGURE 4.5 SPEED CONTROL ALGORITHM FOR A FULLY OBEDIENT PLATOON UNDER DIFFERENT SCENARIOS.	67
FIGURE 4.6 RE-GROUP OF A PLATOON MIXED WITH OVs AND DOVs.	72
FIGURE 4.7 LOGIC OF SPEED CONTROL ALGORITHM.	73
FIGURE 4.8 FUEL CONSUMPTION OF PA UNDER SPEED CONTROL AND FREE DRIVING.	75
FIGURE 4.9 TOTAL FUEL CONSUMPTION UNDER DIFFERENT SCENARIOS.	76
FIGURE 4.10 FUEL CONSUMPTION UNDER DIFFERENT PERMUTATIONS.	77
FIGURE 5.1 TRAFFIC MOVEMENTS AND REGULARS AT UNSIGNALIZED INTERSECTIONS.	80
FIGURE 5.2 TREAT GAPS AND VEHICLE LENGTH AS “SIGNAL TIME”.....	81
FIGURE 5.3 SPEED TRAJECTORIES OF A SINGLE VEHICLE UNDER DIFFERENT SCENARIOS.	82
FIGURE 5.4 IMPACTS OF THE DOWNSTREAM VEHICLES AND THE GAPS.	86
FIGURE 5.5 SCENARIOS FOR TWO-LEVEL PRIORITY INTERSECTIONS WITHOUT THE IMPACT OF THE DOWNSTREAM VEHICLES.....	88
FIGURE 5.6 SCENARIOS FOR TWO-LEVEL PRIORITY INTERSECTIONS CONSIDERING THE IMPACT OF THE DOWNSTREAM VEHICLES.	90

FIGURE 5.7 IMPACTS OF THE DOWNSTREAM VEHICLES AND THE GAPS WITH MULTIPLE STREAMS. .	93
FIGURE 5.8 OVERALL PROCEDURE OF THE PROPOSED SPEED CONTROL ALGORITHM	97
FIGURE 5.9 PRIORITY RANKS AND CONFLICTING POINTS OF THE 8-STREAM INTERSECTION.....	98
FIGURE 5.10 COMPARISON OF FUEL CONSUMPTION AND EMISSION BETWEEN SPEED CONTROL AND FREE DRIVING UNDER SCENARIOS 1 TO 3.	99
FIGURE 5.11 COMPARISON OF FUEL CONSUMPTION AND SPEED PROFILE OF THE TARGET VEHICLE BETWEEN SPEED CONTROL AND FREE DRIVING UNDER SEVERAL CONDITIONS.....	100
FIGURE 6.1 POTENTIAL WEAVING SECTION AT A NEAR-SIDE BUS STATION.....	103
FIGURE 6.2 TRAJECTORY OPTIMIZATION TO PREVENT WEAVING AT A CURB SIDE BUS STATION. ..	106
FIGURE 6.3 A BUS TRAVERSING PWS.	108
FIGURE 6.4 DISTRIBUTION OF PLATOON UPSTREAM OF BUS STATION.	108
FIGURE 6.5 WEAVING DETERMINATION AT PWS.	109
FIGURE 6.6 RANGES OF RK UNDER VARIOUS INITIAL SIGNAL INFORMATION.....	112
FIGURE 6.7 A TWO-PHASE SOLUTION ALGORITHM.	113
FIGURE 6.8 MULTI-STAGE DECISION MAKING FOR VEHICLE TRAJECTORY OPTIMIZATION IN PHASE I.	114
FIGURE 6.9 LOCATION AND LAYOUT OF THE TEST SITE.	122
FIGURE 6.10 COMPARISON OF THE VEHICULAR TRAVEL TIME UNDER CONTROL AND NON-CONTROL ENVIRONMENTS.....	123
FIGURE 6.11 COMPARISON OF VEHICULAR TIME UNDER CONTROL AND NON-CONTROL ENVIRONMENTS.....	124
FIGURE 6.12 COMPARISON OF PERSON TRAVEL TIME UNDER CONTROL AND NON-CONTROL ENVIRONMENTS.....	125
FIGURE 6.13 TRAJECTORIES OF THE LAST CAR AND BUS ON THE 5TH LANE, UNDER THE CONTROL AND NON-CONTROL ENVIRONMENT.....	126
FIGURE 6.14 TRAJECTORIES OF THE CARS AND BUS ON THE 4TH LANE UNDER THE CONTROL AND NON-CONTROL ENVIRONMENT.	126
FIGURE 6.15 TRAJECTORIES OF THE CARS AND BUS ON THE 3TH LANE UNDER THE CONTROL AND NON-CONTROL ENVIRONMENT.	127
FIGURE 6.16 TRAJECTORIES OF THE CAR AND BUS ON THE DESTINATION LANE, UNDER THE CONTROL AND NON-CONTROL ENVIRONMENT.	128
FIGURE 6.17 COMPARISON OF OPTIMAL RATES OF VEHICULAR AND PERSON TRAVEL TIME UNDER THE CONTROL ENVIRONMENT.....	129
FIGURE 6.18 COMPARISON OF OPTIMAL RATES OF PERSON TRAVEL TIME UNDER VARIOUS TRAFFIC DEMAND.....	130
FIGURE 6.19 COMPARISON OF OPTIMAL RATES OF PERSON TRAVEL TIME UNDER VARIOUS DISTANCE.	131
FIGURE 7.1 SPEED GUIDANCE FOR DZ PROTECTION.	136
FIGURE 7.2 LAYOUT OF TYPE I AND TYPE II DZs.	137
FIGURE 7.3 LOGIC OF THE PROPOSED DYNAMIC SPEED GUIDING METHOD.	139
FIGURE 7.4 IDEA FOR DZ DETECTION.....	140
FIGURE 7.5 ARCHITECTURE OF THE TWO-STAGE MODEL.	142
FIGURE 7.6 SAMPLE DP MODEL WITH I STAGES.	143
FIGURE 7.7 VARIOUS INITIAL SIGNAL INFORMATION.....	146
FIGURE 7.8 TRAJECTORIES AVOID TOUCHING THE DZ.	147
FIGURE 7.9 FREQUENT SPEED FLUCTUATION.....	148

FIGURE 7.10 AERIAL VIEW OF THE US 40 AND RED TOAD ROAD INTERSECTION.	151
FIGURE 7.11 LAYOUT OF THE GUIDING AREA.	153
FIGURE 7.12 COMPARISON OF VEHICULAR TRAJECTORY WITH AND WITHOUT GUIDANCE IN SCENARIO 1.	155
FIGURE 7.13 COMPARISON OF VEHICULAR TRAJECTORY WITH AND WITHOUT GUIDANCE IN SCENARIO 2.	156
FIGURE 7.14 COMPARISON OF VEHICULAR TRAJECTORY WITH AND WITHOUT GUIDANCE IN SCENARIO 3.	157
FIGURE 7.15 COMPARISON OF VEHICULAR TRAJECTORY WITH AND WITHOUT GUIDANCE IN SCENARIO 4.	157
FIGURE 7.16 COMPARISON OF TRAVEL TIME, IDLING TIME, AND SPEED FLUCTUATION FREQUENCY UNDER VARIOUS SPACE HEADWAYS.	158
FIGURE 7.17 COMPARISON OF TRAVEL TIME UNDER VARIOUS SCOPE OF DZ GUIDING AREA.	159
FIGURE 7.18 COMPARISON OF SPEED FLUCTUATION FREQUENCY UNDER VARIOUS SCOPE OF DZ GUIDING AREA.....	160

LIST OF TABLES

TABLE 3.1 SYMBOLS AND PARAMETERS.	33
TABLE 3.2 SUMMARY OF PARAMETER SETTINGS.	49
TABLE 3.3 COMPARISON OF IDLING TIME AND SPEED FLUCTUATION UNDER THE CONTROL AND NON-CONTROL ENVIRONMENTS.	52
TABLE 5.1 SAMPLE COEFFICIENTS OF HYBRID REGRESSION MODEL FOR FUEL CONSUMPTION AND CAR EMISSION RATES.	84
TABLE 6.1 SYMBOLS AND PARAMETERS.	106
TABLE 6.2 SUMMARY OF THE MODEL INPUTS.	122
TABLE 7.1 PRE-DESIGN SURVEY FINDINGS OF THE EASTBOUND MOVEMENT.	152
TABLE 7.2 COMPARISON OF DZ PROTECTION METHOD AND TRAVEL TIME WITH AND WITHOUT GUIDANCE.	154
TABLE 7.3 COMPARISON OF IDLING TIME AND SPEED FLUCTUATION OF THE BEST AND RANDOM SPEED PROFILES.	154

ACKNOWLEDGEMENTS

Writing dissertation has been a period of intense learning for me, not only in the academic research, but also on a personal level. Without this valuable experience, I will never know how far I can push myself.

I would like to express the deepest appreciation to my advisor, Dr. Jie Yu, who has provided me with unconditional and countless help and support during the entire graduate study. Her inner passion in research and teaching infected me a lot. Without her guidance and persistent help this dissertation would not have been possible.

I would like to thank my committee members, Dr. Troy Liu, Dr. Chao Zhu, Dr. Yin Wang, and Dr. Matthew E H Petering. Thank you so much for being my committee members, reading my proposal and dissertation draft, and giving me the insightful suggestions and comments.

I am so lucky to have the continuing and strong supports from my family and my friends. When I was upset and stressed, they always encouraged me and cheered me up.

Chapter 1 INTRODUCTION

1.1 Background

Traffic bottleneck is defined as a disruption of traffic flow through a freeway or an arterial (Daganzo, C.F., 1997), which can be divided as two categories: stationary bottleneck and moving bottleneck. The stationary bottleneck is mainly formed by the lane drops in the multi-lane roadways, while the moving bottleneck are due to the very slowing moving vehicles which disrupt the traffic flow (Daganzo et al., 1999). Traditional strategies for eliminating bottlenecks mainly focus on expanding supply including road widening, green interval lengthening and optimization of intersection channelization. A few macroscopic methods are also made to optimize the traffic demand such as routing optimization (V.L. Knoop and W. Daemen, 2017).

One typical urban bottleneck causing congestion is around the curb side bus stops. The bus system, with its cost efficiency, design flexibility, and short construction period, has been widely developed in urban areas as an alternative way to alleviate traffic congestion and improve accessibility. As cities grow in both surface and population, the bus system nowadays often struggles to provide satisfying level of service due to limited road space coupled with increasing traffic demand, especially in developing countries. For example, it is common to observe serious conflicts between buses and cars weaving at a curb side bus station (no matter located near-side or far-side). Such a potential weaving section (PWS) often causes traffic bottlenecks characterized with aggressive lane changes, frequent stops, excessive delays, and frequent accidents especially as road saturation level increases as shown in Figure 1.1.

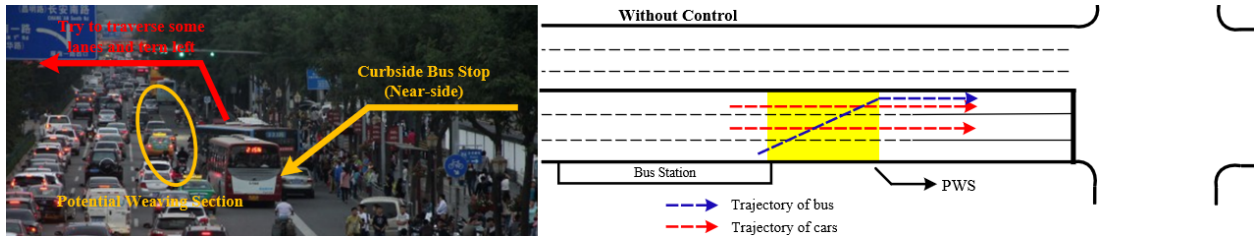


Figure 1.1 Potential weaving section at a near-side bus station.

Compared with far-side locations, near-side bus stations may cause worse traffic congestion in couple with high traffic flow weaving, limited road space, poor geometric design, and improper intersection signal timings.

The bottleneck around linkage between the urban freeway off-ramp and ground intersection is also noteworthy. As the top of Figure 1.2 depicts, traffic on the off-ramps may suffer difficulty in passing through the ground intersection due to its competition with the ground traffic movements.

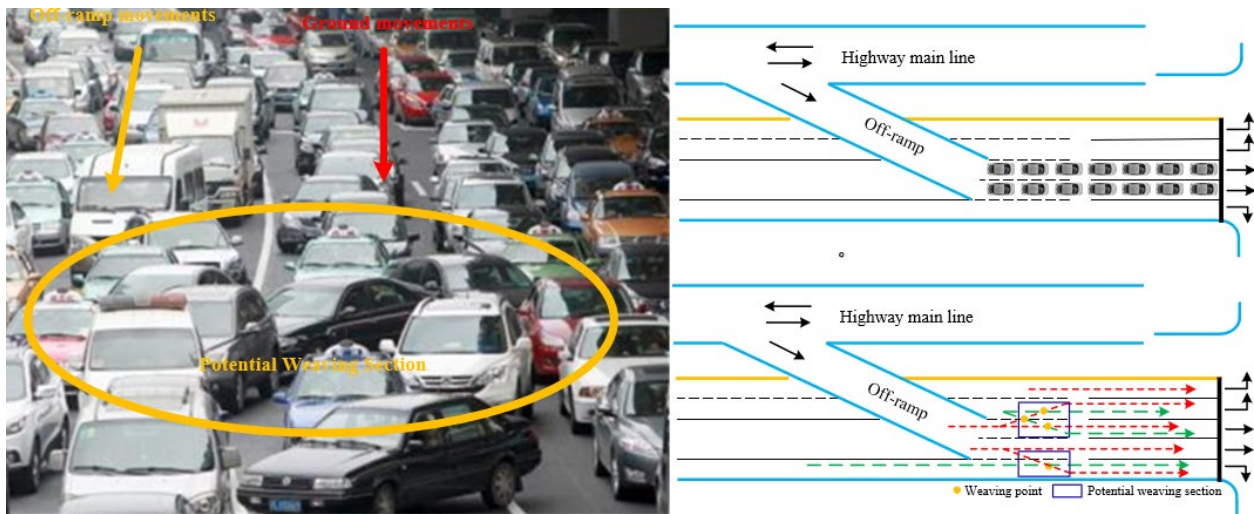


Figure 1.2 Weaving section on the linkage between off-ramp and ground intersection.

There're two main reasons to formulate this bottleneck. The left bottom of Figure 1.2 illustrates one reason that due to the over short linkage which causes the off-ramp movements

blocked so that they cannot merge into the ground traffic flow. The other, depicted by the right bottom, is that to reach the target approaching lane, the off-ramp and ground movements may mutually weave each other.

Improving traffic safety is almost the overriding responsibility of transportation departments at all levels, especially for reducing the risks at those hazardous intersections with deadly accidents. A report from the United States shows in 2016 there were 2,524,000 crashes happened at intersections, where approximately 4470 crashes were fatal (NHTSA 2016). There're two types of bottleneck which take high risk for crashes. The first is high-speed signalized intersection, due to the dilemma zone issue; the other is the unsignalized intersection where the motorists may choose to traverse unsafe gaps.

Dilemma zone (DZ), as a segment in the approach of the intersection, is one of the most contributing factors towards crashes (nearly 40% of urban crashes are caused by DZ), because motorists could neither pass the intersection before the onset of the red phase, causing side-angle crashes; nor stop the car safely, resulting in rear-end collision (Gazis et al. 1960). The idea of DZ was initially proposed by Gazis, who developed a model, "Type-I Model", defining DZ as a space range, where the vehicle could neither clear the intersection safely nor slow down to stop smoothly during the amber phase. Beside the "Type-I Model", a concept of the "Type-II Model" was also raised, expressed as a probability of drivers 'decision for stop (Zegeer 1977). Field observation or graph processing are usually adopted to study DZ boundaries or the drivers' reaction facing DZ. The features of Types I and II DZs are depicted in Figure 1.3.

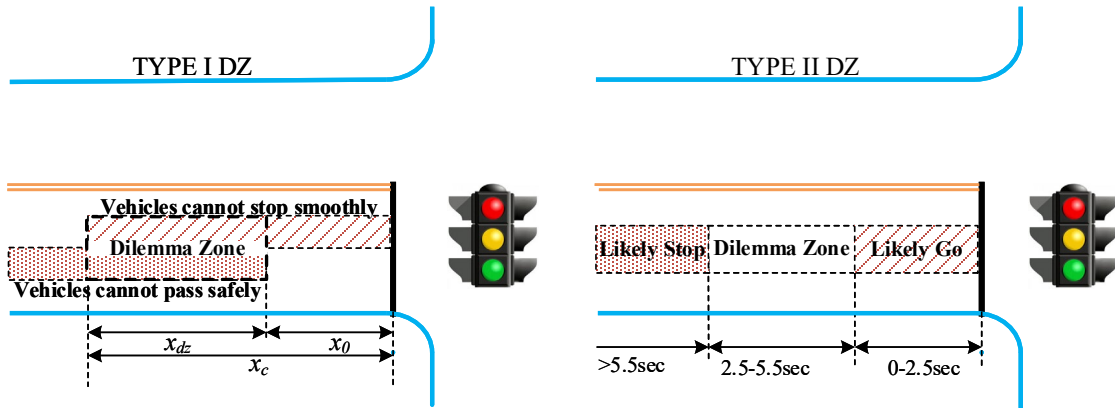


Figure 1.3 Features of Types I and II DZs.

Unlike signalized intersections where the green light gives the right of way, there's no positive indication to the drivers about when to pass through the prior streams at unsignalized intersections. The drivers need to find a safe "gap" themselves. The minimum gap that the driver accept is the critical gap. In traditional environment, the critical gap is sensed by human and is variable toward different people. For the unsignalized intersections, there exists a hierarchy among streams. Some streams have the top priority, while others must yield to higher rank streams. In some cases, streams must yield to some streams which also should yield to others.

The simplest unsignalized intersection, shown in the left part of Figure 1-4, have two streams, from which the minor one yields to the major one. Here is only one conflicting point (the red circle in the left part of Figure 5) in these simplest intersections. While for those having more than two streams, a vehicle may need to avoid several conflicting points, like the right part of Figure 1.4 illustrates.

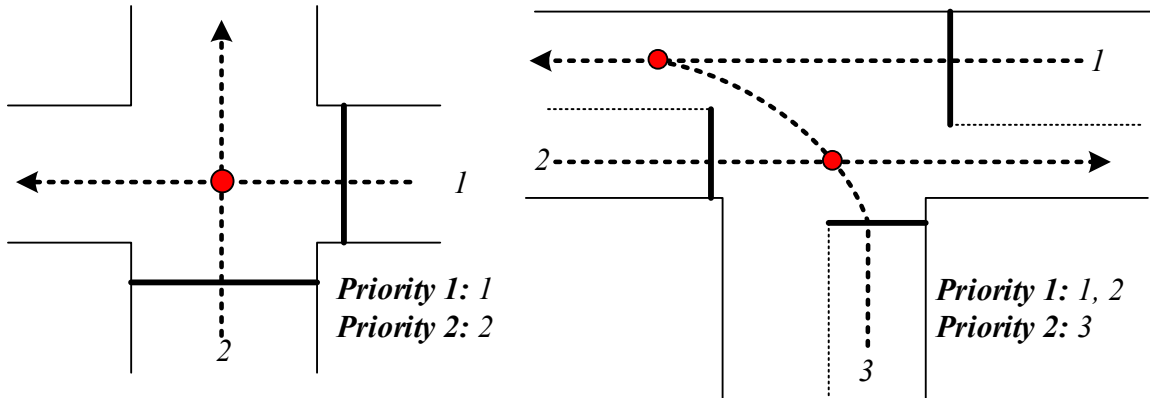


Figure 1.4 Traffic movements and regulars at unsignalized intersections.

1.2 Application of Connected and automated vehicle technology

Nowadays, with the development of Intelligent Transportation Technology (ITS), it is possible to eliminate bottlenecks and improve safety dynamically. As a part of Intelligent Transportation Systems, the Connected and automated vehicle technology (CAV), sponsored by the U.S. DOT Research and Innovative Technology Administration (RITA)/ITS Joint Program Joint Program Office (ITS JPO), focuses on localized Vehicle-to-Vehicle, Vehicle-to-Infrastructure and Vehicle-to-Device Systems (V2X) to support safety, mobility and environmental applications using vehicle Dedicated Short Range Communications (DSRC)/Wireless, as Figure 1.5 depicts.



Figure 1.5 Illustration of connective-vehicle technology.

Based upon the characteristics of CAV, it can be used to improve the traffic safety and efficiency, by adjusting the speed of the traffic movements with the change of traffic environment. For the problems listed above, take the near-side bus stop and DZ as examples, CAV can be implemented as follows.

(1) Near-side bus stop

As Figure 1.6 depicts, under CV environment, the vehicular speed can be guided so that there's no cars inside the weaving section as the bus enters.

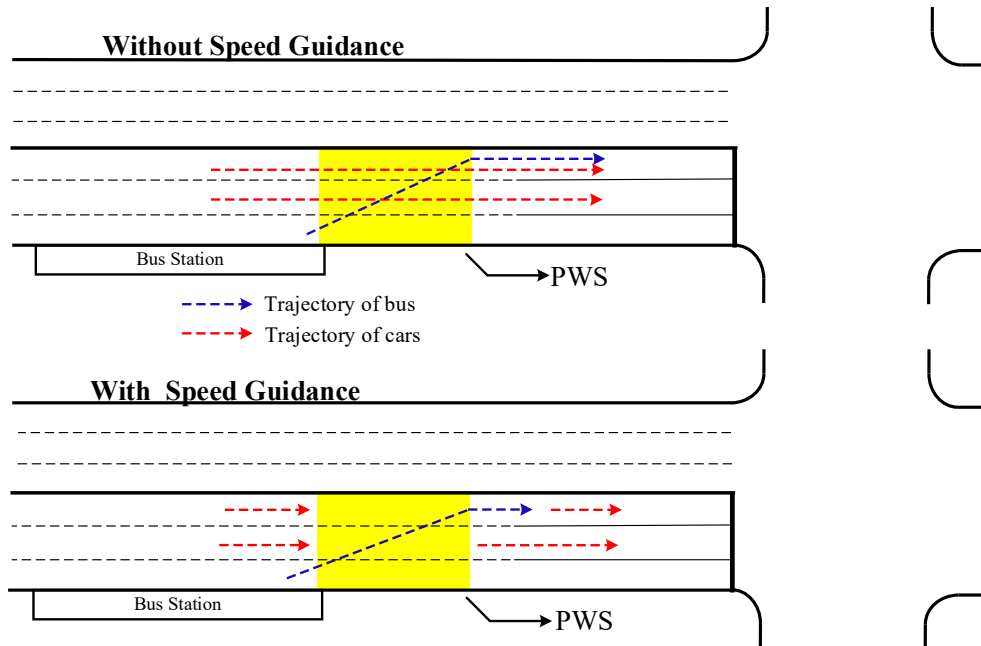


Figure 1.6 Speed control to prevent weaving at a curb side bus station.

(2) DZ protection

Although some kinds of warning systems have been installed to remind motorists of DZ protection, they cannot assist the motorists to change their status smoothly and effectively. Under the CV environment, the motorists can actively follow the system's guidance and decelerate optimally to acquire other benefits such as travel time and idling time saving. The idea can be depicted in Figure 1-7.

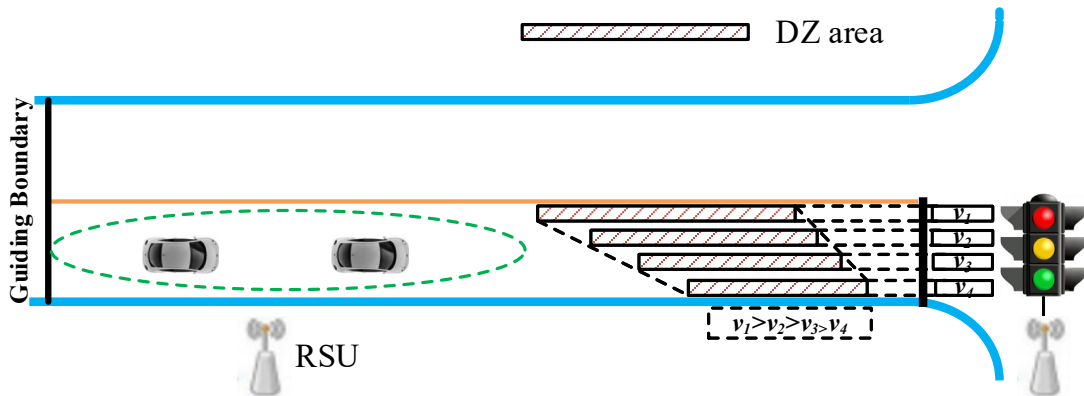


Figure 1.7 Speed control to prevent weaving at a curb side bus station.

1.3 Research Objectives

Therefore, the primary focus of this dissertation is to develop a cooperative vehicular trajectory optimization framework, based on the CAV technology, that can assist vehicles optimizing their trajectories to proactively prevent the urban bottlenecks. More specifically, the proposed models shall have the capabilities to:

- Determine control boundaries, based on the mechanism of vehicles and utilization of temporal and spatial resources;
- Design detection strategy that can determine if bottleneck or safety risk would emerge;
- Design cooperative control plans at the transportation nodes such as near-side bus stop, and intersections, i.e., to eliminate bottleneck or safety risk; and
- Update local control strategies, if vehicle doesn't obey the control command or its status changes.

To accomplish all the above objectives, the proposed framework and models shall have the following features:

- Realistic representation of the complex temporal and spatial interrelations among the selected transportation nodes with acceptable computational efficiency;
- Integration of various levels of control strategies with pre-specified control objectives to ensure the effectiveness of the integrated operations under various scenarios; and
- Development of sufficiently efficient and robust solution algorithms that can solve the proposed optimization formulations and generate target control strategies for a complicated system.

1.4 Dissertation Organization

Based on the proposed research objectives, this study has organized the primary research tasks into eight chapters. The core of those tasks and their interrelations are illustrated in Figure 1.8.

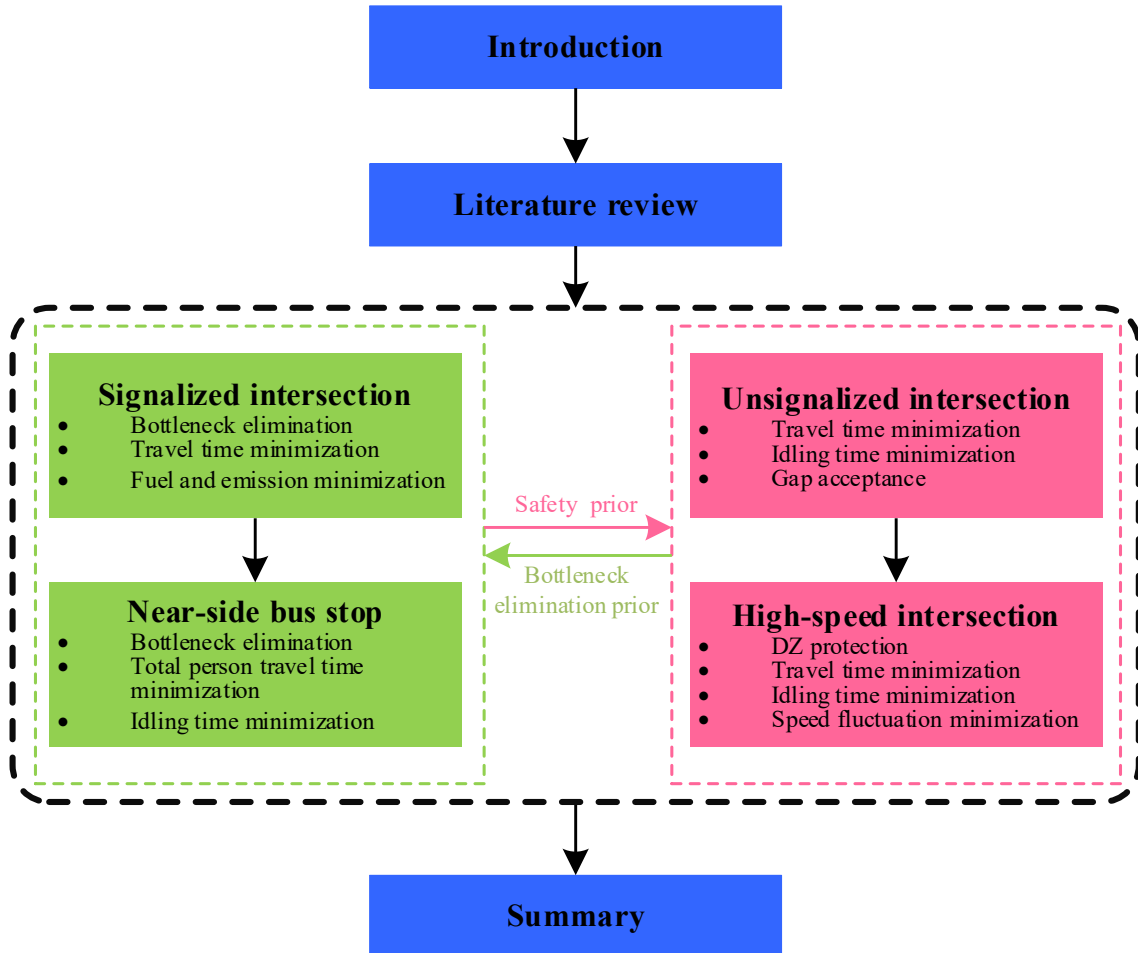


Figure 1.8 Architecture of the thesis outline.

The remaining chapters of this dissertation are organized as follows:

- **Chapter 2** presents a comprehensive literature review of existing studies on various control strategies for traffic bottleneck and safety risk elimination, including both model formulations and solution algorithms. The review focuses on identifying the advantages

and limitations of those strategies, along with their potential enhancements, including the trajectory optimization.

- **Chapters 3 and 4** develops the formulations and solution algorithms for the optimization models necessary to execute the cooperative control strategies at signalized intersections, including determining the control boundaries, confirming the existence of bottleneck, and designing the cooperative control strategies. The cooperative control model is expected to eliminate the bottleneck and minimize the average travel time, idling time and speed fluctuation of the off-ramp and ground movements
- **Chapter 5** develops the gap-based model on the two-way stop unsignalized intersection. The proposed model considers the running status of the target vehicle as well as the impact of the downstream vehicles (if exists) and the gap conditions in real-world traffic environment. Acceleration/deceleration profile, instead of speed trajectories, is optimized for speed guidance. Illustrative examples are provided to validate the proposed algorithm. Results indicate that the proposed control algorithm is effective to minimize the fuel consumption and emission of the target vehicle under various test scenarios.
- **Chapters 6** designs the cooperative control model that optimizes the vehicular trajectories around the near-side bus stop, based on critical issues that need to be considered in the design of control strategies. It specifies the required system inputs, the principal system components and their key functional features, as well as operational interactions. A time rolling horizon-based solution algorithm is introduced to optimize the trajectories step by step that minimizes the total person travel time and idling duration.

- **Chapter 7** focuses on high-speed intersections where a dynamic speed control model is proposed featuring dilemma zone protection and trajectory optimization. The control boundary is divided into two parts where the upstream slow down the over-speed vehicle and the downstream optimizes the vehicular trajectory. The time-rolling-horizon-based algorithm is also applied to solve the model where the vehicular travel time optimization is the primary target. Conditioned on the optimized travel time, idling time and speed fluctuation will be minimized in sequence.
- **Chapter 8** summarizes the contributions of this dissertation and provides future research directions, including the development of an efficient cooperative control model to address the demand surge due to bottleneck and safety risk elimination at transportation nodes, and innovative heuristics for solving the proposed model formulations.

1.5 References

- Daganzo, C.F. (1997). A continuum theory of traffic dynamics for freeways with special lanes. *Transportation Research Part B: Methodological*, 31(2), 83-102
- Gazis, D., Herman R. and Maradudin A. (1960). The problem of the amber signal in traffic flow. *Opns Rex* 8, 112-132.
- NHTSA. (2016). 2015 Motor Vehicle Crashes: Overview. *Traffic safety facts research note, 2016*, 1-9.
- Victor L. Knoop & Winnie Daamen. (2016). Automatic fitting procedure for the fundamental diagram. *Transportmetrica B: Transport Dynamics*, 129-144, DOI: 10.1080/21680566.2016.1256239
- Zegeer, C. V. (1977). Effectiveness of green-extension systems at high-speed intersections. *Kentucky Transportation Center Research Report*, KYP-75-69; HPR-PL-1(12), Part 111-B.
- NHTSA. (2016). 2015 Motor Vehicle Crashes: Overview. *Traffic safety facts research note, 2016*, 1-9.
- Daganzo, C.F. (1997). A continuum theory of traffic dynamics for freeways with special lanes. *Transportation Research Part B: Methodological*, 31(2), 83-102

Chapter 2 LITERATURE REVIEW

This chapter presents a comprehensive literature review of existing studies on various control strategies for traffic bottleneck and safety risk elimination, including both model formulations and solution algorithms. The first section summarizes the traditional research efforts and their deficiencies towards the bottlenecks and safety risks. The second section explores the improvements of those research outcomes under the connected and autonomous vehicles.

2.1 Traditional Research toward Bottlenecks And Safety Risks

2.1.1 Near-side bus stops

The bus system, with its cost efficiency, design flexibility, and short construction period, has been widely developed in urban areas as an alternative to private cars for efficient, reliable and comfortable travel. As cities grow in both surface and population, the bus system often struggles to provide satisfying level of service due to limited road space coupled with increasing traffic demand. For example, it is common to observe serious conflicts between buses and cars weaving at a curb side bus station (no matter located near-side or far-side). Such a potential weaving section (PWS) often causes traffic bottlenecks characterized with aggressive lane changes, frequent stops, excessive delays, and frequent accidents especially as road saturation level increases. Compared with far-side locations, near-side bus stations may cause even worse traffic congestion due to high traffic flow weaving, limited road space, poor geometric design, and improper intersection signal timings.

The impact of curb side bus stations on traffic flow has been investigated in the literature. Previous studies fall into different categories: observational studies, analytical methods, and simulation-based studies. Observational studies usually explore field data to examine the effect

of bus stations on traffic operations. For examples, it was found that far-side bus stations tend to outperform near-side stops in terms of reduced queue, additional vehicle maneuvering space, easier lane changes, and fewer delayed right-turning vehicles (Terry and Thomas, 1971). However, Fitzpatrick (1997) reached the opposite findings. Yu (2014) established a statistical model to quantify the impact of factors such as platform types, bus station lengths, and lane numbers. Feng (2015) statistically investigated the joint impacts of bus station locations, signalized intersections and traffic conditions. Stephen (2016) proposed a statistical model to explore the factors that may affect the bus dwelling time and the time to re-enter to the main traffic flow. These studies are informative but not conclusive due to either limited numerical scenarios or the lack of detailed analysis of the relationships among important affecting factors such as bus frequency, dwelling time, and vehicle volume/distribution in the bus operational environment.

Analytical methods generally open to broader situations with simplified models for tractability. Furth (2006) evaluated the impact of harbor-style bus station location on bus delay with factors of gravity, queue interference at signalized intersections. As for curb side bus stations, queue model was developed to assess disturbance from cars on isolated bus stations, without involving signalized intersections (Gu et al., 2011). Gu (2014) further incorporated signalized intersections to research the impact of far-side and near-side bus stations on traffic efficiency but did not include either oversaturated conditions or instant traffic disturbances such as lane changes, gaps in front of the dwelling bus and turning vehicles.

2.1.2 Intersections

Signalized intersections are one of the most important elements in the urban transportation system. As cities grow in both surface and population, the signalized intersections often struggle to provide satisfying level of service due to limited road space coupled with increasing traffic demand, resulting in over-long travel time and eco-problems. In the United States, the transportation sector uses up nearly 75% of petroleum and emits the second largest carbon dioxides due to the poor operation performance (EPA 2016; Davis et al., 2010). Research findings also indicate that bad driving behaviors resulted from the severe bottlenecks constitute the major contribution to carbon emission and petroleum consumption (Toshiaki and Takumi, 2008). Traditional strategies have little effectiveness for improving the operation research around the signalized intersections (Mensing et al., 2011). Therefore, innovative technologies are urgently needed to address these challenges.

2.1.3 Dilemma zone on high-speed signalized intersections

Dilemma zone (DZ), a segment in the approach of the intersection, is one of the most contributing factors towards those crashes, since motorists can neither pass the intersection before the onset of the red phase, causing side-angle crashes; nor stop the car safely, resulting in rear-end collision (Gazis et al., 1960). The idea of DZ was initially proposed by Gazis (1960), who developed a model, “Type-I Model”, defining DZ as a space range, where the vehicle can neither clear the intersection safely nor slow down to stop smoothly during the yellow phase. Beside the “Type-I Model”, a concept of the “Type-II Model” was also raised, expressed as a probability of motorists’ decision for stop (Zegeer 1977). Field observation or graph processing are usually adopted to study DZ boundaries or the motorists’ reaction facing DZ. A common sense is that DZ range depends on the motorist’s behaviors and the types of vehicles (Liu et al.

2007). Other literatures also show a boundaries range of between 2 to 6 seconds for DZ (Parsonson et al., 1974; Chang et al., 1985; Bonneson and McCoy 1996). In studying with the motorists' behaviors, Van der Horst and Wilmink illustrated that they depend on some objective and subjective factors, such as motorist's emotion, personality, and vehicular speed, et al (Horst and Wilmink 1986). They developed a decision-making process model and some parameters in that model are adopted by some later research (Widodo et al., 2000a; Wu et al., 2010; Asadi and Vahidi 2010; Tielert et al., 2010; Marzoug et al., 2015).

The traditional studies towards DZ protection are mainly divided into two categories: one belongs to the motorist side, trying to alert the motorists in advance; the other belongs to infrastructure, extending the green time to insure the vehicles pass before the onset of the red phase. Over the motorist ride, Moon et al. (Moon et al., 2003) developed an integrated system for assessing a DZ warning system for signalized intersections by a serial of field tests. Results from the tests indicated that the system can be implemented at signalized intersections to avoid the DZ, and to reduce red-light violations and intersection collisions. Martin et al. (Martin et al., 2003) considered the two-advanced warning (AWS) systems presently used in Utah. It found that the setup and performance of the two systems were different. The Texas Transportation Institute has developed a new system named the Advanced Warning for End of Green System (AWEGS) for application of DZ protection (Sunkari et al., 2005). The system was implemented at two sites in Waco and Brenham, Texas. The result indicated that AWEGS consistently improved the DZ protection at intersections and reduced red light running by approximately 40%. Another system is called the Pre-signal Indication System (PSIS) which uses a flashing green or yellow signal at the last of the green phase (Factor et al., 2012; Wu et al., 2017).

Over the infrastructure side, Ma et al. (2010) presents an extensive investigation regarding the impacts of green signal countdown devices (GSCD) on the intersection safety, based on field observation of critical motorist and vehicle related parameters at two similar intersections (one with GSCD and the other without GSCD) in Shanghai. Also, some studies combined those two categories together (Zimmerman et al., 2012; McCoy and Pesti. 2003b; Wang et al., 2016).

2.2 Bottlenecks And Safety Risk Elimination Based on CAV

In the past two decades, wireless communication technologies have been widely used in the transportation system. As a part of Intelligent Transportation Systems, the Connected-vehicle program (formerly called VII or Intellidrive), sponsored by the U.S. DOT Research and Innovative Technology Administration (RITA)/ITS Joint Program Joint Program Office (ITS JPO), focuses on localized Vehicle-to-Vehicle, Vehicle-to-Infrastructure and Vehicle-to-Device Systems (V2X) to support safety, mobility and environmental applications using vehicle Dedicated Short Range Communications (DSRC)/Wireless Access for Vehicular Environments (WAVE) (ITS AMERICA, 2014). In US, major Connected-vehicle projects have been initiated in the states of California, Michigan, and Arizona (Amanna, 2009). In California, a “sniffer” working with a 170-type controller (and conceivably with any controller) is established, combined with a message set, which provides wireless DSRC signal state information to approaching, equipped cars (Dallinger et al., 2013). Michigan DOT developed a self-supporting test bed in 2005. The aim of this program is to provide a real-world laboratory to validate products and technologies related to Connected-vehicle (Underwood et al., 2008; Krueger, 2005). Connected-vehicle-related activities in Arizona are focused on providing emergency

services and supporting incident management activities. The Emergency VII (E-VII) program has identified four key capabilities to improve incident response (Saleem and Nodes, 2008).

2.2.1 CAV on signalized intersection

Leveraging the DSRC technology, approaching vehicles' speeds, positions, and other information with signal data could be obtained at a signalized intersection. Such technologies offer the possibility for vehicles to receive advanced information from signal lights and alter speed trajectories to minimize idling at the stop line of signalized intersection (Chen et al., 2011).

Some studies in this regard aim at minimizing vehicular delay time. In 2014, Guler proposed an algorithm to enumerate various patterns of cars discharging before the stop bar to minimize the vehicular delay using connected-vehicle technology (Guler et al., 2014). Li and Wang developed some trajectories for cars to safely and resulting in minimized delay time (Li and Wang, 2006). In 2012, based on game theory for a cooperative adaptive cruise control system at an intersection, an algorithm was developed to let every single vehicle to avoid conflict and have minimized delay (Zohdy and Rakha, 2012). Abu-Lebdeh proposed an algorithm to study the benefit of the intellidrive technology in terms of delay (Abu-Lebdeh, 2013).

For those delay minimized-related researches, speed trajectories recommended may not be the best for reducing fuel consumption and emission. Therefore, use of ITS technology to propose a fuel-optimal strategy is on the agenda of the eco-driving research (Barth and Boriboonsomsin, 2009; Widodo et al., 2002). In advance, under the connected vehicle technology, a few researches utilized the signal information to reduce fuel consumption and emissions (Wu, G et al., 2002; Asadi and Vahidi, 2010; Tielert et al., 2010; Malakorn and Park, 2010). In 2012, the RITA released a report on eco-driving by controlling speed trajectories of vehicles using V2I technology (US.DOT, 2012), which is based upon the Rakha's research

(Rakha and Kamalanathsharma, 2011). In this report, multiple scenarios are studied at intersections according to the upcoming signal changing information and vehicle's position and speed. In addition to an isolated intersection, an algorithm for vehicles moving along a signalized arterial is also developed and tested by simulations (Barth et al., 2011).

2.2.2 Advanced research at unsignalized intersections

Unlike signalized intersections where the green light indicates the right of way, there's no definite indication to the drivers regarding when to pass through the prior streams at unsignalized intersections. Instead, there usually exist hierarchies of moving priorities among streams. Traffic streams with lower priorities need to yield and find a safe 'gap' to pass through those streams with higher priorities. While for the yield rule, there exist huge risks based upon sight blocking. For example, if there exists a construction at the corner of the intersection, it may block the drivers' sights on both the higher and lower priority lanes, posing a potential risk. Accordingly, studies on unsignalized intersections (or try to eliminate signal control) mainly focus on crash avoidance based on connected-vehicle technology. For example, Milanés et al. (2010) developed a fuzzy-based intersection control algorithm for autonomous vehicles and validated it by a test in Spain. Kamal et al. (2015) used a predictive control model to integrate automated vehicles at an unsignalized intersection to avoid collision. Dresner and Stone (2008) proposed an intersection algorithm for autonomous vehicles to avoid crash at unsignalized intersections. Lee and Park (2012) developed a cooperative vehicle intersection control algorithm without the need signal control. For this algorithm, the fuel consumption and car emissions are neglected to some extent. Speed alteration sharply to avoid a crash may cause huge fuel consumption and emission, which is not environmental friendly. In addition, it is more complicated to develop speed guidance

algorithms at an unsignalized intersection, as the ‘gap’, used to determine when to cross, is dynamic and lacks regularity.

2.2.3 Real-time bus control

With the development of real-time wireless communication technology (e.g. connected vehicle, vehicle to infrastructure communication), TSP strategies have been advanced in recent years. For examples, Hu et al. (2015) developed an algorithm that reached the maximum coverage of TSP buses and reduced the risk of competing movements. Despite its effectiveness in reducing bus delay, implementation of TSP is usually at the cost of general traffic operational performance. The key issue of conflicts between general traffic and buses has not been resolved, especially at the bus stations.

2.2.4 Active DZ protection

Recently, several preliminary studies have been investigated towards applying the real-time communication theory for DZ protection. Sharma et al. (2012) developed a prototype Yellow Onset Motorist Assistance (YODA) system, consisting of a pole-mounted unit (StreetWave) and an in-vehicle unit (MobiWave), to advise the motorists on whether it is safe to proceed through the intersection. Hsu et al. (2014) developed an on-board system which can alert the motorists to slow down to avoid DZ according to the real time driving status, such as speed and position. Dong et al. (2014) presents a dilemma-zone (DZ) avoidance-guiding system for vehicles approaching an intersection. The purpose of the system is to assist motorists in determining the driving behavior and to prevent vehicles from being caught in DZ.

2.3 Summary of Critical Issues

This chapter illustrates current research towards the traffic bottleneck and safety studies including latest model improvements and their benefits in the future transportation system.

There're still several drawbacks need further investigation, which are summarized as follows:

1. Despite its effectiveness in reducing bus delay, implementation of TSP is usually at the cost of general traffic operational performance;
2. The key issue of conflicts between general traffic and buses has not been resolved, especially at the bus stations. Different station layouts within and across real-time crash studies pose doubts on the consistency of findings in different studies;
3. For the freeway entrances and unsignalized intersections, existing methods are unable to prevent weaving effectively; and
4. On the high-speed and unsignalized intersections, although some warning systems can remind the motorists of changing speed, while this inactive deceleration may generate other issues such as drastic speed fluctuation or long-time idling.

2.4 References

- A. Amanna. (2009). *Overview of IntelliDrive / Vehicle Infrastructure Integration (VII)*. Virginia Tech Transportation Institution.
- Abraham, A., Hassanien, A.E., Siarry, P., Engelbrecht, A. (2009). *Foundations of Computational Intelligence Volume 3: Global Optimization, 6th Edition ed.* Springer, Berlin, Germany.
- Abu-Lebdeh G. (2013). Exploring the Potential Benefits of Intellidrive-Enabled Dynamic Speed Control in Signalized Networks. *Proceeding of the 89th Annual Meeting of the Transportation Research Board*. Washington D.C.
- Ahn, K., Trani, A.A., Rakha, H., Van Aerde, M. (1999). Microscopic fuel consumption and emission models. In: *Proceedings of the 78th Annual Meeting of the Transportation Research Board*. Washington DC, USA, CD-ROM.
- Asadi, B. and A. Vahidi. (2010). Predictive Cruise Control: Utilizing Upcoming Traffic Signal Information for Improving Fuel Economy and Reducing Trip Time. *Control Systems Technology, IEEE Transactions*, 1-9.
- Authority, L.A.C.M. (2010). Congestion Management Program. *Metropolitan Transportation Authority: Los Angeles*. p. 9.
- Barth M., Mandava S., Boriboonsomsin K., Haitao Xia H.T. (2011). "Dynamic ECO-Driving for Arterial Corridors," in *Proc. IEEE Forum on Integrated and Sustainable Transportation Systems*, Vienna.
- Barth, M. and K. Boriboonsomsin.(2009). Energy and emissions impacts of a freeway-based dynamic eco-driving system. *Transportation Research Part D: Transport and Environment*,. 14. 400-410.
- Brackstone M.,(1999). Car-following: *A Historical Review*. *Transportation Research Part F*, 2, 181- 1961.
- Cassidy, M.J., Anani, S.B., Haigwood, J.M. (2002). Study of freeway traffic near an off-ramp. *Transportation Research Part A: Policy and Practice volume 36(6)*, 563-572.
- Chang, E. and M. C., (1985). Minimum delay optimization of a maximum bandwidth solution to arterial signal timing. *Transportation Research Record, Vol.1005*. 89-95.
- Chen S, Sun J, Yao J. (2011), Development and Simulation Application of a Dynamic Speed Dynamic Signal Strategy for Arterial Traffic Management. 14th *International IEEE Conference on Intelligent Transportation System (ITSC)*. IEEE. 1349-1354
- Chen, X., Qi, Y., Li, D., Wang, Y. (2014). Dual right-turn lanes in mitigating weaving conflicts at frontage road intersections in proximity to off-ramps. *Transportation Planning and Technology 37(3)*, 307-319.

- Cheu, R.L., Jin, X., Ng, K.C., Ng, Y.L., Srinivasan, D. (1998). Calibration of FRESIM for Singapore Expressway using genetic algorithm. *Journal Of Transportation Engineering-Asce* 124(6), 526-535.
- Cui, Y., S. Chen and J. Liu. (2015). Optimal Locations of Bus stations Connecting Subways near Urban Intersections. *Mathematical Problems in Engineering*. DOI: [10.1155/2015/537049](https://doi.org/10.1155/2015/537049)
- D. Dallinger., S. Gerda., and M. Wietschel M. (2013). Integration of intermittent renewable power supply using grid-connected vehicles– A 2030 case study for California and Germany. *Applied Energy* 104, pp: 666-682.
- Daganzo, C.F., Cassidy, M.J., Bertini, R.L.(1999). Possible explanations of phase transitions in highway traffic. *Transportation Research Part A: Policy and Practice* 33(5), 365–379.
- Daganzo, C.F., Laval, J., Muñoz, J.C., (2002). Ten strategies for freeway congestion mitigation with advanced technologies. University of California, Berkeley, California, USA.
- Dandrea J., (1986). Coaching the professional. *Driver Private Carrier* 23 (3),20.
- Davis S. C., Diegel S. W., Boundy R. G., (2010). “Transportation Energy Data Book,” Oak Ridge, TN,
- Denney, R.W., Curtis, E., Head, L. (2009). Long Green Times and Cycles at Congested Traffic Signals. *Transportation Research Record: Journal of the Transportation Research Board* 2128, 1-10.
- Dion, F. and B. Hellinga. (2002). A rule-based real-time traffic responsive signal control system with transit priority: application to an isolated intersection. *Transportation Research Part B: Methodological*. Vol. 36(4): p. 325-343.
- Ekeila W., Sayed T., Esawey M. E. (2009). Development of dynamic transit signal priority strategy. *Transportation Research Record: Journal of the Transportation Research Board*. pp: 1–9.
- Feng, W., Figliozzi, M., and Bertini, R. L. (2015). Quantifying the joint impacts of stop locations, signalized intersections, and traffic conditions on bus travel time. *Public Transport, Vol. 7, No. 3*, pp. 391-408.
- Fitzpatrick, K., et al. (1996). Guidelines for the location and design of bus stations, in TCRP REPORT. *Transportation Research Board of the National Academies: Washington D.C.*
- Fitzpatrick, K., et al. (1997). Location and design of bus stations, *ITE JOURNAL-INSTITUTE OF TRANSPORTATION ENGINEERS*. Vol. 67(5): p. 36-41.
- Fu, J.L.(2007). Operational research methodology and model, 6th Edition ed. *Fudan University Press*, Shanghai, China.

- Furth, P.G. and J.L. SanClemente, 2006. Near side, far side, uphill, downhill - Impact of bus station location on bus delay, in *TRANSPORTATION RESEARCH RECORD*. p: 66-73.
- Gallivan, S., Heydecker, B. (1988). Optimising the control performance of traffic signals at a single junction. *Transportation Research Part B: Methodological* 22(5), 357-370.
- Garrow, M. and R. Machemehl. (1997). Development and Evaluation of Transit Signal Priority Strategies (Technical Report). Center for Transportation Research the University of Texas at Austin 3208 Red River, Suite 200 Austin, Texas 78705-2650.
- Gu, W., et al. (2011). On the capacity of isolated, curb side bus stations. *Transportation Research Part B-Methodological*. 45(4): p. 714-723.
- Gu, W., et al. (2013). Mitigating negative impacts of near-side bus stations on cars. *Transportation Research Part B: Methodological*. 47: p. 42-56.
- Gu, W., et al. (2014). On the impacts of bus stations near signalized intersections: Models of car and bus delays. *TRANSPORTATION RESEARCH PART B-METHODOLOGICAL*. 68: p. 123-140.
- Guler S.I., Menendez M., Meier L., (2014). Using connected vehicle technology to improve the efficiency of intersections. *Transportation Research Part C Emerging Technologies*. 46, 121-131.
- Günther, G.E., Coeymans, J.E., Muoz, J.C., Herrera, J.C., 2012. Mitigating freeway off-ramp congestion: A surface streets coordinated approach. *Transportation Research Part C Emerging Technologies* 20(1), 27–43.
- H. Rakha. and R.K. Kamalanathsharma. (2011). Eco-driving at signalized intersections using V2I communication. *14th International IEEE Conference on Intelligent Transportation Systems*. Washington, DC, USA.
- Hagen, L., Lin, P.-S., Fabregas, A.D., 2006. A Toolbox for Reducing Queues at Freeway Off-Ramps. University of South Florida, Tampa, Florida, USA.
- Head, L., Gettman, D., Bullock, D.M., Urbanik, T.(2007). Modeling traffic signal operations with precedence graphs. *Transportation Research Record: Journal of the Transportation Research Board* 2035, 10-18.
- Hesham Rakha., Raj Kishore Kamalanathsharma.(2011). Eco-driving at signalized intersections using V2I communication. *14th International IEEE Conference on Intelligent Transportation Systems*, Washington, DC, USA.
- Hu, J., B. Park "Brian", and A. Parkany Emily.(2014). Transit Signal Priority with Connected Vehicle Technology. *Transportation Research Part C-Emerging Technologies*, pp. 20p.
- ITS AMERICA, (2014). The Connected Vehicle: Next Generation ITS. [Online]. Available: <http://www.itsa.org/industryforums/connectedvehicle>.

- J. Lee. and B. Park., (2012). Development and evaluation of a cooperative vehicle intersection control algorithm under the connected vehicles environment. *IEEE Trans. Intell. Transport. Syst.* 13(1), PP: 81–90.
- Jacobson, J. and Y. Sheffi. (1981). Analytical Model of Traffic Delays under Bus Signal Preemption - Theory and Application. *Transportation Research Part B-Methodological.* 15(2): p. 127-138.
- Jin, X., Cheu, R.L., Srinivasan, D. (2002). Development and adaptation of constructive probabilistic neural network in freeway incident detection. *Transportation Research Part C-Emerging Technologies* 10(2), 121-147.
- K. Dresner and P. Stone. (2008). A multiagent approach to autonomous intersection management. *J. Artif. Intell. Res.*, vol. 31, no. 1, pp. 591–656.
- Khasnabis, S., G. Reddy and B. Chaudry. (1991). Signal preemption as a priority treatment tool for transit demand management. *Vehicle Navigat. Inform. Syst.* 2. p. 1093-1111.
- Krueger, G.D., (2005). *VII Michigan Test Bed Program: Concept of Operations*, Michigan Department of Transportation, Editor.
- L. Li. and F.Y. Wang., (2006). Cooperative driving at blind crossings using intervehicle communication. *IEEE Trans. Veh. Technol.* 55(6), pp: 1712–1724.
- Lam, W.H., Poon, A.C., Mung, G.K. (1997). Integrated model for lane-use and signal-phase designs. *Journal of transportation engineering* 123(2), 114-122.
- Lee, J., Park, B., (2012). Development and evaluation of a cooperative vehicle intersection control algorithm under the connected vehicles environment. *IEEE Trans. Intell. Transport. Syst.* 13 (1), 81–90.
- Lee, S., Wong, S.C., Li, Y.C. (2015). Real-time estimation of lane-based queue lengths at isolated signalized junctions. *Transportation Research Part C: Emerging Technologies* 56, 1-17.
- Li, L., Wang, F.Y. (2006). Cooperative driving at blind crossings using intervehicle communication. *IEEE Trans. Veh. Technol.* 55 (6), 1712–1724.
- Li, Z., Chang, G.-L., Natarajan, S. (2009). Integrated Off-Ramp Control Model for Freeway Traffic Management, *Transportation Research Board 88th Annual Meeting, Washington DC*, pp. 1-12.
- Lim, K., Ju, H.K., Shin, E., Kim, D.G. (2011). A signal control model integrating arterial intersections and freeway off-ramps. *Ksce Journal of Civil Engineering* 15(2), 385-394.
- Liu, Y., and Niu, H. (2012). Simulation and analysis of traffic flow model on multi-platform harbor-style bus station. *Journal of Transportation Systems Engineering and Information Technology*, Vol. 12, No. 5, pp. 97–102.

- Liu, Y., Chang, G.L., Yu, J. (2011). An Integrated Control Model for Freeway Corridor Under Nonrecurrent Congestion. *IEEE Transactions on Vehicular Technology* 60(4), 1404 - 1418.
- Liu, Y., Li, P., Wehner, K., Yu, J. (2013). A Generalized Integrated Corridor Diversion Control Model for Freeway Incident Management. *Computer-Aided Civil And Infrastructure Engineering* 28(8), 604-620.
- Long, J., Gao, Z., Zhao, X., Lian, A., and Orenstein. P. (2011). Urban traffic jam simulation based on the cell transmission model. *Networks & Spatial Economics, Vol. 11, No. 1*, pp. 43-64.
- Lu, J., Geng, N., Chen, H. (2010). Impacts of freeway exit ramp configurations on traffic operations and safety. *Advances in Transportation Studies* 22, 5-16.
- Luis Moura, J., et al. (2012). A Two-Stage Urban Bus Station Location Model. *Networks & Spatial Economics. Vol.12(3)*: p. 403-420.
- Ma, W., et al. (2013). Effective Coordinated Optimization Model for Transit Priority Control Under Arterial Progression. *Transportation Research Record*. p. 71-83.
- Ma, W., K.L. Head and Y. Feng. (2014). Integrated optimization of transit priority operation at isolated intersections: A person-capacity-based approach. *Transportation Research Part C-Emerging Technologies. Vol.40*: p. 49-62.
- Malakorn, K.J. and B. Park. (2010). Assessment of mobility, energy, and environment impacts of IntelliDrive-based Cooperative Adaptive Cruise Control and Intelligent Traffic Signal control. in *Sustainable Systems and Technology (ISSST), 2010 IEEE International Symposium.. IEEE*.
- Markel A., Barter P. (2002). A system tool for analysis of advanced vehicle. *J Power Sources* 110, 255–66.
- Mensing, F., Trigui, R., Bideaux, E.(2011). Vehicle trajectory optimization for application in ECO-driving. In: IEEE Vehicle Power and Propulsion Conference. van der Voort, M., 2001. A prototype fuel-efficiency support tool. *Transportation Research Part C* 9, 279–296.
- Mirchandani, P., Head, L.(2001). A real-time traffic signal control system: architecture, algorithms, and analysis. *Transportation Research Part C-Emerging Technologies* 9(6), 415-432.
- Munoz, J.C., Daganzo, C.F. (2002). The bottleneck mechanism of a freeway diverge. *Transportation Research Part A: Policy and Practice* 36(6), 483-505.
- Muñoz, J.C., Laval, J.A. (2006). System optimum dynamic traffic assignment graphical solution method for a congested freeway and one destination. *Transportation Research Part B: Methodological* 40(1), 1–15.

- Newell, G.F. (1999). Delays caused by a queue at a freeway exit ramp. *Transportation Research Part B: Methodological* 33(5), 337-350.
- Ngan, V., T. Sayed, and A. Abdelfatah.(2004). Impacts of Various Parameters on Transit Signal Priority Effectiveness, *Journal of Public Transportation, Vol. 7, No. 3*, pp 71-93
- Pratt, R.H.K., et al.(2000). Traveler Response to Transportation System Changes: *Interim Handbook. TCRP Web Document.*
- Rudjanakanoknad, J.(2012). Capacity Change Mechanism of a Diverge Bottleneck. *Transportation Research Record: Journal of the Transportation Research Board* 2278, 21-30.
- S.E. Shladover. and T. M. Kuhn. (2008). Traffic Probe Data Processing for Full-Scale Deployment of Vehicle–Infrastructure Integration. *Transportation Research Record: Journal of the Transportation Research Board, No. 2086*, pp. 115–123.
- Saleem F., Nodes S.(2008). *Arizona Emergency VII (E-VII): Program Overview and Focus Areas.*
- Salter, R.J. and J. Shahi. (1979). Prediction of Effects of Bus-Priority Schemes by Using Computer Simulation Techniques. *Transportation Research Record.* p. 1-5.
- Schelenz, T., Ángel Suescun, Li, W., and Karlsson, M. A. (2013). Application of agent based simulation for evaluating a bus layout design from passengers’ perspective. *Transportation Research Part C: Emerging Technologies, Vol. 43* , pp. 222-229.
- Schrank D., Lomax T., and Turner S.(2010). *Urban Mobility Report 2010.*
- Shen, W., Zhang, H.M. (2009). On the morning commute problem in a corridor network with multiple bottlenecks: Its system-optimal traffic flow patterns and the realizing tolling scheme. *Transportation Research Part B: Methodological* 43(3), 267–284.
- Sheu, J.B., Yang, H. (2008). An integrated toll and ramp control methodology for dynamic freeway congestion management. *Physica A: Statistical Mechanics and its Applications* 387(16-17), 4327-4348.
- Skabardonis, A. (2000). Control strategies for transit priority, *in Transportation Research Record.* p. 20-26.
- Spiliopoulou, A., Kontorinaki, M., Papageorgiou, M., Kopelias, P. (2014). Macroscopic traffic flow model validation at congested freeway off-ramp areas. *Transportation Research Part C Emerging Technologies* 41, 18-29.
- Stephen, Arhin, Errol, Noel, Melissa, and Anderson, et al. (2016). Optimization of transit total bus station time models. *Journal of Traffic and Transportation Engineering, Vol. 3, No. 2*, pp. 146-153.

- Strakey J.M., Gray S., Watts D. (1988). Vehicle performance simulation and optimization including tire slip. *SAE Trans*, 881733.
- Terry, D.S. and G.J. Thomas. (1971). Farside Bus stations Are Better. *Traffic Engineering*. Vol. 41(6): p. 21-29.
- Thew R.(2007). United evidence and research strategy: driving standards agency, *CIECA*, version number 1.2.1.
- Tian, L. (2012). Traffic flow simulation in a scenario with signalized intersection and bus station. *Journal of Transportation Systems Engineering and Information Technology*, Vol. 12, No. 5, pp. 90–96.
- Tian, Z., Urbanik, T., Gibby, R. (2007). Application of diamond interchange control strategies at closely spaced intersections. *Transportation Research Record: Journal of the Transportation Research Board 2035*, 32-39.
- Tian, Z.Z., Kevin, B., Roelof, E., Larry, R. (2002). Integrated control strategies for surface street and freeway systems. *Transportation Research Record: Journal of the Transportation Research Board 1811*, 92-99.
- Tian, Z.Z., Wu, N. (2012). Probability of Capacity Enhancement and Disruption for Freeway Ramp Controls Analysis by Gap-Acceptance and Queuing Models. *Transportation Research Record: Journal of the Transportation Research Board 2278*, 1-12.
- Tielert, T., et al. (2010). The impact of traffic-light-to-vehicle communication on fuel consumption and emissions. in *Internet of Things (IOT) IEEE*.
- Toshiaki K., Takumi F.(2008). Fuel consumption analysis and prediction model for ‘Eco’ rout search. in *Proc. 15th World ITS congress*, New York.
- TRB. (2010). *Highway Capacity Manual 2010*. Transportation Research Board, Washington, DC.
- Underwood S. E., Cook S.J., and Tansil W. H. (2008). *Line of Business Strategy for Vehicle-Infrastructure Integration Part IV: History and Background*, Michigan Department of Transportation, Editor.
- USDOT, (2012). Eco-Vehicle Speed Control at Signalized Intersections Using I2V Communication. Research and Innovative Technology Administration.
- V. Milanés, J. Perez, E. Onieva, and C. Gonzalez. (2002). Controller for urban intersections based on wireless communications and fuzzy logic. *IEEE Trans. Intell. Transp. Syst.*, vol. 11, no. 1, pp. 243–248.
- Widodo, S., T. Hasegawa, and S. Tsugawa. (2002). Vehicle fuel consumption and emission estimation in environment-adaptive driving with or without inter-vehicle

- communications. in *Proceedings of the IEEE Intelligent Vehicles Symposium 2000 (Cat. No.00TH8511)*. IEEE.
- Wong, C., Wong, S. (2003). A lane-based optimization method for minimizing delay at isolated signal-controlled junctions. *Journal of Mathematical Modelling and Algorithms* 2(4), 379-406.
- Wong, C.K., Heydecker, B. (2011). Optimal allocation of turns to lanes at an isolated signal-controlled junction. *Transportation Research Part B: Methodological* 45(4), 667-681.
- Wu, G., et al. (2010). Energy and Emission Benefit Comparison of Stationary and In-Vehicle Advanced Driving Alert Systems. *Transportation Research Record: Journal of the Transportation Research Board*. 2189: p. 98-106.
- Yang, X., Lu, Y., Chang, G.L.(2014). Dynamic Signal Priority Control Strategy to Mitigate Off-Ramp Queue Spillback to Freeway Mainline Segment. *Transportation Research Record: Journal of the Transportation Research Board* 2438, 1-11.
- Yang, X.F., Cheng, Y., Chang, G.L.(2015). A multi-path progression model for synchronization of arterial traffic signals. *Transportation Research Part C-Emerging Technologies* 53, 93-111.
- Yi, Q., Chen, X., Li, D. (2012). Development of Warrants for Installation of Dual Right-Turn Lanes at Signalized Intersections. Southwest Region University Research Center, Texas, USA.
- Yu, Q., and Li, T. (2014). Evaluation of bus emissions generated near bus stations. *Atmospheric Environment*, Vol. 85, No. 2, pp. 195-203.
- Zhao, X. M., Gao, Z. Y., and Li, K. P. (2008). The capacity of two neighbor intersections considering the influence of bus station. *Physica A: Statistical Mechanics and Its Applications*, Vol. 387, No. 18, pp. 4649-4656.
- Zhong, R.X., Sumalee, A., Pan, T.L., Lam, W.H.K. (2014). Optimal and robust strategies for freeway traffic management under demand and supply uncertainties: an overview and general theory. *Transportmetrica A: Transport Science* 10(10), 849-877.
- Zohdy, I.H., Rakha, H. (2012). Game theory algorithm for intersection-based cooperative adaptive cruise control (CACC) systems. *15th IEEE International Conference on Intelligent Transportation Systems*, pp. 1097-1102.

Chapter 3 SINGLE VEHICLE-BASED TRAJECTORY OPTIMIZATION FOR CONNECTED AND AUTOMATED VEHICLES AT A SIGNALIZED INTERSECTION

This chapter develops a single vehicle-based trajectory optimization model for connected and automated vehicles at a signalized intersection. The proposed model applies when the congestion is detected given the speed, occupancy, location of approaching vehicles and signal timing information. A three-phase solution algorithm is developed to solve the model, where a multi stage based nonlinear programming procedure is developed in Phase I to search trajectories that minimizes the average travel time, while Phases II and III refine the trajectories with a mixed integer linear programming to minimize average idling time and speed fluctuation of the platoon in sequence. Illustrative examples are provided to validate the proposed model. Results indicate that it is effective to prevent congestion while minimizing average travel time, idling time and speed fluctuation. Sensitivity analyses with respect to the impact of initial speeds of the target vehicle on the speed control performance are also conducted, which may help further improve the speed guidance performance by pre-adjusting vehicle speeds before they enter the control scope.

3.1 Introduction

Signalized intersections are one of the most important elements in the urban transportation system. As cities grow in both surface and population, the signalized intersections often struggle to provide satisfying level of service due to limited road space coupled with increasing traffic demand, resulting in over-long travel time and eco-problems. In the United States, the transportation sector uses up nearly 75% of petroleum and emits the second largest carbon

dioxides due to the poor operation performance. Research findings also indicate that bad driving behaviors resulted from the severe bottlenecks constitute the major contribution to carbon emission and petroleum consumption. Traditional strategies have little effectiveness for improving the operation research around the signalized intersections. Therefore, innovative technologies are urgently needed to address these challenges.

In the past two decades, the connected and automated vehicle (CAV) technologies has been widely researched, sponsored by the U.S. DOT Research and Innovative Technology Administration (RITA)/ITS Joint Program Joint Program Office (ITS JPO), focuses on localized Vehicle-to-Vehicle, Vehicle-to-Infrastructure and Vehicle-to-Device Systems (V2X) to support safety, mobility and environmental applications. In the United States, major CAV projects have been initiated in the states of California, Michigan, and Arizona. In California, a “sniffer” working with a 170-type controller is established, combined with a message set, which provides wireless DSRC signal state information to approaching, equipped cars. Shladover and Kuhn validated the CAV probe data for adaptive signal control, incident detection and weather condition monitoring systems. In Michigan, the DOT developed a self-supporting test bed in 2005. The aim of this program is to provide a real-world laboratory to validate products and technologies related to CAV. CAV-related studies in Arizona are originally concentrated on emergency service and adaptive control strategies. For example, Samaranyake et al presented a novel air pollution estimation method that models the highway traffic state, highway traffic-induced air pollution emissions, and pollution dispersion, and describe a prototype implementation for the San Francisco Bay Area. The model is based on the availability of real-time traffic estimates on highways, which is obtained using a traffic dynamics model and an estimation algorithm that augments real-time data from both fixed sensors and probe vehicles.

M. Ramezani and N. Geroliminis integrated the collective effect of dispersed probe vehicle data with traffic flow shockwave analysis and data mining techniques to estimate queue profiles. Z. Wang et al. proposed a nonlinear model predictive control (MPC) approach for emission mitigation via longitudinal control of intelligent vehicles in a congested platoon. The proposed vehicle control strategies are tested using a series of simulations, and results verify that localized and instantaneous control of a few intelligent vehicles could reduce emissions of a platoon of vehicles.

There are a handful of studies focused on trajectory optimization for intersection operation under real-time communication. Li and Wang have proposed safe vehicular trajectories resulting in minimized delay time. Chen et al developed an algorithm assuming that vehicles are able to receive information in advance from signal lights through DSRC and alter their speeds to minimize idling at the stop line. Zohdy and Rakha developed a game theory-based algorithm to allow each single vehicle to avoid conflict and incur minimized delay for a cooperative adaptive cruise control system at an intersection. Using connected-vehicle technology, a cooperative vehicle intersection control algorithm is developed without the need signal control. Abu-Lebdeh proposed an algorithm to study the benefits of the Intellidrive technology in terms of vehicular delay. Guler et al. have proposed an algorithm to enumerate various vehicle discharging patterns before the stop line and minimize vehicular delay using the connected-vehicle technology. Wan et al. proposed a Speed Advisory System (SAS) for pre-timed traffic signals and obtained the fuel minimal driving strategy as an analytical solution to a fuel consumption minimization problem. Wei et al. developed a set of integer programming and dynamic programming models for scheduling longitudinal trajectories with both system-wide safety and throughput requirements taken into consideration. However, very limited efforts have been made for

cooperative trajectory optimization that alters vehicle arrival patterns to proactively eliminate weaving conflicts at a bottleneck. Other researches are conducted toward connected and automated vehicles at an isolated. A review of literature indicates that most previous studies on vehicular speed control algorithms are designed for individual optimization objective. However, very limited efforts have been made for cooperative trajectory optimization that alters vehicle arrival patterns to proactively eliminate bottleneck while minimizing travel time and lower down speed fluctuation and idling time.

Therefore, this study contributes to developing a platoon-based trajectory optimization model for CAV that can effectively and simultaneously shorten the average travel time, idling time and speed fluctuation of platoon through the signalized intersection (Figure 3.1). Due to the wireless communication, the real-time location and speed of each vehicle as well as the signal information can be acquired, helping predict the future traffic situation. As the left part of Figure 4.2 illustrates, if the vehicle is expected to hit the red and cannot speed up to avoid hitting, the system will guide the vehicle to slow down until the next green comes. On the contrary, if acceleration can dodge hitting red, the system will guide the vehicle to speed up and pass the stop line before the red displays.

The proposed model applies when the congestion is detected given the speed, occupancy, location of approaching vehicles and signal timing information. It enables vehicle-vehicle and vehicle-signal cooperation through a three-phase optimization process. A three-phase algorithm is developed to solve the model, where a multi-stage-based nonlinear programming (NLP) procedure is developed in Phase I to search trajectories that minimizes the average travel time, while Phases II and III refine the trajectories with the mixed integer linear programming (MILP) to minimize average idling time and speed fluctuation of the platoon in sequence.

In order to explore the benefits of entire connected and automated environment, the penetration rate of the connected and automated vehicles is set as 100%. Besides, the automation level analyzed in this chapter refer to the high automation, which means human can drive but they don't need to, as the vehicle can drive itself. Therefore, human factors such as response manipulating time can be fully neglected.

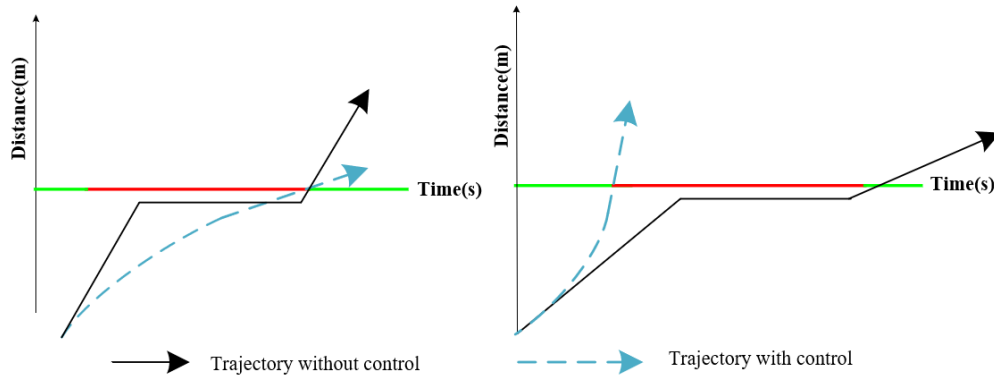


Figure 3.1 Trajectory optimization to prevent congestion.

3.2 Illustration of Control Model

3.2.1 Notation

To facilitate the presentation of model and its solution algorithm, indices and parameters used hereafter are listed in Table 3.1.

Table 3.1 Symbols and Parameters.

<i>Indices</i>	
p	Index of vehicles on a lane, $p = 1, 2, \dots$
s	Index of stages, $s = 0, 1, 2, \dots$
t	Index of times, $t = 0, 1, 2, \dots$
<i>General Constants and Variables</i>	
x_p^0	Initial distance between the stop line and the p^{th} vehicle (m)
x_{scope}	Length of the control scope (m)
x'	Initial location of the nearest downstream vehicle (m)
h_p^0	Initial headway between the p^{th} and $p-1^{th}$ ($p > 1$) vehicles (m)

h_1^0	Initial headway between the leading and its nearest downstream vehicles (m), which is assigned by a very large number if no downstream vehicles exist
v_1^0	Initial speed of the first vehicle (m/s);
l	Average vehicle length (m)
v_{min}	Minimum cruising speed (m/s)
v_{max}	Maximum speed limit (m/s)
a	Maximum acceleration rate (m/s^2)
$-d$	Maximum deceleration rate (m/s^2)
TTR	Time to red indication when the platoon enters the control scope (s), which is negative and its absolute value equals to the duration since the red light has appeared, if the signal light displays red at the instant
C	Signal cycle length (s)
r	Duration of red interval (s)
g	Duration of green interval (s)
R	Ranges of red interval
s^*	Final stage of the multi-stage-based NLP in Phase I
t_p^*	Number of decision variables of the p^{th} vehicle for MILP
I^*	Optimal average idling time (s)
$D_{p,s}$	Accumulated travel distance of the p^{th} vehicle at the s^{th} stage (m)
$d_{p,s}(t)$	Accumulated travel distance of the p^{th} vehicle at the t^{th} second within the s^{th} stage (m)
$d'_s(t)$	Accumulated travel distance of the downstream vehicle at the t^{th} second within the s^{th} stage (m)
$y_{p,s}$	Indicator for idling of the p^{th} vehicle at the s^{th} stage
$t_{p,s}$	Travel time for the p^{th} vehicle at the s^{th} stage (s)
t_{p,s^*}	Travel time of the p^{th} vehicle in the last stage s^* , using time rolling horizon method (s)
$\Delta_{p,s}$	Difference in travel time between the s^{th} and $s+I^{th}$ stages (s)
H	Time interval between two successive stages (s)
t_p	Travel time for the p^{th} vehicle to pass the intersection (s)
Decision Variables	
v_t^p	Speed of the p^{th} vehicle at the t^{th} second (m/s)
Auxiliary Variables	
I_t^p	Indicator for idling for the p^{th} vehicle at the t^{th} second
U_t^p	Indicator for speed fluctuation for the p^{th} vehicle at the t^{th} second

3.2.2 Description of Control Logic

The architecture of the control logic is depicted by a flow chart (see Figure 3.2), which is consisted of four components: (1) platoon detection; (2) bottleneck determination; (3) trajectory optimization; and (4) status tracking.

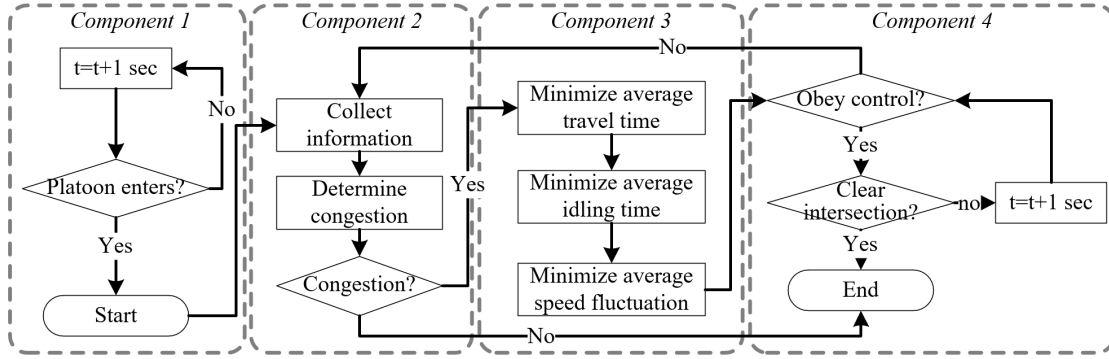


Figure 3.2 Architecture of the control logic.

Platoon Detection

This is the first step of the control mechanism that is activated when the leading vehicle of a platoon enters the control scope. Here, the control scope should be initially determined, since an over short scope cannot provide enough space for the vehicle to change its status according to the control guidance, while the over-long scope may cause waste of time and space resources.

$$\begin{cases} -\frac{1}{2d} \cdot v_{max}^2 + \frac{1}{2a} \cdot v_{max}^2 \leq x_{scope} \\ C \cdot v_{min} \geq x_{scope} \end{cases} \quad (1)$$

According to formulas (1), the control scope x_{scope} should be determined to make sure:

- 1) the vehicle has enough space to stop before the stop line;
- 2) the vehicle has enough space to accelerate to the maximum speed limit;
- 3) vehicular travel time with the minimum cruising speed to the stop line should be no greater than the cycle length when no congestion presents.

It should be noted that the platoon is defined as a list of vehicles where the headway between every two vehicles are less than 5 second. If the headway is larger than 5s, the two vehicles belong to different platoons.

Congestion Determination

The congestion is determined based on the prediction that the platoon with the current speed will be blocked by the downstream vehicles or signal control, which should be satisfied with either of the following formulas.

$$h_1^0 + x' - v_1^0 t' \leq 2v_1^0 \quad (2)$$

$$\begin{cases} TTR + \tau < \frac{x_1^0}{v_1^0} < TTR + \tau + r, & TTR \geq 0 \\ \frac{x_1^0}{v_1^0} < TTR + r \text{ or } \frac{x_1^0}{v_1^0} > TTR + c, & TTR < 0 \end{cases} \quad (3)$$

where, x' is the current location of the nearest downstream; v_1^0 is the initial speed of the first vehicle; t' is the travel time of that vehicle to clear the intersection, which could be acquired by the system control towards the downstream platoon; and TTR is time to red interval when the platoon enters the control scope, which is negative and its absolute value equals to the duration since the red light has appeared, if the signal light displays red at the instant.

If congestion is confirmed, the control logic will proceed to the next component, as optimizing trajectory of the platoon. Otherwise, the control logic will skip to the last component, as the status tracking.

Status Tracking

If no congestion will happen or the trajectory optimization is finished, the system will keep tracking the platoon status to check if the status is violated. If so, the control logic will go

back to the component of congestion determination, and re-process the following steps, until the platoon entirely clears the intersection.

3.2.3 Model Formulation

If the congestion is determined, a platoon-based trajectory optimization model will be formulated, as illustrated below.

Decision Variables

The set of decision variables is the speed profile of each vehicle inside the platoon, given by:

v_t^p = speed of the pth vehicle at the tth second (m/s).

Objective functions

The objectives of the model include: (a) minimizing the average travel time for vehicles in the platoon; (b) conditioned on the outcome of objective (a), minimizing the average idling time; and (c) conditioned on the outcomes of objectives (b) and (c), minimizing the average speed fluctuation, given by:

Objective (a):

$$\min \frac{1}{n} \sum_{p=1}^n t_p \quad (4)$$

Objective (b):

$$\max \frac{1}{n} \sum_{p=1}^n \sum_{t=1}^{t_p} I_t^p \quad (5)$$

Objective (c):

$$\min \frac{1}{n} \sum_{p=1}^n \sum_{t=1}^{t_p} U_t^p \quad (6)$$

where, t_p is the travel time of the p th vehicle; I_t^p is a binary idling indicator of the p th vehicle at the t^{th} second, given by the following formula,

$$I_t^p = \begin{cases} 0, & v_t^p = 0 \cap v_{t-1}^p = 0 \\ 1, & \text{o.w.} \end{cases}, \quad p \in [1, n]; t \in [1, t_p] \quad (7)$$

and U_s^p is a binary indicator for speed fluctuation of the vehicle the p th vehicle at the s th second, illustrated by formula (8).

$$U_t^p = \begin{cases} 0, & v_{t+1}^p - v_t^p = v_{t-1}^p - v_{t-2}^p \\ 1, & \text{o.w.} \end{cases}, \quad p \in [1, n]; t \in [2, t_p - 1] \quad (8)$$

Constraints

The general form of constraints for the model, excepting for the inner connections among those objective functions, are illustrated below.

Vehicular speed should not exceed the maximum speed, given by:

$$0 \leq v_t^p \leq v_{max}, \quad p \in [1, n]; t \in [1, t_p] \quad (9)$$

Furthermore, if the vehicle is cruising, the speed should be beyond a minimum cruising speed, given by:

$$v_t^p \geq v_{min} \text{ if } v_t^p = v_{t-1}^p, \quad p \in [1, n]; t \in [1, t_p] \quad (10)$$

Vehicular acceleration and deceleration rates should be within the reasonable range, given by:

$$-d \leq v_t^p - v_{t-1}^p \leq a, \quad p \in [1, n]; t \in [1, t_p] \quad (11)$$

A safe distance should be always kept between vehicles to avoid rear-end collision. To linearly express the constraint, the “two-second rule” rule is applied herein, which is defined as a rule of thumb by which a driver may maintain a safe trailing distance at any speed. The rule is that a driver should ideally stay at least two seconds behind any vehicle that is directly in front of his or her vehicle, given by:

$$h_p^0 + \frac{1}{2} \left(\sum_{q=1}^t v_q^{p-1} + v_{q-1}^{p-1} \right) - \frac{1}{2} \left(\sum_{q=1}^t v_q^p + v_{q-1}^p \right) \geq 2v_t^p, \quad p \in [1, n]; t \in [1, t_p] \quad (12)$$

$$h_1^0 + \frac{1}{2} \left(\sum_{q=1}^t v'_q + v'_{q-1} \right) - \frac{1}{2} \left(\sum_{q=1}^t v_q^1 + v_{q-1}^1 \right) \geq 2v_t^1, \quad p \in [1, n]; t \in [1, t_p] \quad (13)$$

Formulas (12) and (13) insure all vehicles in the platoon could keep a safe distance, where the set of v_t^1 introduced in formula (13) are the speed of the last downstream vehicle.

Red light violation shall also be completely avoided with the following formulas, as Figure 3.3 depicts.

$$\frac{1}{2} \sum_{q=1}^{r-1} v_q^p + v_{q-1}^p \leq x_p^0, \quad p \in [1, n]; r \in R \cap [1, t_p] \quad (14)$$

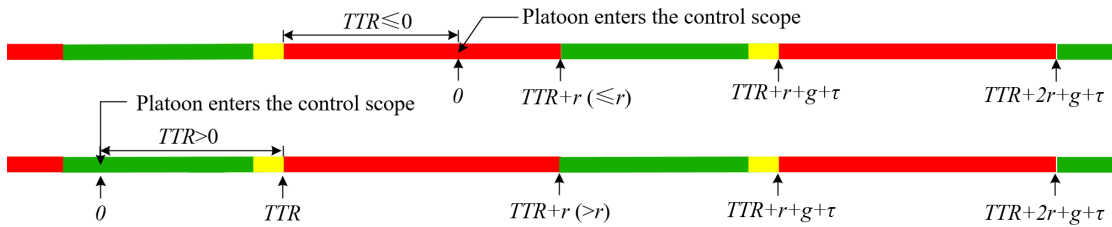


Figure 3.3 Range of red duration under various initial signal information.

Regarding formula (14), the range of R is determined by the initial signal information TTR , denoted as the time to red indication. If the signal displays red when the platoon enters the control scope, the value of TTR would be negative and its absolute value equals to the duration

since the red signal has displayed. Therefore, the remaining red duration under the current cycle can be estimated with $[0, TTR + r]$. Accordingly, the range of R at the z th cycle can be illustrated as:

$$R = [0, TTR + r] \cup [TTR + zC, TTR + r + zC], TTR \leq 0, z = 1, 2, \dots \quad (15)$$

While if the signal displays yellow or green initially, the red duration at the current cycle is estimated with $[TTR, TTR + R]$. Then the range of R at the z th cycle can be given by:

$$R = [TTR + zC, TTR + r + zC], TTR > 0, z = 1, 2, \dots \quad (16)$$

Finally, the entire platoon should clear the intersection, given by:

$$\frac{1}{2} \sum_{q=1}^{t_p} v_q^p + v_{q-1}^p \geq x_p^0, p \in [1, n]; \quad (17)$$

3.3 Solution Algorithm

3.3.1 A Three-phase algorithm

This study provides a three-phase algorithm to solve the platoon-based trajectory optimization model, whose mechanism is depicted in Figure 3.4, where Phase I features a multi-stage-based NLP to minimize the average travel time for the platoon; Phase II develops a MILP to further minimize the average idling time, conditioned on the travel time of each vehicle determined in Phase I; and Phase III advances another MILP to ultimately minimize the average speed fluctuation of the platoon, conditioned on the outcomes of Phases I and II.

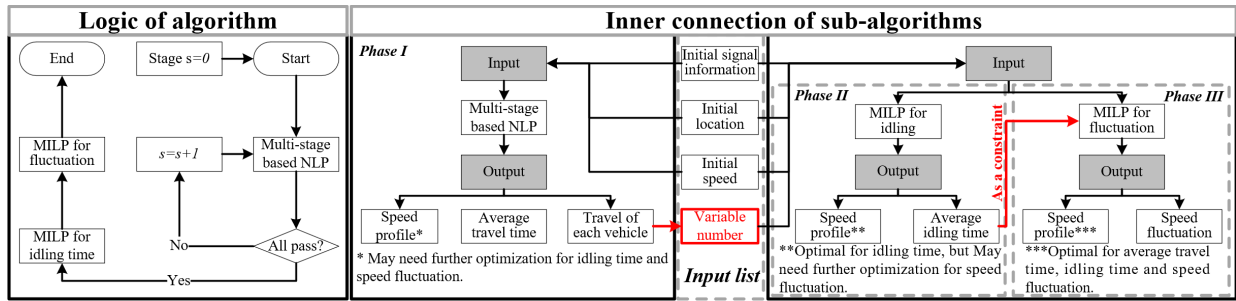


Figure 3.4 Architecture of the three-phase algorithm.

3.3.2 Minimization of average travel time

Average Travel Time Optimization-A Multi-Stage Decision Process

The estimation of travel time is based on the vehicular speed, while it is not stable during a long interval due to the fluctuating speed. Thus, it is difficult to use any “one-off” algorithm to optimize the travel time. Instead, the time rolling horizon-based algorithm applies, as the travel time can be estimated based on the feasible speed at the current stage, and it can be updated stage by stage. Accordingly, a multi-stage optimization process is developed in this study, where in each stage a NLP is used to find the optimal speed for each vehicle inside the platoon that could minimize the average travel time (Figure 3.5).

Regarding the time interval between two successive stages, denoted as H , it should be as short as possible while be sufficient for any vehicle to switch the status between idling and traveling with the maximum speed limit.

As the left part of Figure 3.4 shows, the multi-stage-based NLP is terminated when all vehicles in the platoon clear the intersection. Otherwise, it is assumed that those vehicles who have passed the stop line still participate in the optimization process.

$$D_{p,s+1} = D_{p,s} + d_{p,s}(t)|_{t=sH+H}, \quad D_{0,p} = 0 \quad (20)$$

where, $d_{p,s}(t)$ is the travel distance at the t^{th} second through the s^{th} to $s+1^{\text{th}}$ stages, estimated with:

$$d_{p,s}(t) = \begin{cases} \frac{1}{2}(v_t^p + v_{sH}^p)(t - sH), & v_t^p \neq v_{sH+H}^p \\ \frac{v_{sH+H}^p{}^2 - v_{sH}^p{}^2}{2m_s^p} + v_{sH+H} \left(t - sH - \frac{v_{sH+H}^p - v_{sH}^p}{2m_s^p} \right), & v_t^p = v_{sH+H}^p \end{cases} \quad (21)$$

Update travel time

The multi-stage-based estimation of travel time is illustrated in Figure 3.5. At the s^{th} stage, it can be estimated with:

$$t_{p,s} = \begin{cases} \frac{x_p^0 - D_{p,s}}{v_t^p + y_t^p} + sH, & s > 0, \\ 0, & s = 0 \end{cases}, \quad t = sH \quad (22)$$

where, y_t^p is an indicator for the idling speed given by the following formula. If v_t^p is zero, the travel time will be assigned by a very large number.

$$y_t^p = \begin{cases} 0, & v_t > 0 \\ 0.0001, & v_t = 0 \end{cases} \quad t = sH; s > 0 \quad (23)$$

It can be found from formula (22) that if at the s^{th} stage the vehicle has already cleared the intersection, the value $x^0 - D_s$ is negative, resulting in the travel time is less than sH .

Given the travel time at the s^{th} stage, it can be updated at the $s+1^{\text{th}}$ stage with:

$$t_{p,s+1} = t_{p,s} + \Delta t_{p,s} \quad (24)$$

where,

$$\Delta t_{p,s} = \begin{cases} \frac{x_p^0 - D_{p,s} - d_{p,s}(t)}{v_t^p + y_t^p} - \frac{x^0 - D_{p,s}}{v_{t-H}^p + y_{t-H}^p} + H, & s > 0 \\ \frac{x_p^0 - D_{p,s} - d_{p,s}(t)}{v_t^p + y_t^p} + H, & s = 0 \end{cases}, \quad t = sH + H \quad (25)$$

Then, the update of average travel time for the platoon is given by:

$$T_{p,s+1} = T_{p,s} + \frac{1}{n} \sum_{p=1}^n \Delta t_{p,s}, \quad s > 0 \quad (26)$$

3.3.4 Objective Function

The objective of the multi-stage-based NLP is to minimize the average travel time stage by stage.

At the $s+1^{\text{th}}$ stage, the objective function can be given by:

$$\min \left(T_s + \frac{1}{n} \sum_{p=1}^n \Delta t_{p,s} \right) \quad (27)$$

Essentially, it can be converted to:

$$\min \frac{1}{n} \sum_{p=1}^n \left(\frac{x_p^0 - D_{p,s}^* - d_{s,p}(t)}{v_t^p + z_{p,t}} \right), \quad t = sH + H \quad (28)$$

where, $D_{p,s}^*$ is the optimized accumulated travel distance at the s^{th} stage, and $z_{p,t}$ is an indicator to determine if the travel time should be assigned by a very large value, given by:

$$z_{p,t} = \begin{cases} 0, & v_t^p > 0 \\ 0.0001, & v_t^p = 0 \end{cases}, \quad t = sH + H \quad (29)$$

The multi-stage-based NLP is terminated at the s^* th stage when all vehicles have cleared the intersection. The final stage s^* should satisfy the following formula.

$$D_{p,s^*} > x_p^0, \quad \forall p \quad (30)$$

3.3.5 Constraints

The constraints of the model, illustrated from formulas (9) to (17), should be converted to the stage-based form, as shown in follows.

Constraint of speed limit, given by:

$$0 \leq v_t^p \leq v_{max}, \quad p \in [2, n]; t = sH + H \quad (31)$$

Constraint of cruising speed limit, illustrated by formula (10), can eliminate the “if” condition, illustrated as:

$$v_t^p \geq v_{min}, \quad p \in [2, n]; t = sH + H \quad (32)$$

Constraint of acceleration/deceleration can be loosened herein, as the process of speed update has been determined.

Constraint of safe distance maintenance, illustrated by formulas (12) and (13), can be converted as:

$$h_p^0 + D_{p-1,s}^* + d_{p-1,s}(t) - D_{p-1,s}^* - d_{p-1,s}(t) \geq 2v_t^p, \quad (33)$$

$$p \in [2, n]; t = sH + H, sH + H + 1, \dots \quad (34)$$

$$h_1^0 + D_s' + d_s'(t) - D_{1,s}^* - d_{1,s}(t) \geq 2v_t^1, \quad t = sH + H, sH + H + 1, \dots$$

Constraint of red violation prevention, illustrated by formula (14), should be added a condition that the constraint only works if the vehicle at the previous stage does not exceed the stop line, given by:

$$D_{p,s-1}^* + d_{p,s}(t) \leq x_p^0 \text{ if } D_{p,s-1}^* \leq x_p^0, \quad t \in [sH + H, sH + H + 1, \dots] \cap R \quad (35)$$

Constraint of clearing the intersection can be loosened here, as it is the condition for terminating the multi-stage-based NLP.

3.4 MILP for Further Optimization

3.4.1 Further Optimization of Vehicular Trajectories-A Linear Process

Although Phase I would generate the speed profiles that could minimize the average travel time, they may not be optimal for idling time and speed fluctuation (See Figure 3.6 for illustration).

Therefore, Phases II and III are introduced to further minimize the idling time and speed fluctuation in sequence. These optimization processes could be fulfilled by MILP, as both the objective functions and constraints could be expressed linearly. Another reason is the travel time is determined by Phase I, which means the number of decision variables can be acquired, given by:

$$t_p^* = \lfloor t_{p,s^*} \rfloor + 1 \quad (36)$$

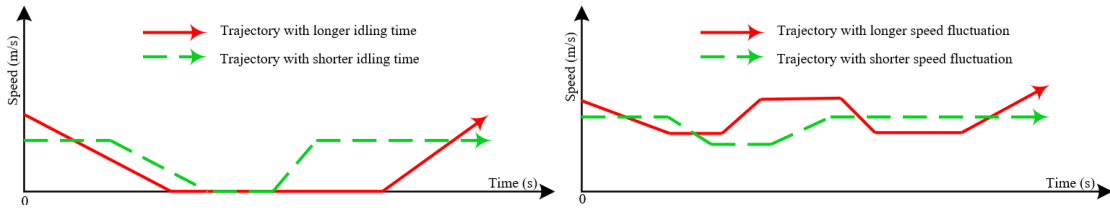


Figure 3.6 Patterns of over-long idling time and speed fluctuation.

Accordingly, the time interval between the last two decision variables is $t_{p,s^*} + 1 - t_p^*$, instead of one second. Then the accumulated travel distance can be linearly estimated with:

$$d_{p,t} = \begin{cases} \frac{1}{2} \sum_{q=0}^{t-1} v_q^p + v_{q-1}^p, & t < t_p^* \\ \frac{1}{2} (v_{t_p^*}^p + v_{t_p^*-1}^p) (t_{p,s^*} + 1 - t_p^*) + \frac{1}{2} \sum_{q=0}^{t_p^*-1} v_q^p + v_{q-1}^p, & t = t_p^* \end{cases} \quad (37)$$

The objective function for average idling time is given by:

$$\max \frac{1}{n} \sum_{t=1}^{t_p^*} I_t^p \quad (38)$$

The objective functions for average speed fluctuation conditions on the outcomes of optimization of average idling time, given by:

$$\max \frac{1}{n} \sum_{t=1}^{t_p^*} U_t^p \quad \text{s. t.} \quad \sum_{t=1}^{t_p^*} I_t^p = I^* \quad (39)$$

where, I^* is the outcome of formula (38).

3.4.2 Constraints

The constraints shared by the two MILP include those depicted in the model section, while they should be converted to the linear form so that they can be used herein, as illustrated below.

The constraints of speed limit, acceleration/deceleration limit, and safe distance maintenance, illustrated by formulas (9), (11), (12) and (13), can be directly used, while for cruising speed limit, as formula (10) shows, should be converted to the linear form, given by:

$$(v_t^p - v_{min})M_1 \geq (v_t^p - v_{t-1}^p) - \alpha_t^p M, \quad , \quad p \in [1, n]; t \in [1, t_p^*] \quad (40)$$

$$(v_t^p - v_{min})M_1 \geq (v_{t-1}^p - v_t^p) - (1 - \alpha_t^p)M, \quad p \in [1, n]; t \in [1, t_p^*] \quad (41)$$

From formulas (40) and (41), two large positive penalty constants M and M_1 ($M \gg M_1$), together with the binary variable α_t , are used to get the rid of the “if-else” condition.

The constraint of red violation avoidance, given by formula (14), should be converted with:

$$(d_{p,t} - x_0^p)M_1 \leq (d_{p,t-1} - x_0^p) - \beta_t^p M, \quad p \in [1, n]; t \in [1, t_p^*] \quad (42)$$

$$(d_{p,t} - x_0^p)M_1 \geq (\beta_t^p - 1)M + M_1, \quad p \in [1, n]; t \in [1, t_p^*] \quad (43)$$

In Formulas (42) and (43), the binary variable β_t , together with the large penalty constants M and M_1 can linearly express the “if” condition.

The constraint of clearing the intersection by formula (12), should be added an additional formula to ensure the value of last speed variable is greater than zero, given by:

$$\frac{1}{2} \sum_{q=1}^{t_p^*} v_q^p + v_{q-1}^p \geq x_0^p, \quad p \in [1, n] \quad (44)$$

$$v_{t_p^*}^p M \geq M_1, \quad p \in [1, n] \quad (45)$$

Finally, the definitions of I_t^p and U_t^p , given by formulas (43) and (44), should also be converted to linear forms, given by:

$$0 \leq I_t^p \leq 1, \quad p \in [1, n]; t \in [1, t_p^*] \quad (46)$$

$$I_t^p \leq (v_t^p + v_{t-1}^p)M, \quad p \in [1, n]; t \in [1, t_p^*] \quad (47)$$

$$(1 - I_t^p)M_1 \leq \gamma_t^p M, \quad p \in [1, n]; t \in [1, t_p^*] \quad (48)$$

$$(v_t^p + v_{t-1}^p)M_1 \leq (1 - \gamma_t^p)M, \quad p \in [1, n]; t \in [1, t_p^*] \quad (49)$$

$$0 \leq U_t^p \leq 1, \quad p \in [1, n]; t \in [1, t_p^*] \quad (50)$$

$$(1 - U_t^p)M \leq (v_{t+1}^p - v_t^p - v_{t-1}^p + v_{t-2}^p)M_1 + \delta_t^p M, \quad p \in [1, n]; t \in [1, t_p^*] \quad (51)$$

$$U_t^p M_1 \leq (1 - \delta_t^p)M, \quad p \in [1, n]; t \in [1, t_p^*] \quad (52)$$

$$(v_{t+1}^p - v_t^p - v_{t-1}^p + v_{t-2}^p)M_1 \leq \delta_t^p M, \quad p \in [1, n]; t \in [1, t_p^*] \quad (53)$$

$$-(v_{t+1}^p - v_t^p - v_{t-1}^p + v_{t-2}^p)M_1 \leq \delta_t^p M, \quad p \in [1, n]; t \in [1, t_p^*] \quad (54)$$

$$(v_{t+1}^p - v_t^p - v_{t-1}^p + v_{t-2}^p)M_1 + \varepsilon_t^p M \geq \delta_t^p, \quad p \in [1, n]; t \in [1, t_p^*] \quad (55)$$

$$(v_{t+1}^p - v_t^p - v_{t-1}^p + v_{t-2}^p)M_1 + (1 - \varepsilon_t^p)M \geq \delta_t^p, \quad p \in [1, n]; t \in [1, t_p^*] \quad (56)$$

Formulas (46) to (49) use M , M_1 and a binary variable γ_t^p to linearly express the values of I_t^p . While from formulas (50) to (56), two binary variables δ_t^p and ε_t^p , together with M and M_1 , linear express the definition of U_t^p .

3.5 AN ILLUSTRATIVE EXAMPLE

3.5.1 Scenarios Establishment

In this section, some examples are illustrated to validate the proposed platoon-based trajectory optimization model. Ten vehicles are selected to form a platoon and various scenarios are established related to TTR. We chose ten vehicles because we think ten vehicles of platoon has an appropriate length. We need to consider two limitations: overlong platoon may cause delay for more than two cycles; and over short platoon cannot reflect all the benefits of the speed control.

The parameter settings in this example are summarized in Table 3.2. Note that the initial speed and headway of each vehicle in the platoon are set as identical.

Table 3.2 Summary of Parameter Settings.

Parameter s	Denotation	Scenarios		
		Scenario 1	Scenario 2	Scenario 3
x_{scope}	Control Scope (m)	200	200	200
x'	Location of downstream vehicle	100	-	85
l	Average vehicle length (m)	6	6	6
h_p^0	Headway (Identical) (m)	21	21	21
v_0^p	Initial speed (Identical)	12	10	10
v_0'	Initial speed of downstream vehicle (m/s)	10	-	0
v_{min}	Minimum cruising speed (m/s)	6	6	6
v_{max}	Maximum speed limit (m/s)	17	17	17
a	Maximum acceleration rate (m/s)	2.8	2.8	2.8
$-d$	Maximum deceleration rate (m/s)	-1.4	-1.4	-1.4
TTR	Time to red (s)	15	20	-35
r	Red interval (s)	60	60	60
g	Green interval (s)	30	30	30
τ	Yellow interval (s)	5	5	5

3.5.2 Evaluation of Travel Time

In this section, the travel time of each vehicle and the average travel time of the platoon under

the control and non-control environments are compared with three scenarios (Figure 3.7). Here, the control environment refers to speed control and therefore, non-control refers to no speed control. Since we are tracking a whole platoon when it is approaching the intersection, there will be only three results, when the speed control is needed: (1) the whole platoon accelerates to pass the intersection before the red light displays; (2) the whole platoon decelerates until the next green interval comes, and then passes the intersection; and (3) the platoon is divided into two sub-platoons, the downstream of which accelerates to pass the intersection, and the upstream of which slows down or even stop until the next green displays. According to the above results, we designed three relative scenarios.

It can be illustrated that Scenario 1 shows significant difference in travel times for the leading and second vehicles of the platoon approaching the intersection under control and non-control environments. Such a difference is due to the fact that those vehicles under control passes the intersection without obstruction from the red light or downstream vehicles when following the control. Nonetheless, without the control the vehicles may experience the process of cruising, deceleration, and idling, resulting in much longer travel time. In Scenario 2, the second and third vehicles experience the similar situation as that in Scenario 1, while the difference in travel time for the leading vehicle is not significant, as even without control the leading vehicle could clear the intersection with no blockage. For other samples, the difference in travel time is due to the elimination of loss time under the control, as no idling happens. In summary, the average travel time of the platoon with the control is shorter than the one without the control.

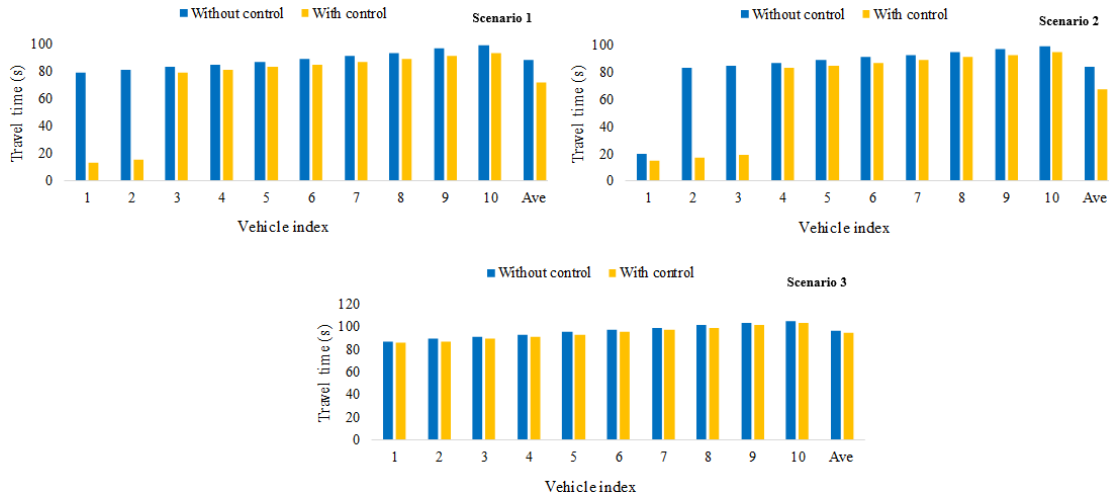


Figure 3.7 Comparison of travel time under the control and non-control environments with various scenarios.

Figure 3.8 further depicts the trajectory of each vehicle under the control environment. For scenarios 1 and 2, the platoon is divided into sub-platoons where the leading one accelerate to clear the intersection while the following one decelerate until the next green interval come. For scenario 3, the idling downstream vehicle let the whole platoon entirely decelerate to clear the intersection without idling.

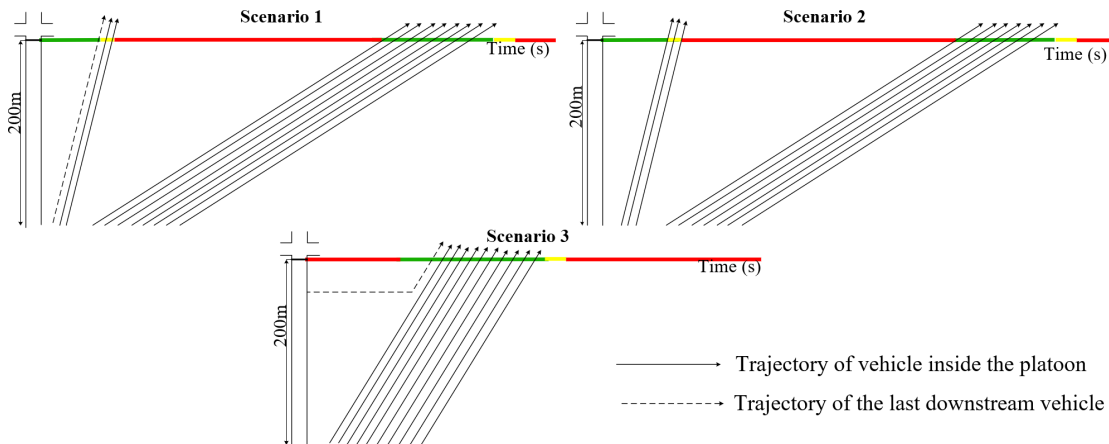


Figure 3.8 Trajectory of platoon under the control environment with various scenarios.

3.5.3 Evaluation of Idling Time and Speed Fluctuation

The idling time and speed fluctuation of each vehicle and the average values with various scenarios are compared under the control and non-control environments (Table 3.3). Note that all values are set as integer. The results indicate that under the control environment, the idling time and speed fluctuation of each vehicle have significant improvement, compared with the those under non-control environment. Furthermore, the average idling time and speed fluctuation of platoon under the control environment are also lower than those without control.

Table 3.3 Comparison of Idling Time and Speed Fluctuation Under the Control and Non-Control Environments.

Vehicle index	Scenarios											
	Scenario 1				Scenario 2				Scenario 3			
	Idling time (s)		Speed fluctuation (times)		Idling time (s)		Speed fluctuation (times)		Idling time (s)		Speed fluctuation (times)	
	With control	Without control	With control	Without control	With control	Without control	With control	Without control	With control	Without control	With control	Without control
1	0	45	1	2	0	0	1	3	0	0	1	3
2	0	44	1	3	0	61	1	2	0	0	1	3
3	0	44	1	3	0	61	1	2	0	0	1	4
4	0	44	1	2	0	62	1	3	0	27	1	3
5	0	43	1	3	0	62	1	3	0	27	1	3
6	0	43	1	3	0	62	1	2	0	26	1	2
7	0	42	1	2	0	62	1	3	0	26	1	2
8	0	42	1	3	0	61	1	1	0	26	1	3
9	0	44	1	3	0	61	1	1	0	26	1	2
10	0	42	1	2	0	61	1	1	0	26	1	2
Ave	0	43	1	3	0	61	1	2	0	26	1	3

To further explore the benefits of lower idling time and speed fluctuation, this study utilizes the VT-micro model to compare the fuel consumption of the platoon under the control and non-control environments.

This research adopts the microscopic fuel consumption and emission model, the VT-micro Model, as it has been proved to be accurate and easy for calibration. The model is given by:

$$MOE_e = \exp\left(\sum_{i=1}^3 \sum_{j=1}^3 L_{i,j}^e v^i a^j\right) \quad (57)$$

where, MOE_e is the instantaneous fuel consumption rate; $L_{i,j}^e$ are the model coefficients for MOE_e at speed power i and acceleration power j ; v is the instantaneous speed; and a is the instantaneous acceleration rate.

The results are depicted by Figures 3.9 and 4.10.

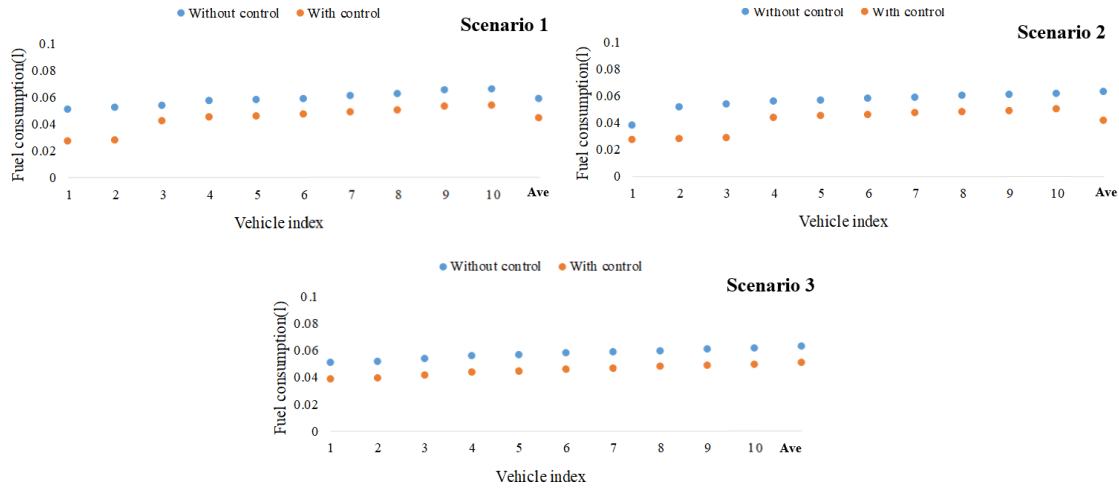


Figure 3.9 Trajectory of platoon under the control environment with various scenarios.

It can be illustrated by Figure 3.9 that in Scenario 1 the leading and second vehicle consume much lower fuel with control, compared with that under non-control environment, due to the significant difference in travel time. The second and third vehicles in Scenario 2 have the similar situation.

For other results, the fuel consumption under the control environment is still lower, due to the optimal idling time and speed fluctuation. The difference in fuel consumption for those samples is not as huge as the previous one, as the travel time with and without control are close.

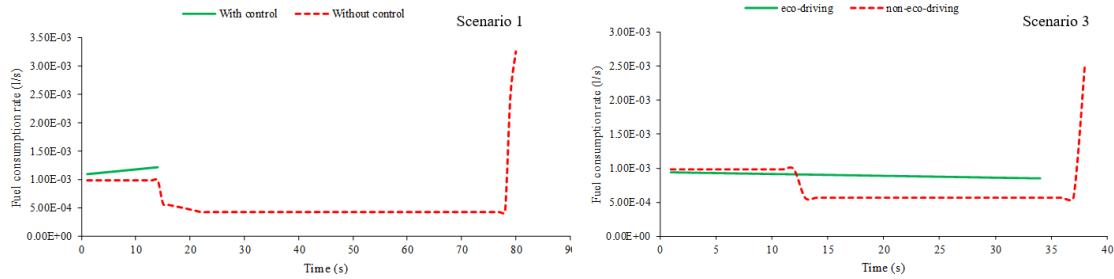


Figure 3.10 Fuel consumption rate for the leading vehicle with and without control in scenarios 1 and 3.

Figure 3.10 discusses the fuel consumption rate of the leading vehicle in Scenarios 1 and 3 in detail (Scenario 2 is neglected here as it is similar to Scenario 1). It can be found that the fuel consumption trajectory of the vehicle undergoing control is smoother than the one without control. For Scenario 1, the fuel consumption curve with control ends much earlier, compared with that without control, resulting in significant energy save. While for Scenario 2, the curve without control ends a little bit later than the one with control, due to the loss time. Furthermore, for the curve without control, as the vehicle aggressively accelerates to pass the intersection, a peak emerges at the end.

3.5.4 Sensitivity Analysis

In this section, a sensitivity analysis is designed to explore the level of average travel time with different initial platoon speed (assume all vehicular speeds are identical), which may further improve the control performance by pre-adjusting the platoon's speed before it enters the control

scope. The average travel time with initial speeds ranging from 6 m/s to 16 m/s with increment step size of 1 m/s, under Scenarios 1 and 3, are summarized in Figure 3.11.

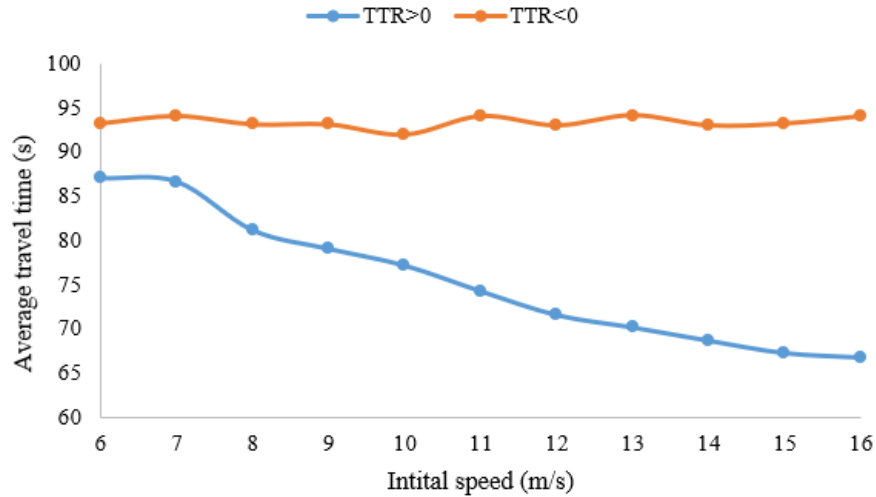


Figure 3.11 Impact of initial speeds on average travel time.

As shown in Figure 3.11, when the signal initially displays green, as $TTR > 0$, the average travel time of platoon declines with the increase of its initial speed. This is probably due to the fact that the higher the initial speed the higher the flexibility for the target vehicle to adjust its speed to avoid blockage by signal control. Nonetheless, if $TTR < 0$, the initial speed seems have little impact on the average travel time, due to the inevitable blockage by signal control.

3.6 Conclusions

This chapter proposes a single vehicle-based trajectory optimization control model for CAV at a signalized intersection. The initial objective of the model is to minimize the average travel time of the platoon. Then, based on the optimal travel time, the speed trajectory of each vehicle is further optimized to minimize the average idling time and speed fluctuation in sequence. A three-phased algorithm is proposed to solve the model, where Phase I features a multi-stage-based NLP to minimize the average travel time for the platoon; Phase II develops a MILP to

further minimize the average idling time, conditioned on the travel time of each vehicle determined in Phase I; and Phase III advances another MILP to ultimately minimize the average speed fluctuation of the platoon, conditioned on the outcomes of Phases I and II.

This study provides several illustrative examples to validate the control model. Firstly, the study compares the travel time of each vehicle in the platoon and the resulted average travel time with and without the control. Results show that both the vehicular travel time and platoon's average travel time decrease significantly. Secondly, this study compares the fuel consumption of each vehicle and the average value of the platoon under the control and non-control environments. Results indicate that due to the lower travel time, idling time and speed fluctuation, the fuel consumption with control is significantly lower than that without control. Furthermore, the time-varying fuel consumption of the leading vehicle in the platoon with respect to control and non-control environments are compared and the fuel consumption curve under control is much smoother. Finally, this study compares the level of average travel time under different initial speeds of a platoon. Results show that when signal displays green initially, the average travel time declines with the increase of initial speed, while no obvious relationship is found when the signal initially displays red. Such findings may help further improve the speed guidance performance by pre-adjusting vehicle speeds before they enter the control scope.

Analysis results of the illustrative examples indicate the validity and effectiveness of the proposed control model. On-going work of this study is to test the model in real-world CAV systems.

Chapter 4 A PLATOON-BASED SPEED CONTROL ALGORITHM AT A SIGNALIZED INTERSECTION

This chapter extends the model in Chapter 3 by proposing a dynamic speed control algorithm for a platoon of vehicles at a signalized intersection to mitigate traffic bottleneck. Both the running status of the target platoon and the impact of the anterior platoon are considered and analyzed. Acceleration/deceleration profile, instead of speed trajectories, is used in this research as the optimization objective to prevent drivers from idling and to let them clear the intersection during the green light as possible as they can. When a platoon is mixed with vehicles obeying or disobeying the system's guidance, the proposed algorithm will group those vehicles into new platoons according to their permutations. Three illustrative examples are provided to validate the proposed algorithm using fuel consumption as the measuring standard. Results indicate that when the platoon needs to accelerate to pass the intersection, a smaller headway causes less fuel consumption; while a larger headway results in less fuel consumption if vehicles decelerate to pass the intersection. In addition, the leading vehicle is found to consume more fuel if it disobeys the system's advice, but if the leading vehicle obeys the system's advice, it is found that the fuel consumption for the following vehicles, even disobeying the advice, may not increase obviously.

4.1 Introduction

In recent years, public attention to the environmental pollution and energy shortage is growing rapidly. In the United States, the transportation sector uses up nearly 75% of petroleum and emits the second largest carbon dioxides. Research findings indicate that urban node bottlenecks constitute the major contribution to carbon emission and petroleum consumption...

In the past two decades, wireless communication technologies have been widely used in the transportation system. As a part of Intelligent Transportation Systems, the Connected-vehicle program (formerly called VII or Intellidrive), sponsored by the U.S. DOT Research and Innovative Technology Administration (RITA)/ITS Joint Program Joint Program Office (ITS JPO), focuses on localized Vehicle-to-Vehicle, Vehicle-to-Infrastructure and Vehicle-to-Device Systems (V2X) to support safety, mobility and environmental applications using vehicle Dedicated Short Range Communications (DSRC)/Wireless Access for Vehicular Environments (WAVE). In US, major Connected-vehicle projects have been initiated in the states of California, Michigan, and Arizona. In California, a “sniffer” working with a 170-type controller (and conceivably with any controller) is established, combined with a message set, which provides wireless DSRC signal state information to approaching, equipped cars. Michigan DOT started developing a self-supporting test bed info-structure in 2005. The aim of this program is to provide a real-world laboratory to test products and technologies related to Connected-vehicle. It aims to provide a geographically scalable system that adopts national standards and is coordinated by USDOT’s Connected-vehicle Consortium. Connected-vehicle-related activities in Arizona are focused on supporting emergency responders and incident management activities. The Emergency VII (E-VII) program has identified four key capabilities to improve incident response.

Leveraging the DSRC technology, approaching vehicles’ speeds, positions, and other information with signal data could be obtained at a signalized intersection. Such technologies offer the possibility for vehicles to receive advanced information from signal lights and alter speed trajectories to minimize idling at the stop line of signalized intersection (18-20). Figure 4.1 shows the operational process of this technology. Two pictures at the bottom of Figure 4.1

illustrate the concept of dynamic speed control that prevents vehicles from idling. In the left picture, the vehicle follows the system's advice to decelerate gradually to pass the intersection and then accelerate back to the original speed. In the right picture, the vehicle accelerates to cross the stop bar and then decelerates back to its original speed.

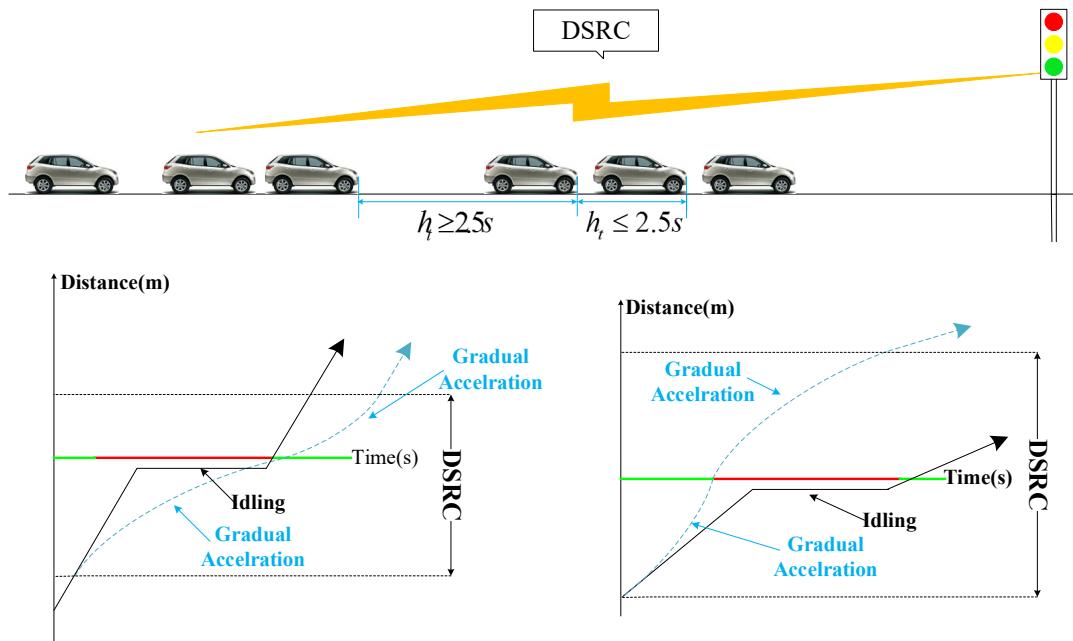


Figure 4.1 Dynamic speed control using V2X.

Many studies in this regard aim at minimizing vehicular delay time; hence the speed trajectories recommended may not be the best for saving fuel consumption and emission. In 2012, the RITA released a report on eco-driving by controlling speed trajectories of vehicles using V2I technology. In this report, multiple scenarios are studied at intersections according to the upcoming signal changing information and vehicle's position and speed. In addition to an isolated intersection, an algorithm for vehicles moving along a signalized arterial is also developed and tested by simulations.

A review of the literature indicates that previous research efforts, focused on minimizing fuel consumption or vehicular delay, lack consideration of many real-world operational

constraints. For example, a platoon rather than a single vehicle shall be considered during speed control. Also, it is necessary to consider the impact of vehicles' in compliance to speed guidance as well as the interactions among platoons.

As an extension, this research contributes to developing a dynamic speed control algorithm to mitigate traffic bottleneck in the measure of fuel consumption, by optimizing the acceleration/deceleration profile for a platoon consisting of obedient and disobedient vehicles rather than the speed trajectories of only one vehicle. Furthermore, besides the signal timing and phasing information, we also analyze the impact of the anterior platoon (for example, queued vehicles) in detail. Finally, this research compares the results of fuel consumption under different headways and permutations (different positions of obedient and disobedient vehicles). Illustrative examples will be provided to validate the proposed algorithm.

4.2 Methodology

4.2.1 Various speed trajectories under the same travel time

Figure 4.2 shows two time-space diagrams representing an acceleration scenario and a deceleration scenario for a single vehicle traverse a signalized intersection. In part (a), the driver needs to accelerate to pass the stop line, while the driver in part (b) needs to decelerate until the signal light turns green, if he/she hopes to avoid idling.

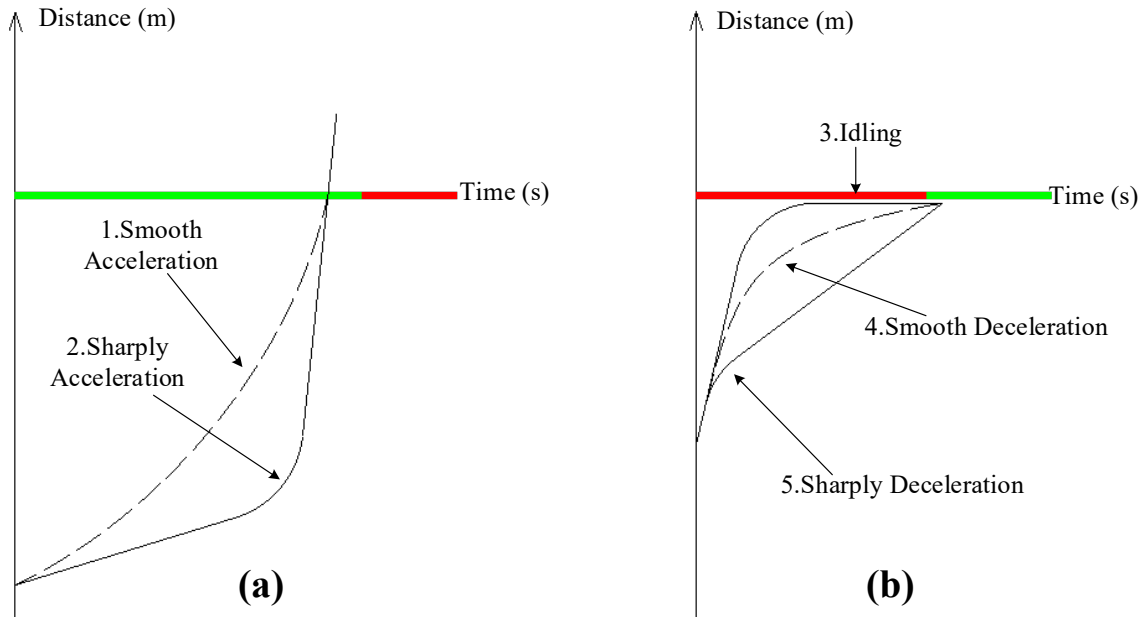


Figure 4.2 Speed trajectories of a single vehicle under different scenarios.

Figure 4.2 indicates five types of speed trajectories corresponding to the acceleration and deceleration scenarios, given by:

- Type 1: The driver accelerates smoothly to pass the stop line during green when he/she knows the possibility of hitting the red light if keeping his/her original speed;
- Type 2: The driver accelerates sharply near the stop line and clears the intersection during the green light;
- Type 3: The driver cruises at the original speed and idles until the signal light turns green;
- Type 4: The driver decelerates smoothly to pass the stop line when the signal light just turns green; and
- Type 5: The driver decelerates sharply at first and cruises the remaining distance until the signal light turns green.

For the same travel distances, the above five speed trajectories result in different levels of fuel consumption. In part (a), the Type 2 trajectory results in more fuel consumption than Type

1. Similarly, the Type 4 trajectory consumes less fuel than the Type 3 and Type 5 in part (b). It is considered that the Type 1 trajectory and the Type 4 trajectory are optimal trajectories for fuel consumption, which encourage drivers to keep a gradual acceleration/deceleration status to pass the stop line during green, rather than accelerating/decelerating sharply (see Figure 4.3 for comparison).

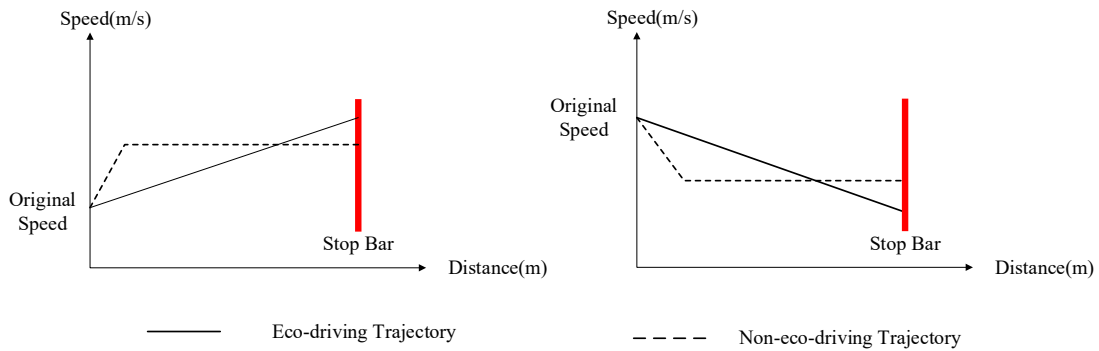


Figure 4.3 Comparison between optimal speed and non-optimal speed trajectories under the same travel time.

It should be noted that there might be a special case where drivers have options to choose Type 1 trajectory and Type 4 trajectory at the same time. In this situation, Type 1 trajectory is suggested due to its savings in travel time.

4.2.2 Assumptions

The following assumptions need to be made to develop the dynamic speed control algorithm in this chapter:

Assumption 1: A platoon of vehicles is divided into two groups, the “obedient vehicles” (OV) and “disobedient vehicles” (DOV). Both groups of vehicles can accomplish real-time communication with infrastructures (V2I) and among themselves (V2V);

Assumption 2: When an OV follows another OV or a DOV, there exist no car-following behavior; when a DOV follows a DOV or an OV, it follows a car-following model.

Assumption 3: When two OVs alter their speeds according to the same speed guidance, they make alterations simultaneously, which means the space/time headway between them is unchanged;

Assumption 4: Effective green and red time used, and the amber time is not considered; and

Assumption 5: Vehicles in a platoon share the same speeds and space headways until they change their running situations.

4.2.3 Acceleration/deceleration models

In order to reach the target speed, the vehicle needs to accelerate or decelerate from its original speed. In this study, we consider a vehicle maintains a constant acceleration/deceleration rate during its speed alteration process, given by:

$$a_n = \frac{v_t - v_0}{t} \quad (1)$$

$$d_n = \frac{v_t - v_0}{t} \quad (2)$$

where, v_0 is the vehicle's original speed; v_t is the target speed, t is the time for acceleration/deceleration; a_n is the acceleration rate for the n th vehicle and d_n is the deceleration rate for the n th vehicle. In this study, the acceleration/deceleration rates are used as the optimization objectives for speed control of a platoon of vehicles.

4.2.4 Car-following model

According to Assumption 2, when a DOV follows a DOV or an OV, a car-following model applies. This chapter chooses the linear GM car-following model (23) due to its simplicity, accuracy and sensibility. The model is given by:

$$a_{n+1}(t + T) = \lambda[v_n(t) - v_{n+1}(t)] \quad (3)$$

where a_{n+1} is the acceleration rate for the $(n+1)^{\text{th}}$ vehicle at the time $(t + T)$; λ is denoted as the sensitivity coefficient; $v_n(t)$ and $v_{n+1}(t)$ are speeds for the n^{th} vehicle and the $(n+1)^{\text{th}}$ vehicle at the time t , respectively. Note that the proposed speed control algorithm offers the flexibility to accommodate other forms of car-following models.

4.2.5 Fuel consumption model

This research adopts the microscopic fuel consumption model, the VT-CPFM-1 Model, as it has been proved to be simple, accurate, and easy for calibration. The model is given by:

$$MOE_e = \begin{cases} \exp\left(\sum_{i=1}^3 \sum_{j=1}^3 L_{i,j}^e v^i a^j\right) & \text{for } a \geq 0 \\ \exp\left(\sum_{i=1}^3 \sum_{j=1}^3 M_{i,j}^e v^i a^j\right) & \text{for } a < 0 \end{cases} \quad (4)$$

where, MOE_e is the instantaneous fuel consumption rate (l/s); $L_{i,j}^e$ are the model coefficients for MOE_e at speed power i and acceleration power j under positive acceleration; $M_{i,j}^e$ is the model coefficients for MOE_e at speed power i and acceleration power j under negative acceleration; v is the instantaneous speed (m/s); and a is the instantaneous acceleration rate (m/s^2).

4.2.6 Impact of anterior platoon and signal timing

When the target platoon enters the communication area, the system shall first judge whether the target platoon needs speed control. The system leverages the DSRC to make real-time communication between vehicles and the infrastructure and among vehicles. Information about the anterior vehicle platoon is also used to determine whether the target vehicle platoon requires speed control or not. The interactions between the target platoon and its anterior platoon are

illustrated in Figure 4.4, in which the solid arrows represent vehicles in the target platoon, and the dotted arrows represent vehicles in the anterior platoon. A total of four cases are analyzed.

Case 1 and Case 2 show that vehicles in the target platoon are not affected by the anterior platoon and the signal timing, resulting in no need of speed control. In Case 1, all vehicles in the target platoon and the last vehicle in the anterior platoon pass the stop line in the same signal cycle. Case 2 indicates that all vehicles in the target platoon pass the stop line in the next cycle. Mathematically, the above two cases should satisfy the inequality (5) and (6) simultaneously:

$$\frac{[h_n(k_n - 1) + X_n]}{v_n} \leq TTR_n - t_{safe} \quad (5)$$

$$X_n > 0 \quad (6)$$

where h_n is the original space headway between two vehicles in the n th platoon (the target platoon); k_n is the number of vehicles in the n th platoon; X_n is denoted as the distance between the stop line and the first vehicle in the n th platoon, which is recorded when the last vehicle in the $(n-1)^{th}$ platoon (the anterior platoon) passes the stop line; It should be noted that if the value of X_n is negative, the target platoon will be blocked by the anterior one. v_n is the original speed of the n th platoon; t_{safe} is denoted as the minimum safe time headway; TTR_n is the time to red recorded when the last vehicle in the $(n-1)$ th platoon passes the stop line. If the signal light is red when the platoon enters the DSRC area, the value of TTR_n is negative and its absolute value equals to the duration since the red light has appeared.

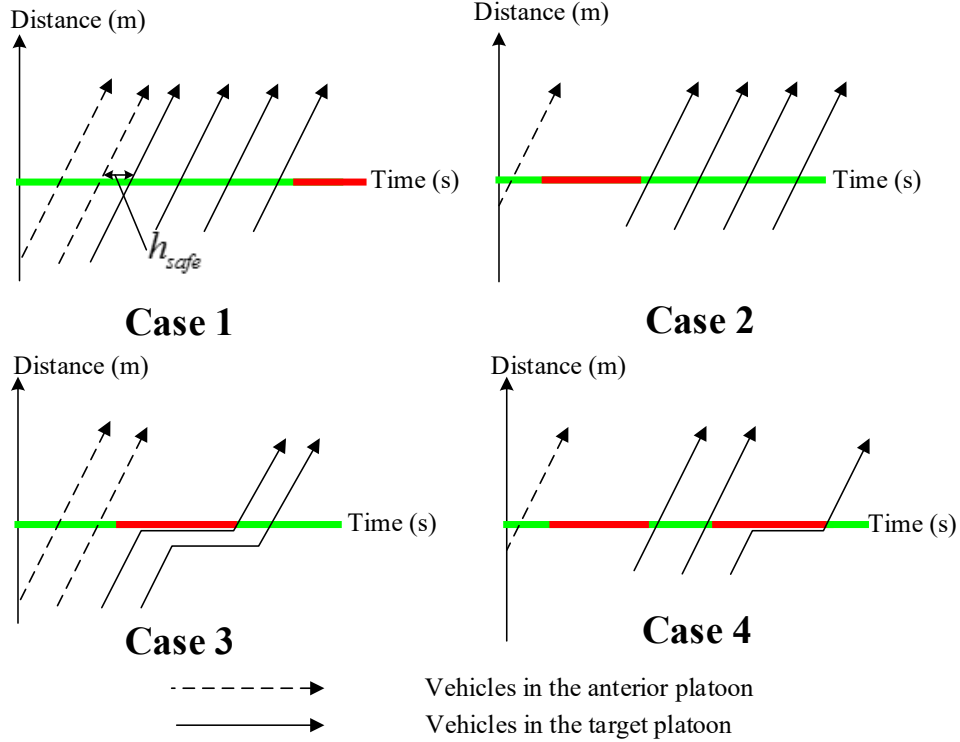


Figure 4.4 Impacts of the anterior platoon and the signal light.

Case 3 and Case 4 indicate that vehicles in the target platoon are affected by the anterior platoon or the signal timing, resulting a potential need of speed control. The following inequality will hold:

$$\frac{[h_n(k_n - 1) + X_n]}{v_n} > TTR_n - t_{safe} \quad (7)$$

For Case 3 or Case 4, how to control the platoon's speed needs further investigation, which will be discussed in details in the next section.

4.2.7 Speed control algorithm for a fully obedient platoon

In this section, we propose a dynamic speed control algorithm for a platoon consisting of all OVs, when they satisfy Case 3 and Case 4 shown in Figure 4.4. When the target platoon enters the DSRC range, based upon the signal information, vehicular position, and the original speed, the system optimizes the acceleration/deceleration values to ensure as many as possible vehicles

hit the green when arriving at the stop line. Even if some vehicles have no chance to pass the stop line without idling, the system will let them slow down at a minimum deceleration rate to save its fuel consumption. Four scenarios are analyzed as shown in Figure 4.5.

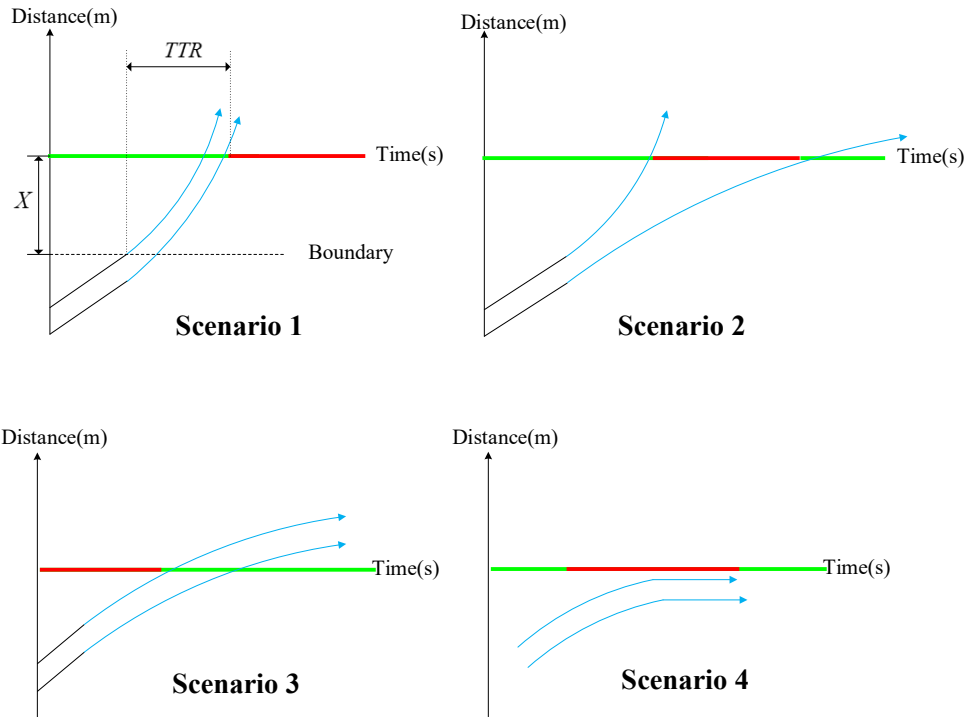


Figure 4.5 Speed control algorithm for a fully obedient platoon under different scenarios.

Scenario 1

The remaining green time (TTR) is not sufficient for the target platoon to clear the intersection but would be sufficient if the platoon accelerates gradually. In addition, if accelerating at a reasonable rate, the target platoon would never bump into the anterior platoon. Then, vehicles in the target platoon are advised to accelerate and clear the intersection. One can compute the suggested acceleration rate with the following equation:

$$a_n = \begin{cases} \frac{2h_n(k_n - 1) + 2X - 2v_n TTR}{TTR^2}, & t_{n-1} = 0 \text{ or } TTR - t_{n-1} > t_{safe} \\ \frac{2h_n(k_n - 1) + 2X - 2v_n(TTR - t_{n-1} - t_{safe})}{(TTR - t_{n-1} - t_{safe})^2}, & o.w. \end{cases} \quad (8)$$

subject to the constraints:

$$\begin{cases} a_n TTR \leq v_{max}, & t_{n-1} = 0 \text{ or } TTR - t_{n-1} > t_{safe} \\ a_n(TTR - t_{n-1} - t_{safe}) \leq v_{max}, & o.w. \end{cases} \quad (9)$$

$$0 < a_n \leq a_{max} \quad (10)$$

where, X is the distance between the upstream boundary of the DSRC range to the stop

line; a_n is the target acceleration rate; a_{max} is the maximum acceleration rate; v_{max} is the maximum speed allowed for safety; t_{n-1} is the time spent by the anterior platoon to clear the intersection, from the moment when the target platoon enters the DSRC range; TTR is the remaining time to red when the platoon enters the DSRC area. If the signal light is red when the platoon enters the DSRC area, the value of TTR_n is negative and its absolute value equals to the duration since the red light has appeared. If $t_{n-1} = 0$ or $TTR - t_{n-1} > t_{safe}$, the target platoon is only affected by the signal timing, otherwise, it is affected by the signal timing and the anterior platoon simultaneously.

Scenario 2

TTR is not sufficient for the target platoon to clear the intersection but would be sufficient for part of the platoon if those vehicles accelerate gradually, and the remaining vehicles need to either decelerate gradually to pass the intersection during the next green time or slow down to make a stop. In this scenario, the target platoon will be split into two parts and the first objective is to maximize the number of vehicles that can accelerate to pass the intersection, given by:

$$max k_{na} = \quad (11)$$

$$\begin{cases} \frac{v_n TTR + \frac{1}{2} a_{max} TTR^2 - X}{h_n} + 1, & t_{n-1} = 0 \text{ or } TTR - t_{n-1} > t_{safe} \\ \frac{v_n (TTR - t_{n-1} - t_{safe}) + \frac{1}{2} a_{max} (TTR - t_{n-1} - t_{safe})^2 - X}{h_n} + 1, & o. w. \end{cases}$$

$$0 < a_n \leq a_{max} \quad (12)$$

subject to the constraint:

$$\begin{cases} v_n + a_{max} TTR \leq v_{max}, & t_{n-1} = 0 \text{ or } TTR - t_{n-1} > t_{safe} \\ v_n + a_{max} (TTR - t_{n-1} - t_{safe}) \leq v_{max}, & o. w. \end{cases} \quad (13)$$

Then, the deceleration rate for the remaining vehicles to pass the intersection during the

next green can be calculated with:

$$d_n = \frac{2maxk_{na}h_n + 2X - 2v_n(TTR + R)}{(TTR + R)^2} \quad (14)$$

subject to constraints:

$$v_n + d_n(TTR + R) \geq v_{min} \quad (15)$$

$$|d_n| \leq |d_{max}| \quad (16)$$

where, the deceleration rate is calculated to satisfy that the leading decelerating vehicle

passes the stop line at the beginning of the next green light. After that, the number vehicles

decelerating to pass the intersection could be calculated with:

$$k_{nd} = \frac{v_n(TTR + R + G) + \frac{1}{2}d_n(TTR + R + G)^2 - X}{h_n} - maxk_{na} + 1 \quad (17)$$

where, R is the effective red time; G is the effective green time; $maxk_{na}$ is the maximum

number of vehicles to accelerate; k_{nd} is the number of vehicles to decelerate v_{min} is the

minimum speed value allowed; d_n is the deceleration rate; d_{min} is the absolute value of the

minimum deceleration rate.

The remaining vehicles (may not exist) that have no chance to avoid idling at the stop line need to slow down with the minimum deceleration rate to stop until the next green light turns on.

Scenario 3

TTR is not sufficient for the target platoon to pass the intersection, but all or part of vehicles could pass during the next green time without idling by reducing the current speed gradually. The suggested deceleration rate can be calculated with the following equation:

$$d_n = \begin{cases} \frac{2X - 2v_n(TTR + R)}{(TTR + R)^2}, & t_{n-1} = 0 \text{ or } TTR - t_{n-1} > t_{safe} \\ \frac{2X - 2v_n(TTR + R - t_{n-1} - t_{safe})}{(TTR + R - t_{n-1} - t_{safe})^2}, & o.w. \end{cases} \quad (18)$$

subject to constraint (15) plus the following equation:

Then, the number of vehicles decelerating to pass the intersection could be calculated as:

$$k_{nd} = \begin{cases} \frac{v_n(TTR + RG)}{h_n} + \frac{d_n(TTR + R + G)^2 - X}{2h_n} + 1, & t_{n-1} = 0 \text{ or } TTR - t_{n-1} > t_{safe} \\ \frac{v_n(TTR + R - t_{n-1} - t_{safe} + G)}{h_n} + \frac{d_n(TTR + R - t_{n-1} - t_{safe} + G)^2 - X}{2h_n} + 1, & o.w. \end{cases} \quad (19)$$

Other vehicles in the platoon that have no chance to avoid idling at the stop line need to slow down with the minimum deceleration rate to stop until the next green light starts.

Scenario 4

The remaining green time is not sufficient clear all vehicles in the target platoon and vehicles cannot avoid idling by either accelerating or decelerating. In this scenario, the algorithm will guide drivers to slow down at a minimum deceleration rate to stop until the next green starts.

4.2.8 Speed control algorithm for a “mixed” platoon

In a platoon mixed with OV_s and DOV_s, DOV_s don't follow the system's speed guidance.

Instead, they will follow the leading vehicles subject to the car-following model given by Eq. (3).

Then, the speed control algorithm will re-group vehicles in the “mixed” platoon into several new platoons according to their permutations.

Figure 4.6 illustrates six different cases of vehicle permutations for an example “mixed” platoon consisting of two OVs and two DOVs. The speed control strategies under different cases are given by:

- Case 1: The first two vehicles are DOVs, which compose a new platoon P1. The following two OVs form another platoon P2. P1 doesn't obey the speed guidance, while the system will give P2 speed control advices based upon information from the signal light and the running status of P1.
- Case 2: The DOVs and the OVs alternate with the first vehicle being a DOV. The first and the last vehicle compose the platoons P1 and P3, respectively, while the two vehicles in-between form the platoon P2. Here, P3 and the OV in the P2 obey the speed guidance, while P1 and the DOV in P2 don't. The DOV in P2 will is subject to the car-following model.
- Case 3: The first three vehicles compose the platoon P1 and the last vehicle forms the platoon P2. The leading OV in P1 and the P2 follow the system's guidance while the two following DOVs show car-following behaviors.
- Case 4: The DOV and the OV alternates with the first vehicle being an OV. The first two vehicles compose the platoon P1, and the following two vehicles form the platoon P2. In each platoon, the leading OV follows the speed guidance and the following DOV is subject to the car-following model.
- Case 5: The first two vehicles are OVs and the following two vehicles are DOVs. No need to re-divide the target platoon. The first two vehicles obey the speed guidance, and the latter DOVs just follow.

- Case 6: The first and the last vehicle are DOVs, and the two vehicles in-between are OVs. The first vehicle composes the platoon P1, and the latter three vehicles form the platoon P2. P1 doesn't obey the speed guidance, while the first two vehicles in P2 follow the instructions, and the last DOV in P2 just follows the leading OV.

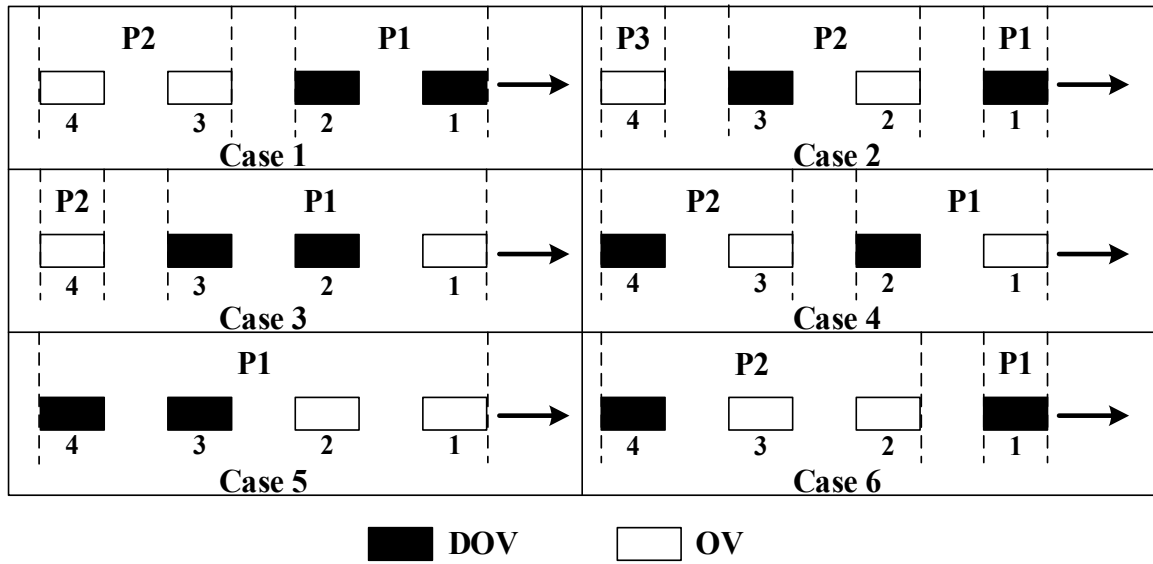


Figure 4.6 Re-group of a platoon mixed with OVs and DOVs.

After re-grouping vehicles in the “mixed” platoon into several new platoons, the system will successively send speed control guidance to those new groups according to the algorithms stated in the previous section, even these groups have DOVs.

If the leading vehicle is an OV, it will follow the system’s guidance. The algorithm to optimize its acceleration/deceleration is the same as presented in the previous section. But if a following vehicle is a DOV, its acceleration/deceleration at time $(t + T)$ is calculated with the car-following model (Eq. (3)) specified with:

$$v_n(t) = v_n(0) + a_n t \tag{20}$$

$$T = 1 (s) \tag{21}$$

$$\lambda = 0.8 \tag{22}$$

where, $v_n(t)$ and $v_n(0)$ are the speeds of the OV ahead of the DOV at time t and at the initial time, respectively; a_n is the acceleration rate of the OV suggested by the system.

After acquiring the value of a_n , we update the acceleration rate of the following DOV every one second.

If the leading vehicle is a DOV, it is not subject to speed control until it hits the red before the stop line. Here, we set the value of deceleration for the leading DOV to be 2.5m/s².

Deceleration rates for the following DOV can be calculated with Eq. (3) and Eqs. (20-22).

In summary, the logic of the proposed platoon-based speed control algorithm is shown in Figure 4.7.

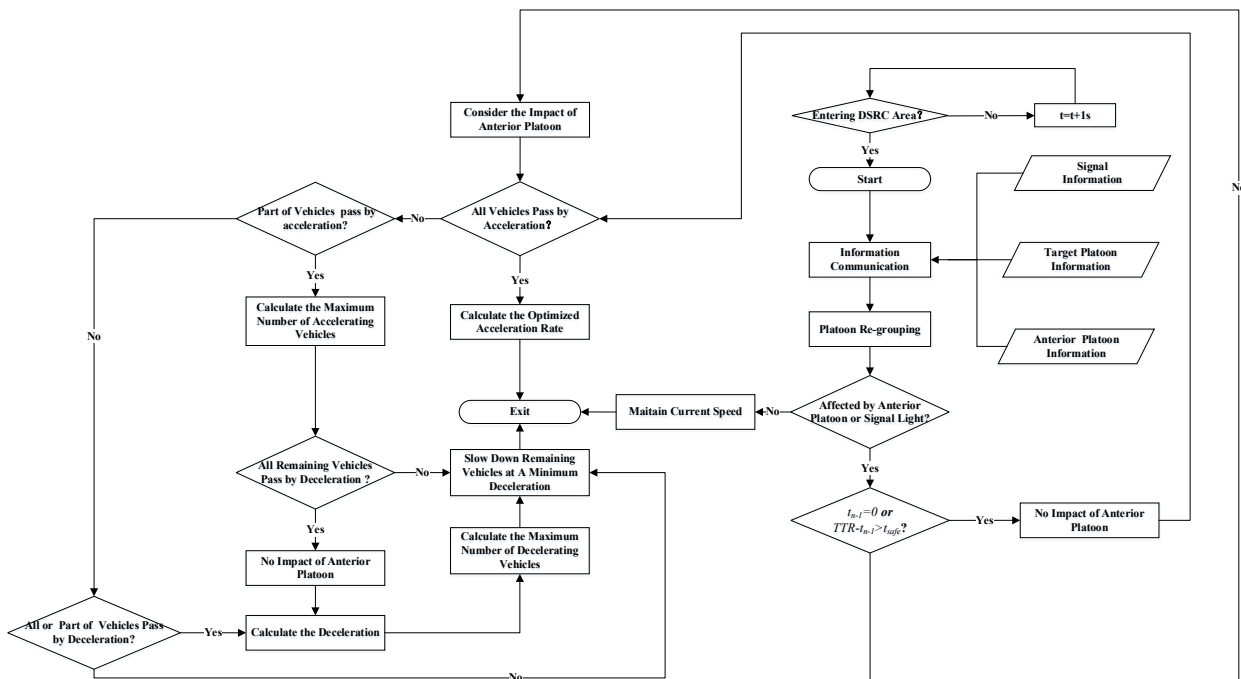


Figure 4.7 Logic of speed control algorithm.

4.3 Illustrative Examples

In this section, three examples are presented to validate the proposed speed control algorithm.

The first example is used to discuss the impact of the anterior platoon, the second one is designed

to analyze fuel consumptions under different time headways, and the third is to compare the results of fuel consumption under different permutations of vehicles in a “mixed” platoon.

In the examples, we set the original speed of the target platoon (named PA) at 20m/s. PA consists of four vehicles. The distance from the upstream boundary of the DSRC range to the stop line is 300m. The safety time headway t_{safe} is set to 0.5s.

4.3.1 Fuel consumption rate comparison

There is an anterior platoon (named PB), consisting of four vehicles, 120m ahead of PA. PB will pass the intersection at its original speed (15m/s) without any speed alternation. We set the value of TTR_n at 2s and time headway to be 0.6s. Then, one can calculate the value of X_n to be 76m.

The relationship between $[h_n(k_n - 1) + X_n]/v_n$ and $TTR_n - t_{safe}$ satisfies the Eq. (7), indicating the PA falls into Case 3 or Case 4 and may need speed control.

The calculation results indicate that PA needs to follow the system’s guidance to change its speed. Then, one can use Eq. (8) to calculate the acceleration rate as approximately 0.67m/s², which is less than the maximum value. It shows that all vehicles in PA could accelerate to pass the intersection. Further calculation shows that the PA is in Case 4 and is not affected by the PB. The VT-Micro Model is used to calculate the fuel consumption of PA and the time-varying comparison of fuel consumption with and without speed control is shown in Figure 4.8.

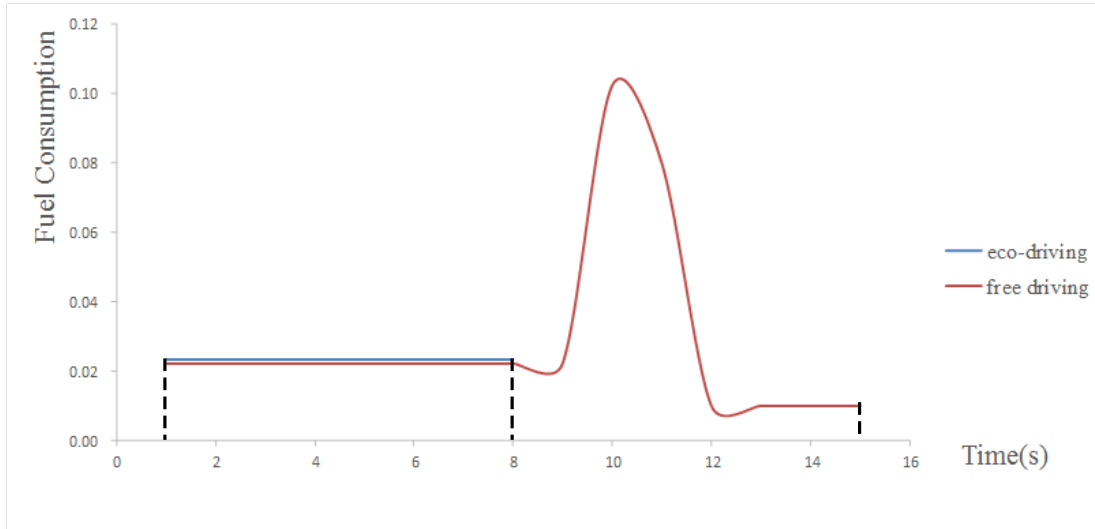


Figure 4.8 Fuel consumption of PA under speed control and free driving.

As shown in Figure 4.8, the blue line represents the second-by-second fuel consumption of PA under speed control, while the red line represents the free driving fuel consumption. It is clear that the blue line is almost horizontal, while there is a crest in the red line, indicating a dramatic increase in fuel consumption due to the sharp deceleration near the stop line.

It is clear that the fuel consumption trajectory under speed control ends at 8s, while the one for free driving ends at 15s. This is due to the fact that the PA under free driving needs to idle for approximately 7 seconds, resulting significantly less fuel consumption of speed control than free driving.

4.3.2 Fuel consumption under various headways

No anterior platoon is considered in this example. We just compare the total fuel consumptions of the PA with the time headways ranging from 0.5s to 2.5s with an increment of 0.5s. We analyze the scenario 1 and the scenario 3 (see Figure 4.5). The results are illustrated in Figure 4.9.

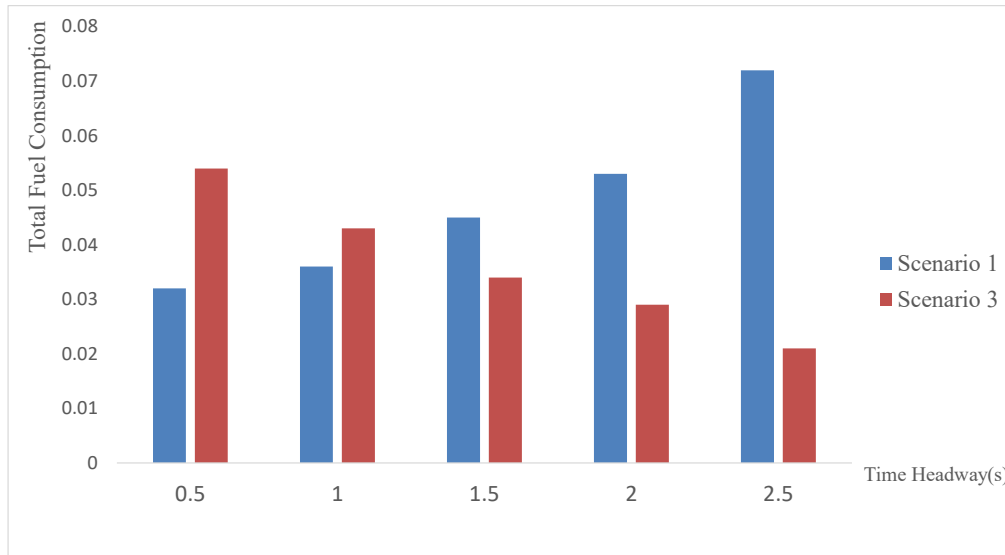


Figure 4.9 Total fuel consumption under different scenarios.

As shown in Figure 4.9, under scenario 1, the total fuel consumption grows with the increase of time headway. While under scenario 3, it declines. This is because under scenario 1 where all vehicles could accelerate to pass the intersection, the bigger the time headway, the less the time (TTR) for following vehicles to cross the intersection, causing a larger acceleration rate; while under scenario 3 where all vehicles need to decelerate until the green time starts, a larger time headway leads to less time for a vehicle to wait for the green light, causing a less deceleration rate.

4.3.3 Fuel consumption under various permutations

We compare the fuel consumptions under different permutations like Figure 4.6 shows. It is considered that the PA consisting of two OV and two DOV falls into scenario 3, where all vehicles need to decelerate. The fuel consumptions under different permutations are shown in Figure 4.10.

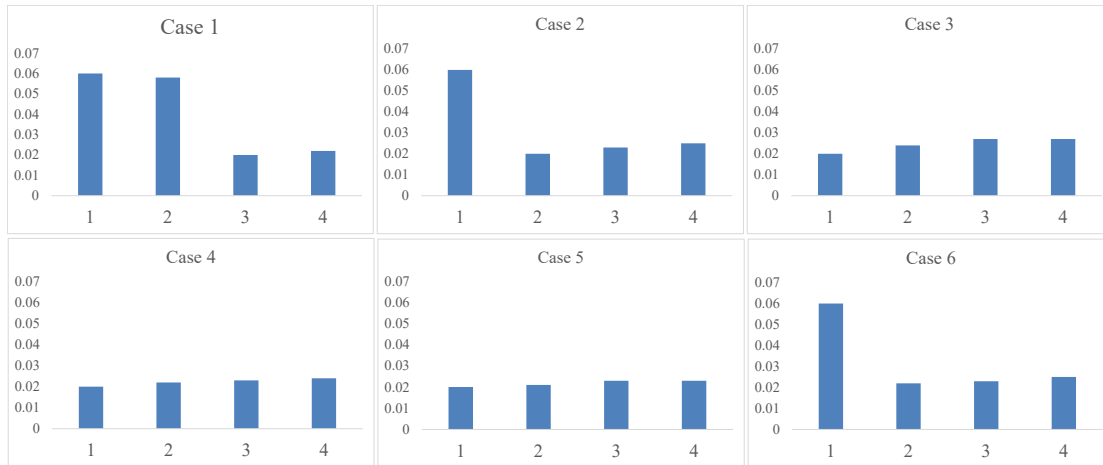


Figure 4.10 Fuel consumption under different permutations.

As Figure 4.10 shows, if the leading vehicle is a DOV, then its fuel consumption is much larger because it doesn't obey the speed guidance and needs to decelerate sharply to wait for the green light. Nevertheless, when the leading vehicle is an OV, it seems that the fuel consumption for the following vehicles, even for DOVs, may not increase obviously. This is because the DOV follows the OV tightly to pass the intersection.

4.4 Conclusions

This chapter extends the single vehicle model by proposing a dynamic speed control algorithm toward a vehicle platoon at a signalized intersection. The algorithm not only considers the running status of the target platoon but also analyzes the impact of the anterior platoon.

Acceleration/deceleration rates, instead of speed, are used as the optimized target to guide the drivers to avoid idling and to hit the green light as possible as they can. Depending on the status of the platoon and signal timing, the speed control algorithms under different scenarios are discussed in details. The proposed algorithms not only work for a fully obedient platoon, but also for a mixed platoon by re-grouping vehicles into several new platoons according to their permutations.

The research provides three examples provided to validate the algorithm. In the first one, considering the impact of the anterior platoons, we compare the time-varying fuel consumptions of the target platoon between the speed control mode and the free driving mode. Results indicate that the platoon under free driving will idle for some time, resulting in significantly more fuel consumption than the speed control mode using the proposed speed control algorithms.

In the second example, we compare the levels of fuel consumptions under different time headways. Results show that in an acceleration scenario, a smaller headway results in less fuel consumption; while in a deceleration scenario, a smaller headway causes a little more fuel consumption.

In the third example, fuel consumptions under different permutations are analyzed. The conclusion implies that if the leading vehicle is a DOV, the target platoon's fuel consumption is much larger. However, when the leading vehicle is an OV, it seems that the fuel consumption for the following vehicles in the target platoon, even for DOVs, may not increase obviously.

Analysis results of the illustrative examples indicate the validity and effectiveness of the proposed platoon-based speed control algorithm. On-going work of this study is to apply the proposed algorithm in real-world projects and evaluate its effectiveness with calibrated fuel consumption models.

Chapter 5 DYNAMIC VEHICULAR SPEED CONTROL TOWARDS BOTTLE MITIGATION AND SAFETY IMPROVEMENT AT AN UNSIGNALIZED INTERSECTION

This chapter develops a dynamic vehicular speed control algorithm towards bottleneck elimination at an unsignalized intersection using the CAV technology. The proposed algorithm considers the running status of the target vehicle as well as the impact of the downstream vehicles (if exists) and the gap conditions in real-world traffic environment.

Acceleration/deceleration profile, instead of speed trajectories, is optimized for speed guidance. Illustrative examples are provided to validate the proposed algorithm in the measure of fuel consumption and emissions. Results indicate that the proposed control algorithm is effective to minimize the fuel consumption and emission of the target vehicle under various test scenarios.

5.1 Introduction

5.1.1 Regulars and gaps at unsignalized intersections

Unlike signalized intersections where the green light gives the right of way, there's no positive indication to the drivers about when to pass through the prior streams at unsignalized intersections. The drivers need to find a safe "gap" themselves. The minimum gap that the driver accept is the critical gap. In traditional environment, the critical gap is sensed by human and is variable toward different people. While under the connected-vehicle technology, especially for automatic vehicles, the critical gap information could be acquired in advance, which makes it uniform to all vehicles.

For the unsignalized intersections, there exists a hierarchy among streams. Some streams have the top priority, while others have to yield to higher rank streams. In some cases, streams have to yield to some streams which also have to yield to others.

The simplest unsignalized intersection, shown in the left part of Figure 5.1, have two streams, from which the minor one yields to the major one. Here is only one conflicting point (the red circle in the left part of Figure 5.1) in these simplest intersections. While for those having more than two streams, a vehicle may need to avoid several conflicting points, like the right part of Figure 5.1 illustrates.

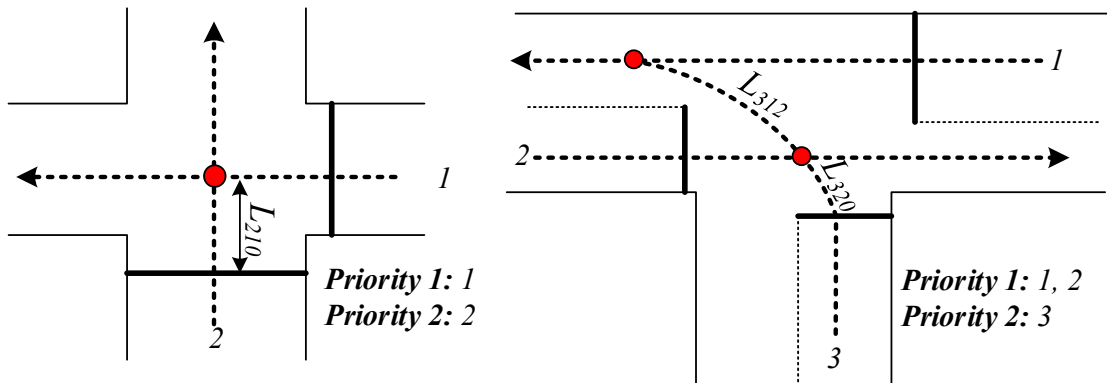


Figure 5.1 Traffic movements and regulars at unsignalized intersections.

Many studies have been conducted towards signalized intersections where the signal status is a very important parameter to achieve connected-vehicle efficiency. While in the unsignalized intersection, as mentioned above, the gap determines if the vehicle needs stop. Here, we function the gap and the vehicle length as the signal status, as Figure 5.2 shows.

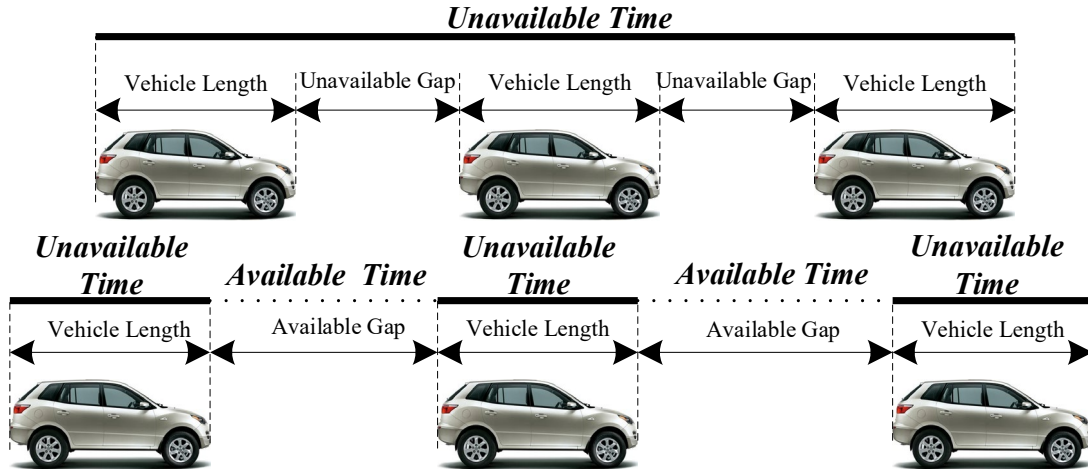


Figure 5.2 Treat gaps and vehicle length as “signal time”.

In Figure 5.2, the top part represents three vehicles with two successive unavailable gaps, where those unavailable gaps and vehicle length are integrated as a whole unavailable time, as the function of “red time”. In the below part, two successive available gaps between three vehicles are available times, treated as “green time”, while those vehicle lengths are treated as “red time”.

It should be noted that, these times are dynamic, depending on the velocity of the vehicle. Thanks to the V2X communication, the information of gaps, vehicle lengths, velocities and positions can be acquired in advanced, which makes it possible to achieve the algorithm proposed in this chapter.

5.1.2 Speed trajectories of various trajectories under the same travel time

Figure 5.3 illustrates two time-space diagrams representing an acceleration scenario and a deceleration plus idling scenario for a single vehicle passing through an unsignalized intersection. If the driver decides to avoid idling, in Part (a), he/she needs to accelerate to pass through the stop bar and the available gap (the gap greater than the critical gap), while the driver in Part (b) needs to decelerate until the next available gap shows.

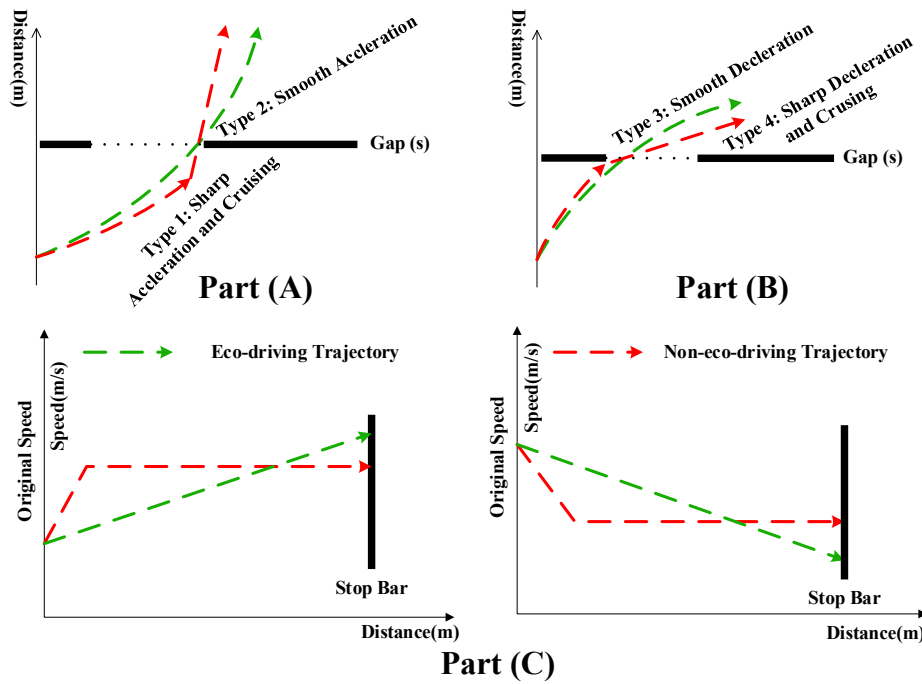


Figure 5.3 Speed trajectories of a single vehicle under different scenarios.

There are four types of speed trajectories corresponding to the acceleration and deceleration scenarios, given by:

Type 1: The vehicle accelerates smoothly to pass the stop line during the available gap when he/she knows the possibility of hitting the unavailable gap if keeping his/her initial speed;

Type 2: The vehicle accelerates sharply near the stop line and clears the intersection during the available gap;

Type 3: The vehicle decelerates smoothly to pass the stop line when the available gap just shows; and

Type 4: The vehicle decelerates sharply at first and cruises the remaining distance until the available gap comes.

For the same travel distances, the above five speed trajectories result in different levels of fuel consumption. In part (a), the Type 2 trajectory results in more fuel consumption than Type

3. Similarly, the Type 3 trajectory consumes less fuel than the Type 3 and Type 4 in part (b). It is considered that the Type 2 trajectory and the Type 3 trajectory are eco trajectories, which encourage drivers to keep a gradual acceleration/deceleration status to pass the stop line during the available gap, rather than accelerating/decelerating sharply (see part (c) of Figure 5.3 for comparison).

Importantly, there might be a special case where vehicles have options to choose Type 2 trajectory and Type 3 trajectory at the same time. In this situation, Type 2 trajectory is suggested due to its savings in travel time. The manipulating order for eco trajectories is as follows:

- (1) If the vehicle could pass or avoid crashing without idling with its original velocity, it does nothing;
- (2) Else if the vehicle could pass or avoid crashing by acceleration, it accelerates smoothly;
- (3) Else if the vehicle could pass or avoid crashing by deceleration, it decelerates smoothly, and
- (4) Else, it decelerates and idles smoothly.

5.1.3 VT-micro model

This research adopts the microscopic fuel consumption and emission model, the VT-micro Model, as it has been proved to be accurate and easy for calibration. The model is given by:

$$MOE_e = \exp\left(\sum_{i=1}^3 \sum_{j=1}^3 L_{i,j}^e v^i a^j\right) \quad (1)$$

$$v \leq 120 \quad (2)$$

where, MOE_e is the instantaneous fuel consumption rate (l/s) or the instantaneous emission (CO emission, NOx emission, HC emission) (kg/s) ; $L_{i,j}^e$ are the model coefficients for

MOE_e at speed power i and acceleration power j ; v is the instantaneous speed (m/s); and a is the instantaneous acceleration rate (m/s²). Coefficients for estimating fuel consumption rates, CO emission, NO_x emission and HC emission are summarized in Table 5.1.

Table 5.1 Sample coefficients of hybrid regression model for fuel consumption and car emission rates.

FUEL CONSUMPTION				
Coefficients	Constant	v	v^2	v^3
Constant	-7.537	0.443809	0.171641	-0.042024
a	0.097326	0.051753	0.002942	-0.007068
a^2	-0.003014	-0.000742	0.000109	0.000116
a^3	0.000053	0.000006	-0.000010	-0.000006
CO EMISSION				
Coefficients	Constant	v	v^2	v^3
Constant	-12.9281	0.488324	0.328837	-0.047675
a	0.23292	0.041656	-0.032843	0
a^2	-0.008503	0.003291	0.0057	-0.000532
a^3	0.000163	-0.000082	-0.000118	0
NO _x EMISSION				
Coefficients	Constant	v	v^2	v^3
Constant	-14.8832	0.834524	0.095433	-0.033549
a	0.152306	0.166647	0.101565	-0.037076
a^2	-0.00183	-0.004591	-0.006836	0.000737
a^3	0.00002	0.000038	0.000091	-0.000016
HC EMISSION				
Coefficients	Constant	v	v^2	v^3
Constant	-14.544	0	0.251563	-0.003284
a	0.081857	0.1092	-0.01942	-0.012745
a^2	-0.00226	-0.00353	0.004356	0.001258
a^3	0.000069	0.000072	-0.00008	-0.000021

5.1.4 Assumptions

This study makes the following assumptions to develop the dynamic speed control algorithm:

Assumption 1: All vehicles are automated vehicles and fully compliant to the system's guidance;

Assumption 2: The road and the weather conditions are optimal for vehicles to run;

Assumption 3: If there exist downstream vehicles when the target vehicle enters the DSRC area, those vehicles could be discharged in the nearest accepted gap (maybe the current or the next);

Assumption 4: Delay time for real time communication or manipulation is ignored;

Assumption 5: If vehicles enters the intersection, it keeps its acceleration/deceleration until passing the intersection, and;

Assumption 6: All movements (left and straight through) share the same critical gap.

5.2 Methodologies

The target of this research is proposing rational algorithms to mitigate traffic bottleneck so that the vehicle could pass the intersection safely and eco-friendly. The control strategy discussed in this chapter begins with the simplest intersection with only two streams, and then extended to the one with more streams.

5.2.1 Impact of downstream vehicles and gaps

When the target vehicle enters the control area, the system shall first judge whether it needs speed control. The system leverages the DSRC to make real-time communication between vehicles and between the infrastructure and the vehicles. Information about the downstream vehicles is also used to determine whether the target vehicle requires speed control or not. The interactions between the target vehicle and its downstream vehicles are illustrated in Figure 5.3, where the solid green arrows represent target vehicle without any blockage, while the dotted red arrows represent the target vehicle blocked by the unavailable gaps (those gaps less than the critical gap) or the downstream vehicles. In addition, the solid red arrows represent the last downstream vehicle. A total of five cases are analysed as illustrated in Figure 5.4.

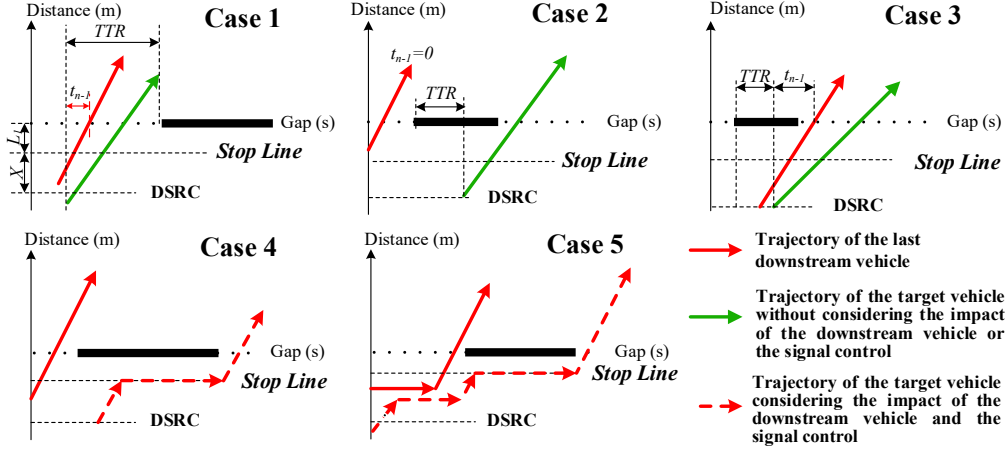


Figure 5.4 Impacts of the downstream vehicles and the gaps.

Case 1, Case 2 and Case 3 show that the target vehicle is not affected by the downstream vehicle or the unavailable gaps, resulting in no need for speed control. In Case 1 and Case 3, the target vehicle and its downstream vehicles pass the stop line in the same available gap, while Case 2 indicates that the target vehicle and its downstream vehicle pass the stop line at different available gaps. Mathematically, the above three cases should satisfy the following inequality:

$$T_x^1 \leq (X + L_1)/v_n \leq T_y^1 \quad (3)$$

where

$$T_x^1 = \begin{cases} t_{n-1} + t_{safe}, & TTU1 > t_{n-1} + t_{safe} \neq t_{safe} \\ 0, & TTU1 > t_{n-1} + t_{safe} = t_{safe} \\ t_{n-1} + t_{safe} + UG1, & TTU1 < t_{n-1} + t_{safe} \neq t_{safe} \\ TTU1 + UG1, & TTU1 < t_{n-1} + t_{safe} = t_{safe} \text{ or} \\ & TTU1 = t_{n-1} + t_{safe} \end{cases} \quad (4)$$

$$T_y^1 = \begin{cases} TTU1, & TTU > t_{n-1} + t_{safe} \\ TTU1 + UG1 + AG1, & TTU \leq t_{n-1} + t_{safe} \end{cases} \quad (5)$$

$TTU1$ is the time to the nearest unavailable gap recorded when the target vehicle enters the DSRC area. If the gap is unacceptable when the vehicle enters the DSRC area, the value of $TTU1$ will be negative and its absolute value equals to unavailable gaps duration since the unavailable gaps has already come.

L_1 is the target vehicle trajectory's distance between the stop line and the conflicting point; T_x^1 is the earliest time when the target vehicle could pass; X is the distance between the upstream boundary of the DSRC range to the stop line; T_y^1 is the total time for the target vehicle to pass the intersection; t_{safe} is denoted as the minimum safe time headway; t_{n-1} is the time spent by the last downstream vehicle to clear the intersection. If $t_{n-1} = 0$, the target vehicle is only affected by the gap, otherwise, it is affected by gap and the downstream vehicles simultaneously. T_x , T_y and t_{n-1} are all recorded from the moment when the target vehicle enters the DSRC control area.

Case 4 and Case 5 indicate that the target vehicle is affected by both the downstream vehicles and the unavailable gaps (i.e. do not satisfy (3)), indicating a potential need for speed control, which will be discussed in detail in the next section.

5.2.2 Speed control algorithm for the two-streams intersection

In this section, towards the simplest two-stream intersection, a dynamic speed control algorithm is developed for Case 4 and Case 5 as shown in Figure 5.3. When the target vehicle enters the DSRC range, based upon the gap information, vehicular position, and the initial speed, the system optimizes the acceleration/deceleration profile to make possible that the vehicle could hit the available gap when arriving at the stop line. Even if the vehicle has no chance to pass the stop line without idling, the system will let it slow down at an appropriate deceleration rate to reduce fuel consumption and emission. Five different scenarios are discussed to develop the speed control algorithm.

Scenario 1

The remaining available gap (TTU1) is not sufficient for the target vehicle to clear the intersection but would be sufficient if the vehicle accelerates gradually.

As Scenario of Figure 5.5 shows, if accelerating at a reasonable rate, the target vehicle would never bump into the downstream vehicle or hit the unavailable gap inside the intersection. Here, the target vehicle is advised to accelerate and clear the intersection by the end of the current available gap. One can compute the suggested acceleration rate with the following equation:

$$a_{n1} = (2X + 2L_1 - 2v_n T_y^1) / (T_y^1)^2 \quad (6)$$

subject to the constraints:

$$0 < a_{n1} \leq a_{max} \quad (7)$$

$$v_n + a_{n1} T_y \leq v_{max} \quad (8)$$

where, a_{n1} is the target acceleration rate; a_{max} is the maximum acceleration rate to make sure the vehicles could accelerate smoothly; v_n is the original speed of the target vehicle; v_{max} is the maximum speed allowed for safety. If a_{n1} falls beyond the constraints listed above, it means the vehicle is not adaptable for scenario 1.

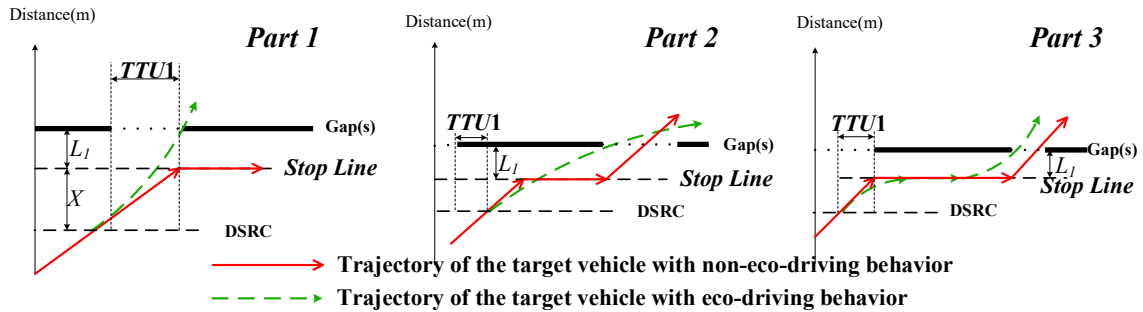


Figure 5.5 Scenarios for two-level priority intersections without the impact of the downstream vehicles.

Scenario 2

TTU1 is not sufficient for the target vehicle to pass the intersection, but the target vehicle could pass at the beginning of the next available gap without idling by reducing the current speed gradually. In addition, there are no downstream queue at the stop line, as Part 2 illustrates.

The suggested deceleration rate can be calculated with the following equation:

$$d_{n2} = [2X + 2L_1 - 2v_n(TTU1 + UA1)] / (TTU1 + UA1)^2 \quad (9)$$

subject to constraints:

$$d_{min} \leq d_{n2} < d_{max} \quad (10)$$

$$v_n + d_{n2}(TTU1 + UA1) > v_{min} \quad (11)$$

where, d_{n2} is the target deceleration rate; d_{min} is the minimum deceleration rate to make sure the vehicles could decelerate smoothly; v_{min} is the minimum speed allowed.

Scenario 3

Without any downstream vehicles, the remaining available gap is not sufficient and the vehicle cannot avoid idling by either accelerating or decelerating. The algorithm suggests the target vehicle to slow down with an appropriate deceleration rate so that it just stops when reaching the stop line, as Part 3 shows.

The appropriate deceleration rate could be calculated with the following equation:

$$d_{n3} = -2(X + L_1) / v_n^2 \quad (12)$$

subject to the constraints:

$$d_{n3} \geq d_{min} \quad (13)$$

where, d_{n3} is the optimal deceleration rate for the target vehicle that has no chance to avoid idling for Scenario 3.

Scenario 4

There exist downstream vehicles when the target vehicle enters the DSRC area.

Nonetheless, if the target vehicle alters its speed appropriately, it may avoid being blocked by the queue. The first three sub-scenarios shown in Figure 5.6 illustrate an avoidance of bumping into the downstream vehicle.

Grounded on V2V communication, when the target vehicle enters the DSRC control range, the status of its downstream vehicles, such as speeds, idling time and acceleration/deceleration rates, could be acquired, and the time for the last vehicle in the downstream queue to move could be calculated by the shock wave theory.

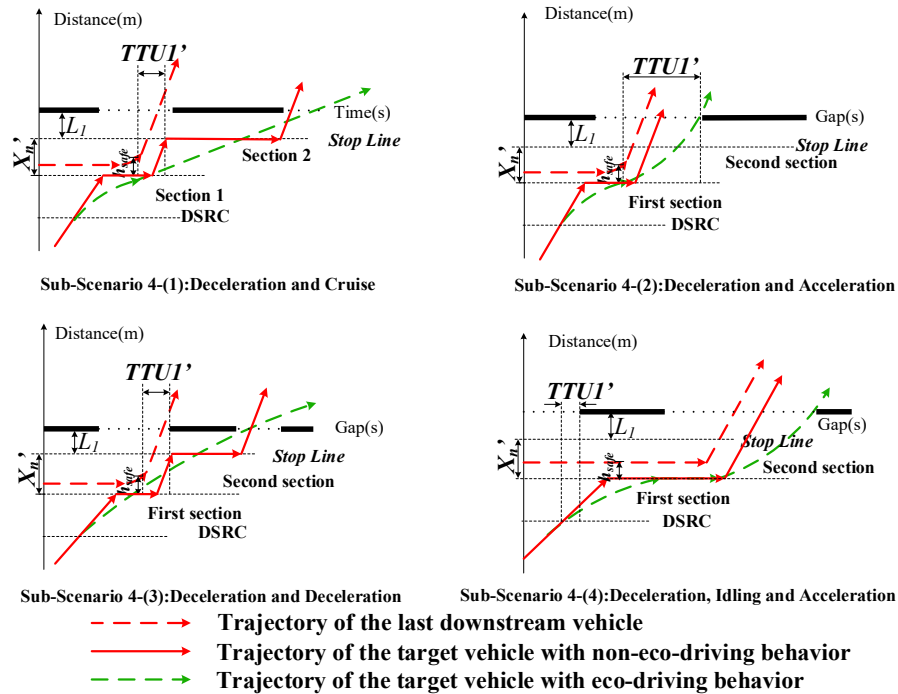


Figure 5.6 Scenarios for two-level priority intersections considering the impact of the downstream vehicles.

Given the impact of downstream queue, the trajectory of the target vehicle should be divided into two sections. The first section is a deceleration process so that the target vehicle

could avoid bumping into the last downstream vehicle. One can compute the deceleration rate with the following equation:

$$d_{n41} = 2[(X + L_1 - k_{n-1}h_{que}) - v_n t_{n-1}^{idle}] / t_{n-1}^{idle^2} \quad (14)$$

subject to the constraints:

$$d_{min} \leq d_{n41} < d_{max} \quad (15)$$

$$0 < v_n + d_{n41} t_{n-1}^{idle} \leq v_{n-1} \quad (16)$$

where,

$$t_{n-1}^{idle} = (k_{n-1} - 1)(h_{move} - h_{que}) / v_{n-1} \quad (17)$$

d_{n41} is the deceleration rate in the first section of the trajectory in Scenario 4; h_{safe} is the minimum safe space headway between two vehicles; k_{n-1} is the number of vehicles consisting the downstream queue; h_{que} is the space headway for a stop queue; h_{move} is the space headway when the queue begins to move; v_{n-1} is the initial speed for the last downstream vehicle if it is moving; t_{n-1}^{idle} is the total stop time for the downstream queue. It should be noted that all those parameters above are recorded when the target vehicle enters the DSRC control range.

After the first section, the target vehicle starts the second section, and the system needs to re-consider if the target vehicle could pass the intersection. If the remaining available gap, $TTU1'$, is sufficient, the target vehicle will cruise to pass the intersection (see Sub-scenario 4-(1) in Figure 5.6); otherwise, the target vehicle will be guided with a proper acceleration/deceleration rate (see Figure 5.6) using a similar calculation method to Scenarios 1 to 3.

Considering the impact of the downstream vehicles, there is a worst case where the target vehicle cannot avoid idling because of the blockage of the downstream queue, as shown in sub-scenario 4-(4). Similarly, the trajectory of the target vehicle has two sections similar to other sub-

scenarios. In the first section, the algorithm suggests the vehicle to slow down with an appropriate deceleration rate so that it just stops when joining the end of downstream queue.

The appropriate deceleration rate could be calculated with the following equation:

$$d_{n5} = -2(X + L_1 - k_{n-1}h_{que})/t_{n-1}^{idle^2} \quad (18)$$

subject to the constraints:

$$d_{n5} \geq d_{min} \quad (19)$$

where, d_{n5} is the optimal deceleration rate for the target vehicle that has no chance to avoid idling in Scenario 5.

In the second section, the algorithm is as same as in sub-scenarios 4-(1) to 4-(3).

5.2.3 The speed control algorithm for the intersection with more than two streams

Towards the intersection with more than two streams, the algorithms are more complicated, while the scenarios discussed are the same as the two-stream intersection.

Go back to the right part of Figure 5.1. In this case, the target vehicle (stream 3) needs to pass through stream 2 and to be converged with stream 1, which means the algorithm should seek for two successive available gaps for the target vehicle. The sequences of the higher priority streams the target vehicle needs to pass depends on the positions of the conflicting points, as Figure 5.7 shows.

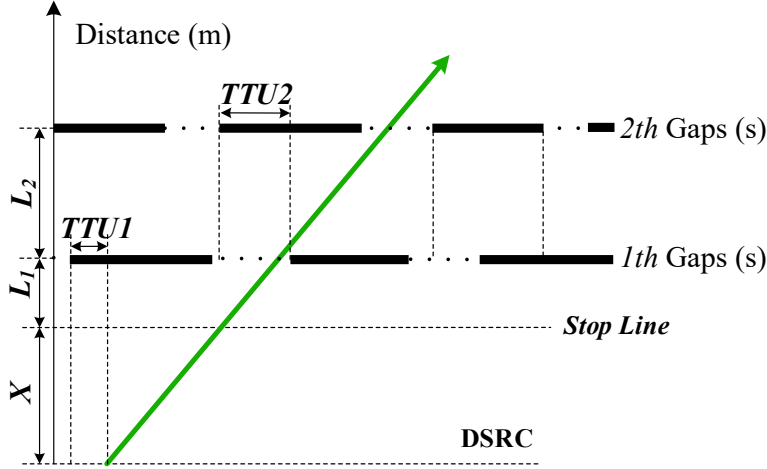


Figure 5.7 Impacts of the downstream vehicles and the gaps with multiple streams.

Similar to Section 3.1, we shall firstly judge if the target vehicle is blocked by the downstream vehicles or the unavailable gap. If the vehicle needs no speed alteration, it should satisfy the following inequality systems:

$$\begin{cases} T_x^1 \leq (X + L_1)/v_n \leq T_y^1 \\ T_x^2 \leq L_2/v_n \leq T_y^2 \end{cases} \quad (20)$$

where,

$$T_x^2 = \begin{cases} t_{n-1}^2 + t_{safe}, & TTU2 > t_{n-1}^2 + t_{safe} \neq t_{safe} \\ 0, & TTU2 > t_{n-1}^2 + t_{safe} = t_{safe} \\ t_{n-1}^2 + t_{safe} + UG2, & TTU2 < t_{n-1}^2 + t_{safe} \neq t_{safe} \\ TTU2 + UG2, & TTU2 < t_{n-1}^2 + t_{safe} = t_{safe} \text{ or} \\ & TTU2 = t_{n-1}^2 + t_{safe} \end{cases} \quad (21)$$

$$T_y^2 = \begin{cases} TTU2, & TTU2 > t_{n-1}^2 + t_{safe} \\ TTU2 + UG2 + AG2, & TTU2 \leq t_{n-1}^2 + t_{safe} \end{cases} \quad (22)$$

L_2 is the trajectory's distance between the first and the second conflicting points; Other parameters, recorded from the moment when the target vehicle passes through the first conflicting point, have the similar meanings to those in Eqs.(3) to (5).

More generally, if the target vehicle needs to pass n higher priority streams, it should satisfy the following equations:

$$\left\{ \begin{array}{l} T_x \leq (X + L_1)/v_n \leq T_y \\ T_x^2 \leq L_2/v_n \leq T_y^2 \\ \vdots \\ T_x^n \leq L_n/v_n \leq T_y^n \end{array} \right. \quad (23)$$

where,

$$T_x^n = \begin{cases} t_{n-1}^n + t_{safe}, & TTUn > t_{n-1}^n + t_{safe} \neq t_{safe} \\ 0, & TTUn > t_{n-1}^n + t_{safe} = t_{safe} \\ t_{n-1}^n + t_{safe} + UGn, & TTUn < t_{n-1}^n + t_{safe} \neq t_{safe} \\ TTUn + UGn, & TTUn < t_{n-1}^n + t_{safe} = t_{safe} \text{ or} \\ & TTUn = t_{n-1}^n + t_{safe} \end{cases} \quad (24)$$

$$T_y^2 = \begin{cases} TTUn, & TTUn > t_{n-1} + t_{safe} \\ TTUn + UGn + AGn, & TTUn \leq t_{n-1} + t_{safe} \end{cases} \quad (25)$$

L_n is the trajectory's distance between the first and the second conflicting points; Other parameters are recorded from the moment when the target vehicle passes through the (n-1)th conflicting point.

If the situation does not match the above conditions, then we need to consider the speed guidance with the same scenarios as those for the two-stream intersection.

Scenario 1 (Acceleration without the impact of the downstream vehicles)

The target acceleration rate is as follows:

$$a_{n1} = \min(a_1, a_2, \dots, a_n) \quad (26)$$

where,

$$\left\{ \begin{array}{l} a_1 \geq \frac{2X + 2L_1 - 2v_n T_y^1}{(T_y^1)^2} \\ a_2 \geq \frac{2X + 2L_1 + 2L_2 - 2v_n T_y^1 - 2v_n T_y^2}{(T_y^1 + T_y^2)^2} \\ \vdots \\ a_n \geq \frac{2X + 2 \sum_{k=1}^n L_k - 2v_n \sum_{k=1}^n T_y^k}{(\sum_{k=1}^n T_y^k)^2} \end{array} \right. \quad (27)$$

subject to the constraints:

$$0 < a_{n1} \leq a_{max} \quad (28)$$

$$v_n + a_{n1} \sum_{k=1}^n T_y^k \leq v_{max} \quad (29)$$

where, a_n is the acceleration considering the vehicle could pass the nth higher priority stream. If a_{n1} falls beyond the constraints listed above, it means the vehicle is not adaptable for scenario 1.

Scenario 2 (Deceleration without the impact of the downstream vehicles)

The suggested deceleration rate can be calculated with the following equation:

$$d_{n2} = \max(d_1, d_2, \dots, d_n) \quad (30)$$

where,

$$\left\{ \begin{array}{l} d_1 \leq \frac{[2X + 2L_1 - 2v_n(TTU1 + UA1)]}{(TTU1 + UA1)^2} \\ d_2 \leq \frac{[2X + 2L_1 + 2L_2 - 2v_n(TTU1 + UA1 + TTU2 + UA2)]}{(TTU1 + UA1 + TTU2 + UA2)^2} \\ \vdots \\ d_n \leq \frac{\{2X + 2L_1 + 2 \sum_{k=1}^n L_k - 2v_n[\sum_{k=1}^n (TTUk + UAk)]\}}{[\sum_{k=1}^n (TTUk + UAk)]^2} \end{array} \right. \quad (31)$$

subject to constraints:

$$d_{min} \leq d_{n2} < d_{max} \quad (32)$$

$$v_n + d_{n2} \sum_{k=1}^n (TTUk + UAk) > v_{min} \quad (33)$$

where, d_n is the deceleration considering the vehicle could pass the nth higher priority stream.

Scenario 3 (Deceleration and idling without the impact of the downstream vehicles)

It is totally as same as the one for the two-stream intersection.

Scenario 4 (With the impact of the downstream vehicle)

Similarly, we divide the trajectory into two section. The deceleration of the first section is computed as the one for the two-stream intersection. Then the second section is processed as Scenarios 1-3 for intersections with more than two streams.

In summary, the logic of the proposed speed control algorithm is summarized in Figure 5.8.

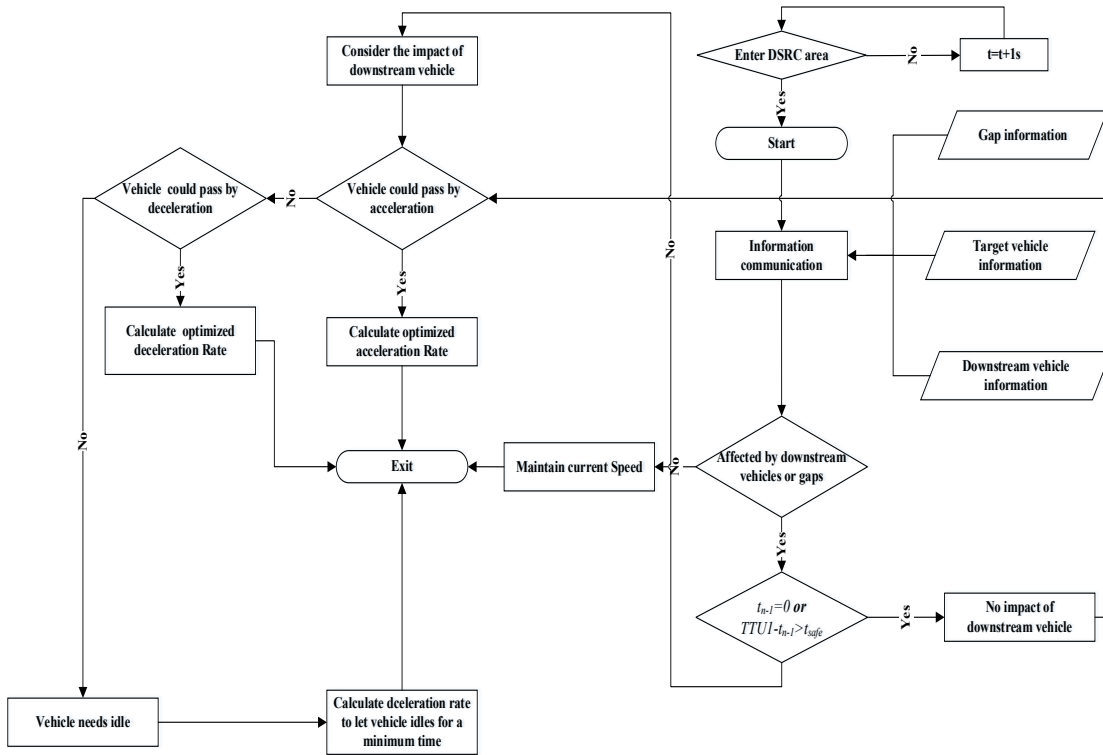


Figure 5.8 Overall procedure of the proposed speed control algorithm

5.3 Illustrative Examples

In this section, an example is illustrated to validate the proposed speed control algorithm. Here, fuel consumption and emission are recorded from the moment when the vehicle enters the DSRC range until the front bumper of that vehicle passes the stop line.

There is a four-leg unsignalized intersection where every leg has one straight approaching lane, one left-turn approaching lane and one exit lane. The priority levels of every stream is shown in Figure 5.9.

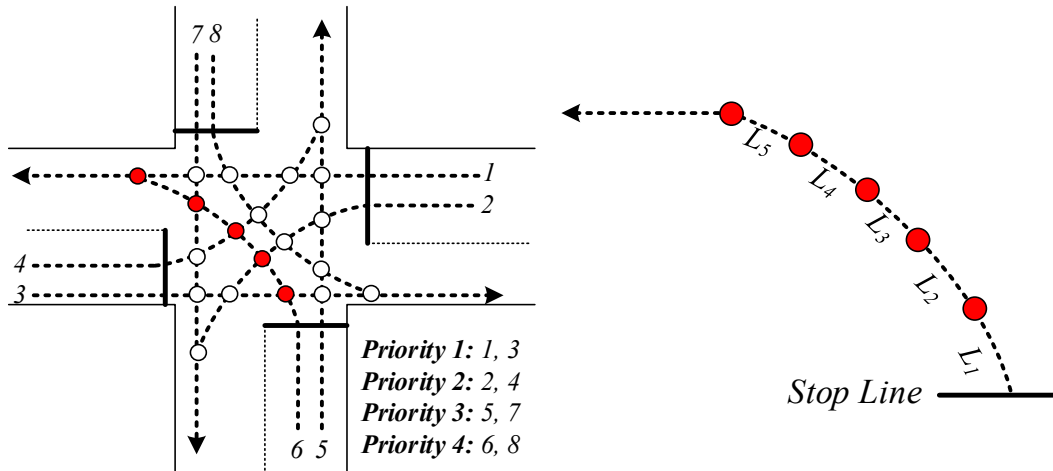


Figure 5.9 Priority ranks and conflicting points of the 8-stream intersection.

We choose a vehicle in the 6th stream as our target vehicle. Then it needs to pass five higher priority levels, whose conflicting points are shown at the right part of Figure 5.9.

Firstly, the effectiveness of the proposed speed control algorithm is investigated with respect to fuel consumption and emission assuming no downstream vehicles (corresponding to Scenarios 1 to 3 defined in Section 3.2).

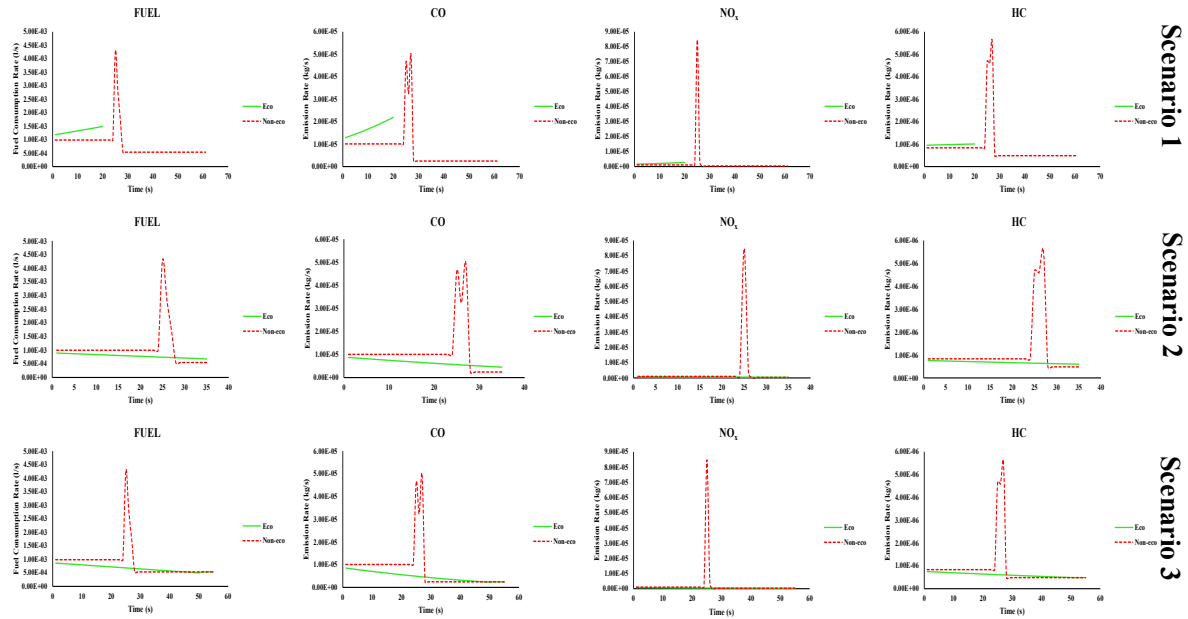


Figure 5.10 Comparison of fuel consumption and emission between speed control and free driving under Scenarios 1 to 3.

Figure 5.10 further shows the comparison of second-by-second fuel consumption and emission rates between speed control and free driving for the target vehicle.

Scenario 1 in Figure 5.10 shows significant difference in travel times for the target vehicle approaching the intersection (21s vs. 64s) under speed control and free driving. Such a difference is due to the fact that the vehicle under speed control passes the intersection without obstruction from the unavailable gaps or the downstream vehicles when following the speed guidance by the proposed algorithm. Nonetheless, without speed control the vehicle may experience the processes of cruising, deceleration and idling, resulting in much higher level of fuel consumption and emission. For other scenarios, although the travel time for the target vehicle under speed control is almost the same as that without eco-driving, the level of fuel consumption and emission is quite different (a surge of fuel consumption and emission can be observed for non-eco driving).

Then, we analyse driving behaviours and fuel consumption under the impact of the downstream vehicles and gap condition (corresponding to Scenarios 4 and 5). Emission analysis is very similar to fuel consumption therefore is skipped in this example.

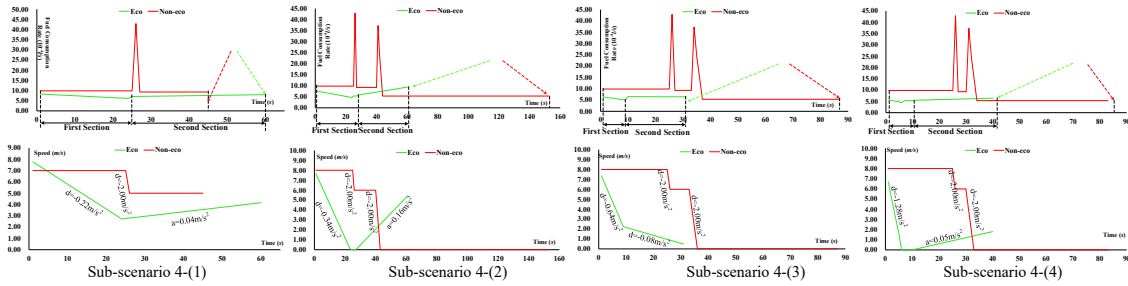


Figure 5.11 Comparison of fuel consumption and speed profile of the target vehicle between speed control and free driving under several conditions.

As shown in Figure 5.11, due to the presence of downstream vehicles and queue, the target vehicle without the proposed speed control algorithm usually needs to abruptly decelerate twice in its speed profile, first avoiding bumping into its downstream vehicles and second braking down due to the available gaps. However, the speed profile of the target vehicle with the proposed speed control algorithm is relatively smooth and flat, resulting much lower fuel consumption and emission.

5.4 Conclusions

This chapter proposes a dynamic speed control algorithm towards bottleneck mitigation at an unsignalized intersection, in the measure of fuel consumption and emissions. The algorithm not only considers the running status of the target vehicle but also captures the impact of downstream vehicles. Acceleration/deceleration rates, instead of speeds, are used as the control objective for speed guidance. Depending on the status of a target vehicle and gap conditions, the speed control algorithms under different scenarios are discussed in details. The proposed

algorithm not only works for an “ideal” situation, but also for a realistic environment where there exist downstream vehicles and initial queue at the stop line. This study provides illustrative examples to validate the algorithm. Firstly, without considering the impact of the downstream platoons, this study compares the time-varying fuel consumption and emission of the target vehicle with respect to speed control and free driving behaviours. Results indicate that the vehicle under the proposed algorithm experience significantly lower fuel consumption and emission than that under free driving. Then, considering the impact of the downstream vehicles and queue, this study compares the level of fuel consumption of the target vehicle with and without the proposed speed control. Results demonstrate the promising application of the proposed speed control algorithm in a realistic traffic environment.

Analysis results of the illustrative examples indicate the validity and effectiveness of the proposed speed control algorithm. On-going work of this study is to test the proposed algorithm in real-world projects and evaluate its effectiveness with calibrated fuel consumption models.

Chapter 6 COOPERATIVE BUS-CAR TRAJECTORY OPTIMIZATION TO ELIMINATE WEAVING BOTTLENECK AROUND CURB SIDE BUS STATIONS

This chapter develops a cooperative bus-car trajectory optimization model towards the elimination of weaving bottleneck at curb side (near-side) bus stations around signalized intersections. A two-phase algorithm is developed to solve the model, where a multi-stage-based nonlinear programming procedure is developed in Phase I to search trajectories that eliminate the conflicts in PWS and minimize the total person travel time and Phase II refines the trajectories with a mixed integer linear programming to minimize idling time of vehicles. An illustrative example is provided to validate the proposed model. Results indicate that the model is effective to eliminate the weaving bottleneck at curb side bus stations while minimizing the total person travel time and vehicular idling time. Sensitivity analysis is conducted, and it implies that with the increase of bus person number, the optimal rate of the total vehicular time declines, while of the total person travel time rises.

6.1 INTRODUCTION

The bus system, with its cost efficiency, design flexibility, and short construction period, has been widely developed in urban areas as an alternative to private cars for efficient, reliable and comfortable travel. As cities grow in both surface and population, the bus system often struggles to provide satisfying level of service due to limited road space coupled with increasing traffic demand. For example, it is common to observe serious conflicts between buses and cars weaving at a curb side bus station (no matter located near-side or far-side, see Figure 6.1). Such a potential weaving section (PWS) often causes traffic bottlenecks characterized with aggressive

lane changes, frequent stops, excessive delays, and frequent accidents especially as road saturation level increases. Compared with far-side locations, near-side bus stations may cause even worse traffic congestion due to high traffic flow weaving, limited road space, poor geometric design, and improper intersection signal timings.

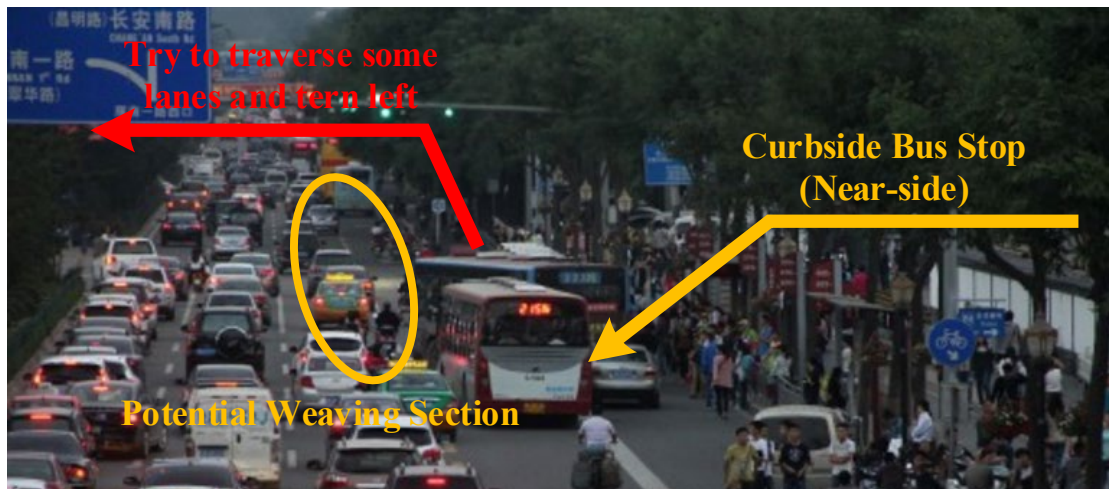


Figure 6.1 Potential weaving section at a near-side bus station.

The impact of curb side bus stations on traffic flow has been investigated in the literature. Previous studies fall into different categories, including observational studies, analytical methods, and simulation-based studies. Observational studies usually explore field data to examine the effect of bus stations on traffic operations. For examples, it was found that far-side bus stations tend to outperform near-side stops in terms of reduced queue, additional vehicle maneuvering space, easier lane changes, and fewer delayed right-turning vehicles. However, Fitzpatrick reached the opposite findings. Yu established a statistical model to quantify the impact of factors such as platform types, bus station lengths, and lane numbers. Feng statistically investigated the joint impacts of bus station locations, signalized intersections and traffic conditions. Stephen proposed a statistical model to explore the factors that may affect the bus dwelling time and the time to re-enter to the main traffic flow. These studies are informative but

not conclusive due to either limited numerical scenarios or the lack of detailed analysis of the relationships among important affecting factors such as bus frequency, dwelling time, and vehicle volume/distribution in the bus operational environment.

Analytical methods generally open to broader situations with simplified models for tractability. Furth evaluated the impact of harbor-style bus station location on bus delay with factors of gravity, queue interference at signalized intersections. As for curb side bus stations, queue model was developed to assess disturbance from cars on isolated bus stations, without involving signalized intersections. Gu further incorporated signalized intersections to research the impact of far-side and near-side bus stations on traffic efficiency but did not include either oversaturated conditions or instant traffic disturbances such as lane changes, gaps in front of the dwelling bus and turning vehicles.

Simulations are widely used to investigate the microscopic interactions between the bus and vehicles. As a highly developed simulation method, Cellular automation (CA) model has been used to evaluate the impact of bus station locations on traffic flow dynamics. In CA models, roads are generally divided into cells with lengths equal to the bus. Long proposed a CA model to find the congestion mechanism due to bus stations located around on-ramp or off-ramp roads. Liu developed a CA model to explore the impact of bus stations on traffic flow, with consideration of bus parking style, bus station length, bus station spacing and bus proportion. In multi-lane mixed traffic flows, the CA model has been used to study the effect of bus proportion in traffic flow. Moreover, as an inexpensive and efficient procedure, agent-based simulation was applied to evaluate bus station layout design in relation to passengers' preferences, needs and expectations.

Continuous efforts have been made to eliminate the traffic bottleneck caused by mixed traffic dynamics near bus stations, including relocation/redesign optimization and signal control strategies. For examples, Moura et al. developed a two-stage model by first minimizing the social cost at the macroscopic scale and then maximizing the commercial speed along with sensitivity analysis in terms of traffic flow, bus flows and signaling sequences. Gu et al. used kinematic wave theory to formulate models for locating near-side stops to achieve target levels of residual queueing among cars. A multi-objective optimization model was employed for multi-objective optimization of bus station location to improve accessibility and minimize vehicle delay. Though optimizing the location or redesigning bus station may alleviate traffic congestion to some extent, its real-world application is usually limited by available road space, construction limitations, and complicated flow composition.

Therefore, this study contributes to developing a cooperative bus-car trajectory optimization model that can effectively prevent weaving conflicts between buses and general traffic around a curb side bus station (see Fig. 6.2), while minimizing total person travel time and idling time of traffic through the signalized intersection. The proposed model applies when a potential conflict is detected in the PWS given the speed, occupancy, location of approaching vehicles and signal timing information. It enables bus-car and vehicle-signal cooperation through a two-phase optimization process, where a multi stage based nonlinear programming (NLP) procedure is developed in Phase I to search trajectories that eliminate the conflicts in PWS and minimize the total person travel time and Phase II refines the trajectories with a mixed integer linear programming (MILP) to minimize idling time of vehicles.

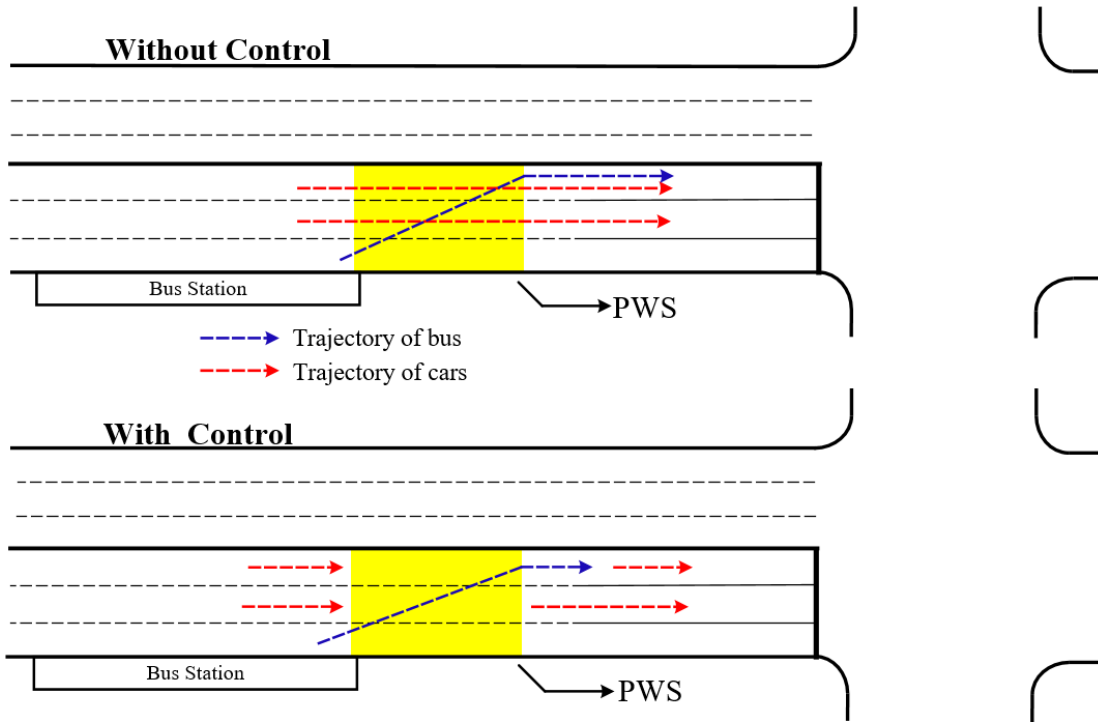


Figure 6.2 Trajectory optimization to prevent weaving at a curb side bus station.

6.2 Trajectory Optimization Model

6.2.1 Notation

To facilitate model presentation, indices and parameters used hereafter are listed in Table 6.1.

Table 6.1 Symbols and parameters.

<i>Index</i>	
k	Index of lanes, $k = j, j + 1, \dots i$
p	Index of cars on a lane, $p = 1, 2, \dots$
t	Index of time steps, $t = 0, 1, 2, \dots$
<i>General Constants and Variables</i>	
x_{PWS}	Length of the PWS (m)
x_C	Distance between the downstream boundary of PWS and the stop line (m)
$x_{k,p}^0$	Initial distance between the stop line and the p^{th} car on the k^{th} lane (m)
x_{bus}^0	Initial distance between the stop line and bus (m)
x_{scope}	Length of the control scope (m)
$x_{k,p}^{PWS}$	Distance between the upstream boundary of the PWS and the front bumper of the p^{th} car on the k^{th} lane (m), and its value is negative if the car has already entered the PWS
x^{0r}	Initial location for the nearest downstream vehicle (m)
v_t'	Speed at time t for the nearest downstream vehicle (m/s)
w	Lane width (m)

l_{bus}	Length of bus (m)
l_{car}	Average length of a car (m)
v_{max}	Maximum speed limit (m/s)
v_{med}	Median speed (m/s)
v_{min}	Minimum cruising speed (m/s)
a_{car}	Maximum acceleration rate for cars (m/s^2)
$-d_{car}$	Maximum deceleration rate for cars (m/s^2)
a_{bus}	Maximum acceleration rate for bus (m/s^2)
$-d_{bus}$	Maximum deceleration rate for bus (m/s^2)
t_{board}	Time for bus boarding and alighting (s)
t_{ij}	Time for bus to traverse from the curb side lane i to destination lane j (s)
$t_{k,p}^{PWS}$	Time for the p^{th} car on the k^{th} lane to hit the PWS (s)
$t'_{k,p}$	Time for the p^{th} car on the k^{th} lane inside the control boundary to traverse the PWS (s)
$t_{k,p}$	Time for the p^{th} car on the k^{th} lane inside the control boundary to pass the intersection (s)
$t_{k,0}$	Time for the last downstream vehicle on the k^{th} lane to pass the intersection (s)
TTR_k	Time to red indication for the k^{th} lane when the bus just stops at the station (s), which is negative and its absolute value equals to the duration since the red light has appeared, if the signal light displays red at the instant
C	Signal cycle length (s)
r_k	Duration of red interval for the k^{th} lane (s)
g_k	Duration of green interval for the k^{th} lane (s)
R_k	Ranges of red interval for the k^{th} lane
n_k	Number of cars on the k^{th} lane (pcu)
$P_{k,p}$	Number of passengers in the p^{th} car on the k^{th} lane
P_{bus}	Number of passengers in the bus ($person$)
Decision Variables	
$v_t^{k,p}$	Speed of the p^{th} car on the k^{th} lane at time t (m/s)
v_t^{bus}	Speed of bus at time t (m/s)
Auxiliary Variables	
$U_t^{p,k}$	Indicator of idling for the p^{th} car on the k^{th} lane at time t
U_t^{bus}	Indicator of idling for the bus at time t

6.2.2 Weaving determination

When a bus leaves the curb side station, it may traverse one or more lanes in the PWS to enter its destination lane to clear the intersection, as shown in Fig. 6.3. The time for the bus to traverse from the curb side lane i to destination lane j ($i > j$) is given by:

$$t_{ij} = (\sqrt{(x_{PWS})^2 + [(j - i + 1)w]^2} + l_{bus}) / v_{bus} \quad (1)$$

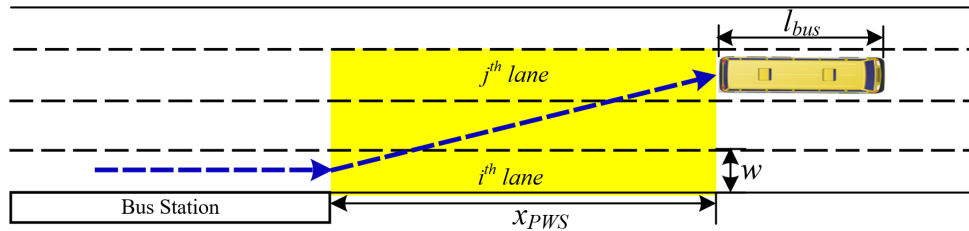


Figure 6.3 A bus traversing PWS.

Fig. 6.4 illustrates the distribution of cars on the k th lane ($i > k > j$), when the bus just stops at the station. At the instant, the time for the p th car (counted from the stop line) inside the control boundary to hit PWS can be estimated with:

$$t_{k,p}^{PWS} = \begin{cases} \frac{x_{PWS}}{v_{k,p}}, & x_{k,p}^{PWS} > 0 \\ 0, & x_{k,p}^{PWS} \leq 0 \end{cases}, p \in [1, n_k] \quad (2)$$

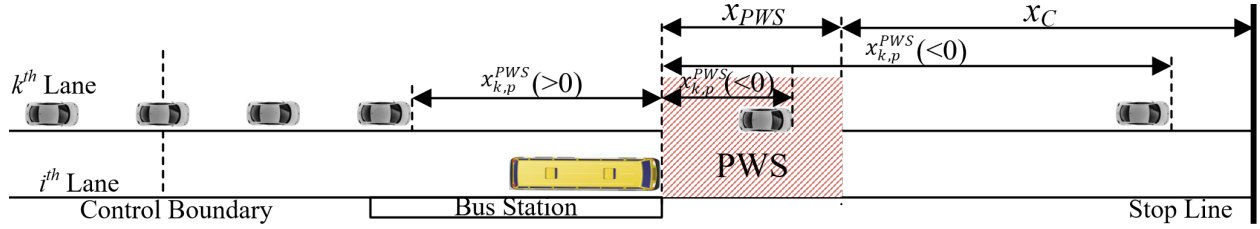


Figure 6.4 Distribution of platoon upstream of bus station.

Therefore, the time for the p th car on the k th lane inside the control boundary to traverse the PWS can be estimated with:

$$t'_{k,p} = \begin{cases} \frac{x_{k,p}^{PWS} + x_{PWS}}{v_{k,p}}, & x_{k,p}^{PWS} + x_{PWS} > 0 \\ 0, & x_{k,p}^{PWS} + x_{PWS} \leq 0 \end{cases}, k \in [j, i]; p \in [1, n_k] \quad (3)$$

Note that the speed $v_{k,p}$ can be zero, due to the impact of signal control or initial queue. If so, $t_{k,p}$ and $t'_{k,p}$ may be infinity. Given (1) - (3), potential weaving between the dwelling bus and the upstream platoon in the PWS under the current speed can be determined with (see Fig. 6.5 for illustration) either of the following formulas.

$$\begin{cases} t_{k,p}^{PWS} > t_{board} \\ t_{k,p}^{PWS} < t_{board} + t_{ij} \end{cases}, \forall k; \forall p \quad (4)$$

$$\begin{cases} t_{board} > t_{k,p}^{PWS} \\ t_{board} < t'_{k,p} \end{cases}, \forall k; \forall p \quad (5)$$

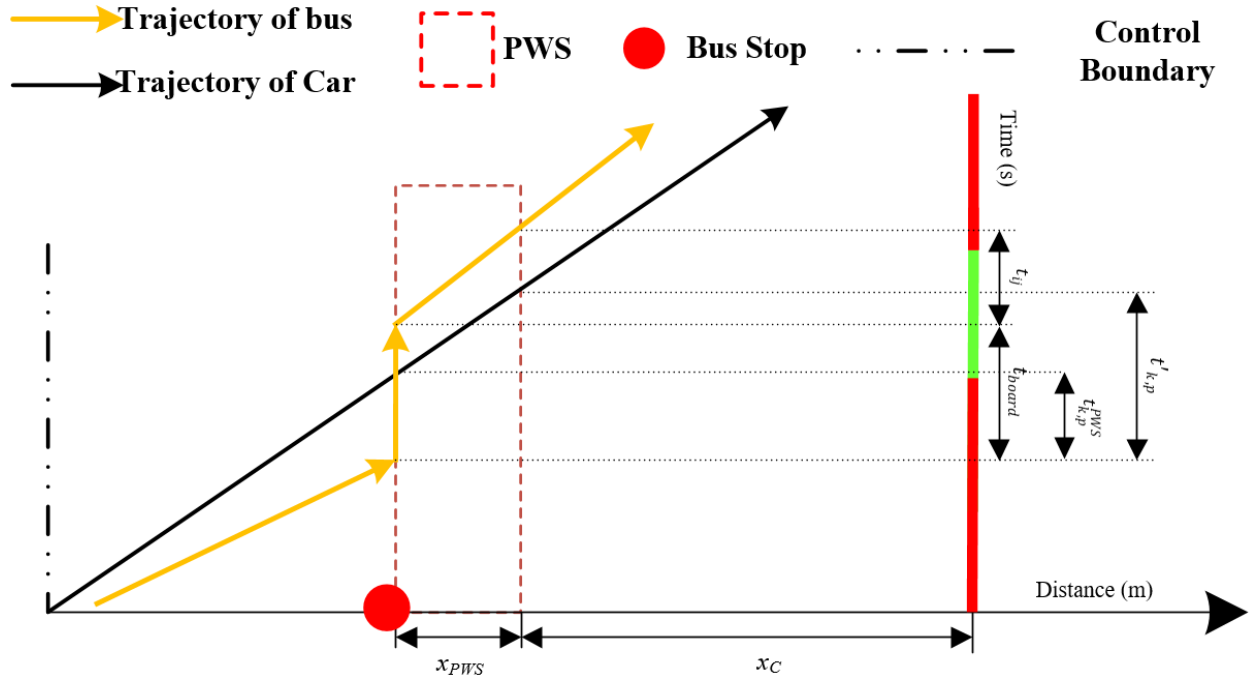


Figure 6.5 Weaving determination at PWS.

6.2.3 Determination of control scope

If weaving within the PWS is identified, the proposed cooperative bus-car trajectory optimization model will be applied to control the status of bus and cars within a predetermined control scope. An over short scope cannot provide enough space for the vehicle to change its status according to the control guidance, while the motorist cannot keep the optimized status if the control scope is too long. In this study, the scope can be estimated with:

$$-\frac{1}{2d_{car}} \cdot v_{max}^2 + \frac{1}{2a_{car}} \cdot v_{max}^2 \leq x_{scope} \quad (6)$$

$$c \cdot v_{min} \geq x_{scope} \quad (7)$$

$$g \cdot v_{med} \geq x_{scope} \quad (8)$$

According to formulas (6) to (8), the control scope x_{scope} should be determined to make sure: (1) the car has enough space to stop before the stop line; (2) the car has enough space to accelerate to the maximum speed limit; (3) travel time with the minimum cruising speed to the

stop line should be no greater than the cycle length; and (4) travel time with the median speed to the stop line should be no greater than the green interval when no congestion presents.

6.2.4 Model formulation

If a weaving conflict is determined at PWS, the following model can be formulated for cooperative bus-car trajectory optimization.

Objective functions

The objectives of the model include: (1) minimizing the total person travel time, and (2) conditioned on the objective (1), minimizing the sum of vehicular idling time, given by:

$$\min \left(\sum_{p=1}^{n_k} \sum_{k=j}^i t_{k,p} \cdot P_{k,p} \right) + t_{bus} \cdot P_{bus} \quad (9)$$

$$\max \left(\sum_{p=1}^{n_k} \sum_{k=j}^i \sum_{t=1}^{t_{k,p}} U_t^{p,k} + \sum_{t=1}^{t_{bus}} U_t^{bus} \right) \quad (10)$$

where,

$U_t^{p,k}$ = indicator of idling for the p^{th} car on the k^{th} lane at time t , given by:

$$U_t^{p,k} = \begin{cases} 0, & v_t^{k,p} = 0 \\ 1, & o.w. \end{cases}, k \in [j, i]; p \in [1, n_k]; t \in [1, t_{k,p}] \quad (11)$$

U_t^{bus} = indicator of idling for the bus at time t , given by:

$$U_t^{bus} = \begin{cases} 0, & v_t^{bus} = 0 \\ 1, & o.w. \end{cases}, t \in [1, t_{bus}] \quad (12)$$

Constraints

Vehicular speeds should not exceed the maximum speed limit, given by:

$$0 \leq v_t^{k,p} \leq v_{max}, \quad k \in [j, i]; p \in [1, n_k]; t \in [0, t_{k,p}] \quad (13)$$

$$0 \leq v_t^{bus} \leq v_{max}, \quad t \in [0, t_{bus}] \quad (14)$$

where $v_t^{k,p}$ is the speed of the p^{th} car on the k^{th} lane at time t , and v_t^{bus} is the speed of the bus at time t .

Furthermore, the cruising speed should not be less than a minimum value, given by:

$$v_t^{k,p} \geq v_{min} \text{ if } v_t^{k,p} = v_{t-1}^{k,p}, \quad k \in [j, i]; p \in [1, n_k]; t \in [1, t_{k,p}] \quad (15)$$

$$v_t^{bus} \geq v_{min} \text{ if } v_t^{bus} = v_{t-1}^{bus}, \quad t \in [1, t_{bus}] \quad (16)$$

Vehicular acceleration/deceleration rate should not exceed the limit, given by:

$$-d_{car} \leq v_t^{k,p} - v_{t-1}^{k,p} \leq a_{car}, \quad k \in [j, i]; p \in [1, n_k]; t \in [1, t_{k,p}] \quad (17)$$

$$-d_{bus} \leq v_t^{bus} - v_{t-1}^{bus} \leq a_{bus}, \quad t \in [1, t_{bus}] \quad (18)$$

A safe distance should always be maintained between two successive vehicles to prevent colliding. To express the constraints linearly, the safe distance calculation is simplified with the ‘‘Three-second rule’’, given by:

$$x_{k,p}^0 - \frac{1}{2} \sum_{q=0}^{t-1} (v_q^{k,p} + v_{q+1}^{k,p}) - x_{k,p-1}^0 + \frac{1}{2} \sum_{q=0}^{t-1} (v_q^{k,p-1} + v_{q+1}^{k,p-1}) \geq 3v_t^{k,p}, \quad (19)$$

$$k \in [j, i]; p \in [2, n_k]; t \in [1, t_{k,p}] \cap [1, t_{k,p-1}]$$

$$x_{k,1}^0 - \frac{1}{2} \sum_{q=0}^{t-1} (v_q^{k,1} + v_{q+1}^{k,1}) - x_{0'}^0 + \frac{1}{2} \sum_{q=0}^{t-1} (v_q' + v_{q+1}') \geq 3v_t^{k,1}, \quad k \in [j, i]; t \in [1, t_{k,p}] \cap [1, t_{k,0}] \quad (20)$$

$$x_{bus}^0 - \frac{1}{2} \sum_{q=0}^{t-1} (v_q^{bus} + v_{q+1}^{bus}) - x_{j,p}^0 + \frac{1}{2} \sum_{q=0}^{t-1} (v_q^{j,p} + v_{q+1}^{j,p}) \geq 3v_t^{bus}, \quad (21)$$

$$p \in [1, n_j]; t \in [0, t_{j,p}] \cap t \in [1, t_{bus}]$$

$$\text{if } x_{bus}^0 - \frac{1}{2} \sum_{q=0}^{t-1} (v_q^{bus} + v_{q+1}^{bus}) < x_{j,p}^0 - \frac{1}{2} \sum_{q=0}^{t-1} (v_q^{j,p} + v_{q+1}^{j,p}) \cap x_c \geq x_{bus}^0 - \frac{1}{2} \sum_{q=0}^{t-1} (v_q^{bus} + v_{q+1}^{bus})$$

$$x_{j,p}^0 - \frac{1}{2} \sum_{q=0}^{t-1} (v_q^{j,p} + v_{q+1}^{j,p}) - x_{bus}^0 + \frac{1}{2} \sum_{q=0}^{t-1} (v_q^{bus} + v_{q+1}^{bus}) \geq 3v_t^{j,p}, \quad (22)$$

$$p \in [1, n_j]; t \in [0, t_{j,p}] \cap [1, t_{bus}]$$

$$\text{if } x_c \geq x_{bus}^0 - \frac{1}{2} \sum_{q=0}^{t-1} (v_q^{bus} + v_{q+1}^{bus}) \text{ or } > x_{bus}^0 - \frac{1}{2} \sum_{q=0}^{t-1} (v_q^{bus} + v_{q+1}^{bus}) \geq x_{j,p}^0 - \frac{1}{2} \sum_{q=0}^{t-1} (v_q^{j,p} + v_{q+1}^{j,p})$$

Formulas (19) and (20) maintains the safe distance between cars, where $x^{0'}$ and v_t' are the initial location and speed at time t for the nearest downstream vehicle, and $t_{k,0}$ is the time for the last downstream vehicle to pass the intersection. Formulas (21) and (22) process this

constraint between cars and bus on the destination lane j , whether or not the bus is ahead of the car. For other lanes, these constraints can be handled with weaving elimination, given by:

$$x_{k,p}^0 - \frac{1}{2} \sum_{q=0}^{t-1} (v_q^{k,p} + v_{q+1}^{k,p}) - x_C > x_{PWS} \text{ or } x_{k,p}^0 - \frac{1}{2} \sum_{q=0}^{t-1} (v_q^{k,p} + v_{q+1}^{k,p}) - x_C < -x_{PWS}, \quad (23)$$

$$\text{if } \frac{1}{2} \sum_{q=0}^{t-1} (v_q^{bus} + v_{q+1}^{bus}) \leq x_{bus}^0 - x_C + l_{bus}, \quad k \in [j, i]; p \in [1, n_k]; t \in [0, t_{k,p}] \cap t \in [1, t_{bus}]$$

$$\frac{1}{2} \sum_{q=0}^{t-1} (v_q^{bus} + v_{q+1}^{bus}) > x_{bus}^0 - x_C + l_{bus} \text{ or } \frac{1}{2} \sum_{q=0}^{t-1} (v_q^{bus} + v_{q+1}^{bus}) = 0, \quad (24)$$

$$\text{if } x_{k,p}^0 - \frac{1}{2} \sum_{q=0}^{t-1} (v_q^{k,p} + v_{q+1}^{k,p}) - x_C - x_{PWS} \leq 0,$$

$$k \in [j, i]; p \in [1, n_k]; t \in [0, t_{k,p}] \cap t \in [1, t_{bus}]$$

The constraints of weaving elimination prevent the bus and cars from conflicting in the PWS simultaneously, where formula (23) applies when the bus is in the PWS and formula (24) holds when a car is inside the PWS.

Red light violation shall also be strictly prohibited with the following constraints, as illustrated in Fig. 6.6.

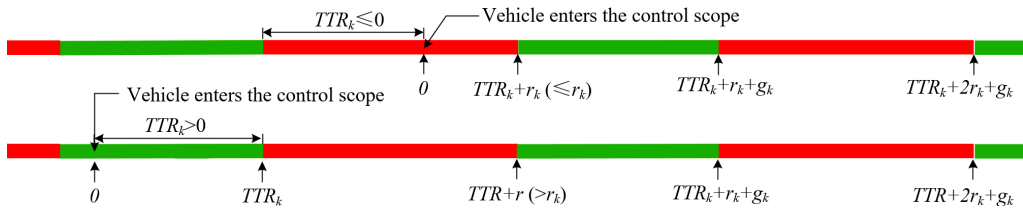


Figure 6.6 Ranges of R_k under various initial signal information.

$$\frac{1}{2} \sum_{q=0}^{r-1} (v_q^{k,p} + v_{q+1}^{k,p}) \leq x_{k,p}^0, \quad k \in [j, i]; p \in [1, n_k]; r \in R_k \cap [1, t_{k,p}] \quad (25)$$

$$\frac{1}{2} \sum_{q=0}^{r-1} (v_q^{bus} + v_{q+1}^{bus}) \leq x_{bus}^0, \quad r \in R_j \cap [1, t_{bus}] \quad (26)$$

It can be found in Fig.6.6 that, if the signal for the k th lane initially displays red, TTR_k is negative and its absolute value equals to the duration since the red light has displayed (the yellow

duration is categorized to the green interval). Thus, the remaining red interval during the current cycle can be expressed with $TTR_k + r_k$. Accordingly, the red interval of the next cycle can be expressed with $[TTR_k + r_k + g_k, TTR_k + r_k + g_k + r_k]$, equivalent to $[TTR_k + C, TTR_k + r_k + C]$. While if the signal initially displays green, the TTR_k is positive and equals to the remaining green interval, and the red interval of the next cycle can be expressed with $[TTR_k + g_k, TTR_k + g_k + r_k]$. Therefore, the range of the red interval for each lane can be summarized by the following formulas.

$$R_k \in [0, TTR_k + r_k] \cup [TTR_k + zC, TTR_k + r_k + zC], TTR_k \leq 0, z = 1, 2, \dots \quad (27)$$

$$R_k \in [TTR_k + r_k + zC, TTR_k + (z + 1)C], TTR_k > 0, z = 0, 1, 2, \dots \quad (28)$$

6.3 Solution algorithm

This study proposes a two-phase algorithm to solve the proposed optimization model, as illustrated in Fig. 6.7, where Phase I features a multi-stage-based NLP to minimize the total person travel time and eliminate conflict in the PWS between bus and cars; and Phase II develops a MILP to further minimize the vehicular idling time conditioned on the travel time of each vehicle determined in Phase I.

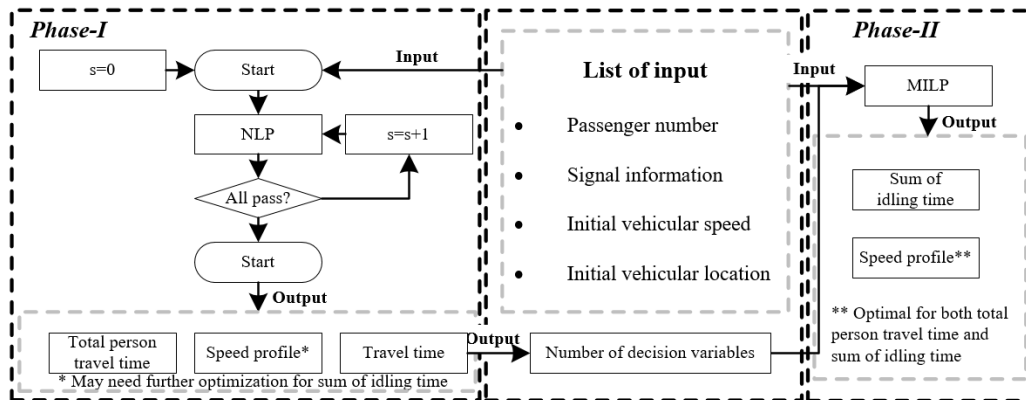


Figure 6.7 A two-phase solution algorithm.

6.3.1 Phase I – Conflict elimination and total person travel time minimization

Due to the time-varying fluctuation of traffic conditions, it is infeasible and impractical to optimize vehicular trajectories over the entire control horizon with any “one-off” algorithms. Rather, a rolling-based solution algorithm can be developed and applied in a stage-by-stage decision process in Phase I. As illustrated in Fig. 6.8, based on the information from the previous stage, the algorithm will find the optimal vehicle and bus speed trajectories to prevent conflicts in the PWS while minimizing the total person travel time with the assumption that the speeds will be maintained till the clearance of vehicles through the intersection. The optimization process repeats itself with the time horizon moving one stage ahead at the end of the current stage. The interval of a stage, denoted as H , should be as short as possible but be sufficient for any vehicle to switch between idling and traveling with the maximum speed limit. The following sections will detail the stage state transfer functions along with stage-based objective functions and constraints for the rolling algorithm.

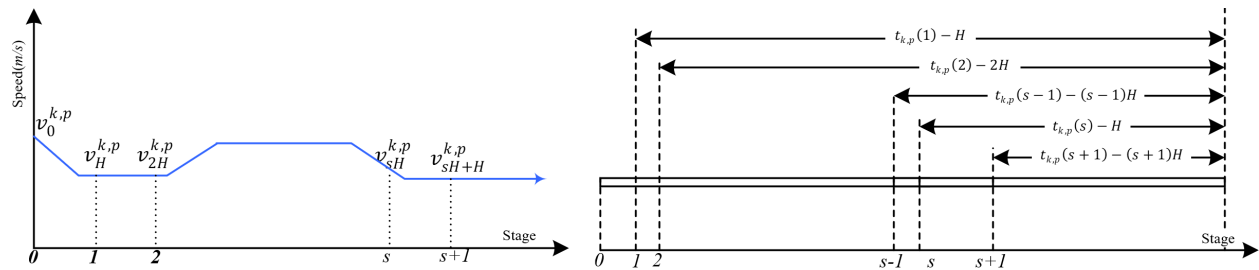


Figure 6.8 Multi-stage decision making for vehicle trajectory optimization in Phase I.

During the rolling-based optimization algorithm, the optimization in the current stage is based upon the outcome of in the previous one. Therefore, the state transfer function in the two successive stages is proposed as follows.

Update speed

Given the interval H , the time index at the s^{th} stage (start from 0) can be expressed as $t=sH$.

Accordingly, the speed variables for the car between the s^{th} and $s+1^{\text{th}}$ stages can be updated with:

$$v_t^{k,p} = \begin{cases} v_{sH}^{k,p}, & t = sH \\ v_{sH+H}^{k,p}, & t = sH + H \\ \max(v_{sH}^{k,p} + m_s^{k,p}(t - sH), v_{sH+H}^{k,p}), & m_s^{k,p} < 0, sH < t < sH + H \\ \min(v_{sH}^{k,p} + m_s^{k,p}(t - sH), v_{sH+H}^{k,p}), & m_s^{k,p} > 0, sH < t < sH + H \end{cases} \quad (29)$$

where, $m_s^{k,p}$ is an indicator for speed update, given by:

$$m_s^{k,p} = \begin{cases} a_{car}, & v_{sH+H}^{k,p} > v_{sH}^{k,p} \\ -d_{car}, & v_{sH}^{k,p} \leq v_{sH+H}^{k,p} \end{cases} \quad (30)$$

The update of bus speed is similar, given by:

$$v_t^{bus} = \begin{cases} v_{sH}^{bus}, & t = sH \\ v_{sH+H}^{bus}, & t = sH + H \\ \max(v_{sH}^{bus} + m_s^{bus}(t - sH), v_{sH+H}^{bus}), & m_s^{bus} < 0, sH < t < sH + H \\ \max(v_{sH}^{bus} + m_s^{bus}(t - sH), v_{sH+H}^{bus}), & m_s^{bus} > 0, sH < t < sH + H \end{cases} \quad (31)$$

$$m_s^{bus} = \begin{cases} a_{bus}, & v_{sH+H}^{bus} > v_{sH}^{bus} \\ -d_{bus}, & v_{sH}^{bus} \leq v_{sH+H}^{bus} \end{cases} \quad (32)$$

Update travel distance

Given the speed update process, the accumulated travel distance for a car can be updated with:

$$D_{k,p,s+1} = D_{k,p,s} + d_{s,k,p}(t)|_{t=sH+H}, \quad D_{k,p,0} = 0 \quad (33)$$

where, $d_{s,k,p}(t)$ is the travel distance at time t for the p^{th} car on the k^{th} lane, given by:

$$d_{s,k,p}(t) = \begin{cases} \frac{1}{2}(v_t^{k,p} + v_{sH}^{k,p})(t - sH), & v_t^{k,p} \neq v_{sH+H}^{k,p} \\ \frac{v_{sH+H}^{k,p}{}^2 - v_{sH}^{k,p}{}^2}{2m_s^{k,p}} + v_{sH+H}^{k,p} \left(t - sH - \frac{v_{sH+H}^{k,p} - v_{sH}^{k,p}}{m_s^{k,p}} \right), & v_t^{k,p} = v_{sH+H}^{k,p} \end{cases} \quad (34)$$

The travel distance at time t for the bus $d_{s,bus}(t)$ can be obtained with a similar procedure, given by:

$$D_{bus,s+1} = D_{bus,s} + d_{s,bus}(t)|_{t=sH+H}, \quad D_{bus,0} = 0 \quad (35)$$

$$d_{s,bus}(t) = \begin{cases} \frac{1}{2}(v_t^{bus} + v_{sH}^{bus})(t - sH), & v_t^{bus} \neq v_{sH+H}^{bus} \\ \frac{v_{sH+H}^{bus^2} - v_{sH}^{bus^2}}{2m_s^{k,p}} + v_{sH+H}^{bus} \left(t - sH - \frac{v_{sH+H}^{bus} - v_{sH}^{bus}}{m_s^{k,p}} \right), & v_t^{bus} = v_{sH+H}^{bus} \end{cases} \quad (36)$$

Update travel time

As shown in Fig. 6.8, the travel time at the sth stage for the pth car on the kth lane can be given by:

$$t_{k,p,s} = \frac{x_{k,p}^0 - D_{k,p,s}}{v_{sH}^{k,p} + y_s^{k,p}} + sH \quad (37)$$

In formula (33), $y_s^{k,p}$ is an auxiliary variable applied to the travel time in case the vehicle's speed is zero, given by:

$$y_s^{k,p} = \begin{cases} 0, & v_{sH}^{k,p} > 0 \\ \varepsilon, & v_{sH}^{k,p} = 0 \end{cases} \quad (38)$$

where, ε is a very small positive number.

The travel time of bus has the similar update process, given by:

$$t_{bus,s} = \frac{x_{bus}^0 - D_{bus,s}}{v_{sH}^{bus} + y_s^{bus}} + sH; y_s^{bus} = \begin{cases} 0, & v_{sH}^{bus} > 0 \\ \varepsilon, & v_{sH}^{bus} = 0 \end{cases} \quad (39)$$

It can be found from formula (33) that at the sth stage if the vehicle has already cleared the intersection, the result of $x_{k,p}^0 - D_{k,p,s}$ is negative, and therefore the travel time will be less than Hs .

Finally, the transfer function of travel time between the sth and the s+1th stage is given by:

$$t_{k,p,s+1} = t_{k,p,s} + \Delta t_{k,p,s} \quad (40)$$

where,

$$\Delta t_{k,p,s} = \begin{cases} \frac{x_{k,p}^0 - D_{k,p,s} - d_{s,k,p}(sH + H)}{v_{s+sH}^{k,p} + y_{s+1}^{k,p}} + H, & s = 0 \\ \frac{x_{k,p}^0 - D_{k,p,s} - d_{s,k,p}(sH + H)}{v_{s+sH}^{k,p} + y_{s+1}^{k,p}} - \frac{x_{k,p}^0 - D_{k,p,s}}{v_{sH}^{k,p} + y_s^{k,p}} + H, & s > 0 \end{cases} \quad (41)$$

Similarly, the state transfer function of travel time for the bus between the s^{th} and the $s+1^{\text{th}}$ stage can be given by:

$$t_{bus,s+1} = t_{bus,s} + \Delta t_{bus,s} \quad (42)$$

$$\Delta t_{bus,s} = \begin{cases} \frac{x_{bus}^0 - D_{bus,s} - d_{s,bus}(sH + H)}{v_{s+sH}^{bus} + y_{s+1}^{bus}} + H, & s = 0 \\ \frac{x_{bus}^0 - D_{bus,s} - d_{s,bus}(sH + H)}{v_{s+sH}^{bus} + y_{s+1}^{bus}} - \frac{x_{bus}^0 - D_{bus,s}}{v_{sH}^{bus} + y_s^{bus}} + H, & s > 0 \end{cases} \quad (43)$$

Update total person travel time

The total person travel time for all vehicles within the control scope at the s^{th} stage, is defined as the sum of each vehicular product of travel time and passenger number, given by:

$$T_s = \begin{cases} 0, & s = 0 \\ \sum_{p=1}^{n_k} \sum_{k=j}^i (t_{k,p,s} \cdot P_{k,p}) + t_{bus,s} \cdot P_{bus}, & s > 0 \end{cases} \quad (44)$$

The state transfer function between the s^{th} and the $s+1^{\text{th}}$ stage can then be updated with:

$$T_{s+1} = T_s + \sum_{p=1}^{n_k} \sum_{k=j}^i (\Delta t_{k,p,s} \cdot P_{k,p}) + \Delta t_{bus,s} \cdot P_{bus} \quad (45)$$

Note that x_{bus}^0 is estimated with:

$$x_{bus}^0 = x_C + \sqrt{(x_{PWS})^2 + [(j - i + 1)w]^2} \quad (46)$$

Given the state transfer functions between stages, the objective function of Phase I can be rewritten as minimizing the difference of total person travel time between two successive stages, given by

$$\min \sum_{p=1}^{n_k} \sum_{k=j}^i (\Delta t_{k,p,s} \cdot P_{k,p}) + (\Delta t_{k,p,s} \cdot P_{bus}) |_{D_{k,p,s^*} > x_{k,p}^0; D_{bus,s^*} > x_{bus}^0, \forall k; \forall p} \quad (47)$$

where, s^* represents the final stage; D_{k,p,s^*} and D_{bus,s^*} are the accumulated travel distance

at the stage s^* for the p th car on the k th lane and the bus, respectively.

Accordingly, the constraints listed in Section 6.2.4 can be converted to their stage-based forms, given as follows:

Constraints of speed limit and cruising speed limit:

$$0 \leq v_t^{k,p} \leq v_{max}, \quad k \in [j, i]; p \in [1, n_k]; t = sH \quad (48)$$

$$0 \leq v_t^{bus} \leq v_{max}, \quad t = sH \quad (49)$$

$$v_t^{k,p} \geq v_{min}, \quad k \in [j, i]; p \in [1, n_k]; t = sH \quad (50)$$


$$v_t^{bus} \geq v_{min}, \quad t = sH \quad (51)$$

Constraint of safe distance maintenance:

$$x_{k,p}^0 - D_{k,p,s-1} - d_{s,k,p}(t) - [x_{k,p-1}^0 - D_{k,p-1,s-1} - d_{s,k,p-1}(t)] \geq 3v_t^{k,p}, k \in [j, i]; p \in [1, n_k]; t \in [sH, s^*H] \quad (52)$$

$$x_{bus}^0 - D_{bus,s-1} - d_{s,bus}(t) - [x_{j,p-1}^0 - D_{j,p-1,s-1} - d_{s,j,p}(t)] \geq 3v_t^{bus}, \quad p \in [1, n_j]; t \in [sH, s^*H] \quad (53)$$

$$x_{k,p}^0 - D_{j,p,s-1} - d_{s,j,p}(t) - [x_{bus}^0 - D_{bus,s-1} - d_{s,bus}(t)] \geq 3v_t^{j,p}, \quad p \in [1, n_j]; t \in [sH, s^*H] \quad (54)$$

If the bus on the destination lane should never exceeds the stop line before the algorithm is terminated, given by 

$$x_{bus}^0 - D_{bus,s-1} - d_{s,j,p}(t) \leq x_C, \quad t \in [sH, s^*H] \quad (55)$$

Constraint of weaving elimination:

$$x_{k,p}^0 - D_{k,p,s-1} - d_{s,k,p}(t) - x_C > x_{PWS} \text{ or } x_{k,p}^0 - D_{k,p,s-1} - d_{s,k,p}(t) - x_C < -x_{PWS}, \quad (56)$$

$$\text{if } D_{bus,s-1} + d_{s,bus}(t) \leq x_{bus}^0 - x_C + l_{bus}; k \in [j, i]; p \in [1, n_k]; t \in [sH, s^*H] \quad (57)$$

$$\text{if } x_{k,p}^0 - D_{k,p,s-1} - d_{s,k,p}(t) - x_C - x_{PWS} \leq 0; k \in [j, i]; p \in [1, n_k]; t \in [sH, s^*H]$$

Constraint of red violation prevention:

$$D_{k,p,s-1} + d_{s,k,p}(t) \leq x_{k,p}^0, k \in [j, i]; p \in [1, n_k]; t + sH - H \in R_k \cap [sH - H, s^*H]; \text{if } D_{k,p,s-1} \leq x_{k,p}^0 \quad (58)$$

$$D_{bus,s-1} + d_{s,bus}(t) \leq x_{bus}^0, t + sH - H \in R_j \cap [sH - H, s^*H]; \text{if } D_{bus,s-1} \leq x_{bus}^0 \quad (59)$$

6.3.2 Phase II- Idling minimization

Phase II of the algorithm aims to further tune vehicular trajectories from Phase I so that the idling time for each vehicle is minimized for energy and environmental considerations.

Objective function

The objective function of the MILP is to minimize the sum of idling time for each vehicle. It can be fulfilled by maximizing the number of non-zero idling indicators at each second. One can express this function with:

$$\max \left(\sum_{p=1}^{n_k} \sum_{k=j}^i \sum_{t=0}^{t_{k,p}^*} U_t^{p,k} + \sum_{t=0}^{t_{bus}^*} U_t^{bus} \right) \quad (60)$$

Given the travel time for the cars and bus optimized in Phase I denoted as $t_{k,p}(s^*)$ and $t_{bus}(s^*)$, the number of decision variables for each vehicle can be estimated with:



$$t_{k,p}^* = \lfloor t_{k,p}(s^*) \rfloor + 1; \quad t_{bus}^* = \lfloor t_{bus}(s^*) \rfloor + 1, \quad k \in [j, i]; \quad p \in [1, n_k] \quad (61)$$

The accumulated travel distance for the p^{th} car on the k^{th} lane at time t is given by:

$$D_t^{k,p} = \begin{cases} \frac{1}{2} \sum_{q=0}^{t-1} v_q^{k,p} + v_{q+1}^{k,p}, & t < t_{k,p}^* \\ \frac{1}{2} (v_{t_{k,p}^*-1}^{k,p} + v_{t_{k,p}^*}^{k,p}) (t_{k,p}(s^*) + 1 - t_{k,p}^*) + \frac{1}{2} \sum_{q=0}^{t_{k,p}^*-1} (v_q^{k,p} + v_{q+1}^{k,p}), & t = t_{k,p}^* \end{cases}, \quad k \in [j, i]; \quad p \in [1, n_k] \quad (62)$$

The second row of formula [62](#) implies the time interval between the last two speed variables is $t_{k,p}(s^*) + 1 - t_{k,p}^*$, instead of one second.

Constraints

All constraints, listed in Section 6.2.4, should be converted to the linear form, which is neglected in this chapter. While the condition for algorithm termination, as vehicles should finally pass the intersection, should be added to the constraint list. One can express the condition with:

$$x_{k,p}^0 - D_{t_{k,p}^*}^{k,p} \leq 0, \quad (63)$$

$$x_{bus}^0 - D_{t_{bus}^*}^{bus} \leq 0 \quad (64)$$

$$v_{t_{k,p}^*}^{k,p} M \geq M_1 \quad (65)$$

$$v_{t_{k,p}^*}^{bus} M \geq M_1 \quad (66)$$

Regarding formulas (63) to (66), the large positive penalty constants M and M_1 ($M \gg M_1$) help fulfill the constraint that the vehicle is not idling when it hits the stop line.

Besides, the definitions of $U_s^{p,k}$ and U_s^{bus} , illustrated by formulas (11) and (12), should be converted to the linear forms, given by:

$$0 \leq U_t^{p,k} \leq t_{k,p}^* + 1 - t, \quad k \in [j, i]; p \in [2, n_k]; t \in [0, t_{k,p}^*] \quad (67)$$

$$U_t^{p,k} \leq v_t^{k,p} M_1, \quad k \in [j, i]; p \in [2, n_k]; t \in [0, t_{k,p}^*] \quad (68)$$

$$(t_{k,p}^* + 1 - t - U_t^{p,k}) M_1 \leq \epsilon_{t,k,p} M + M_2, \quad k \in [j, i]; p \in [2, n_k]; t \in [0, t_{k,p}^*] \quad (69)$$

$$v_t^{k,p} M_1 \leq (1 - \epsilon_{t,k,p}) M, \quad k \in [j, i]; p \in [2, n_k]; t \in [0, t_{k,p}^*] \quad (70)$$

$$0 \leq U_t^{bus} \leq t_{bus}^* + 1 - t, \quad t \in [0, t_{bus}^*] \quad (71)$$

$$U_t^{bus} \leq v_t^{bus} M_1, \quad t \in [0, t_{bus}^*] \quad (72)$$

$$(t_{bus}^* + 1 - t - U_t^{bus}) M_1 \leq \epsilon_{t,bus} M + M_2, \quad t \in [0, t_{bus}^*] \quad (73)$$

$$v_t^{bus} M_1 \leq (1 - \epsilon_{t,bus}) M, \quad t \in [0, t_{bus}^*] \quad (74)$$

Regarding formulas (67) to (74), the binary variables $\epsilon_{t,k,p}$ and $\epsilon_{t,bus}$, together with the large positive penalty constants M , M_1 and M_2 ($M \gg M_1 \gg M_2$) help linearly express the constraint under the “if-else” condition.

6.4 Validation and results

6.4.1 The test site

This study validates the proposed model using a simulated experiment at Zhangyang Road and Fushan Road in Shanghai, China, where the eastbound of the intersection (as illustrated in Fig. 6.9) is selected as the test site. There are five approach lanes in the eastbound approach and the lanes are numbered from the median to the curb. The traffic demand during the peak hour in this leg is around 5000 vph, and during off-peak hour is nearly 2000 vph. The signal timing plan are different between peak hour and off-peak hour. During off-peak hour, the green time and cycle length are summarized in table 6.2. While during the peak hour, the green time for the straight movement is 44s and for the left turn movement is 37, and the cycle length is 310s.

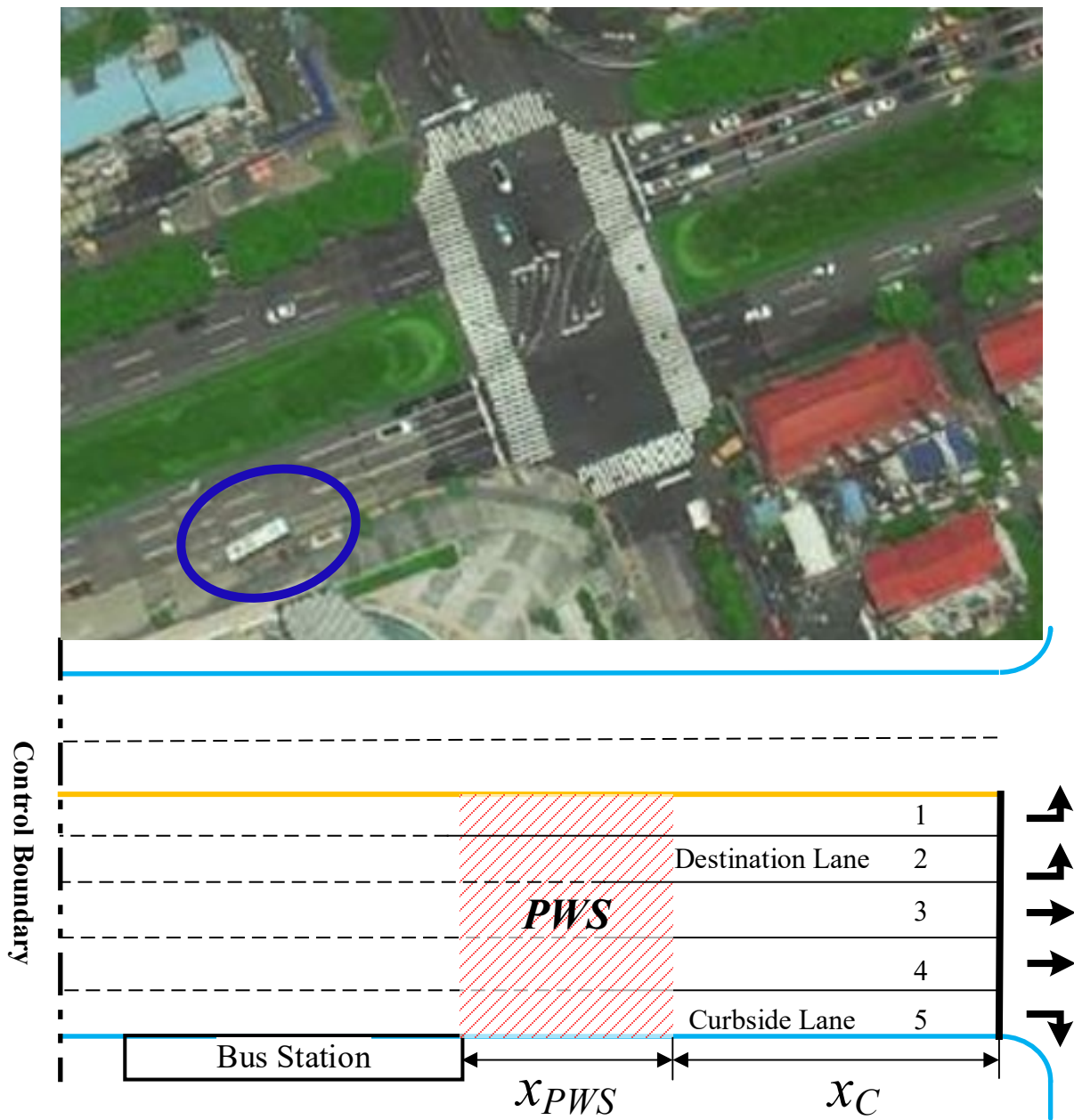


Figure 6.9 Location and layout of the test site.

As Fig. 6.9 shows, there're five approaching lanes, where the 2th ($j=2$) lane is the destination lane, and the 5th ($i=5$) lane is the curbside lane.

The inputs of the model are summarized in Table. 6.2.

Table 6.2 Summary of the model inputs.

Parameters	Sequence number of approaching lanes (k value)
------------	---

	2	3	4	5
x_{pws} (m)	10	10	10	10
x_c (m)	40	40	40	40
w (m)	4	4	4	4
l_{bus} (m)	10	10	10	10
n_k (pcu)	10	10	10	10
$v_0^{k,p}$ (m/s)	10	8	8	8
v_{max} (m/s)	18	18	18	18
C (s)	100	100	100	100
g_k (s)	20	30	30	∞
r_k (s)	80	70	70	0
TTR_k (s)	-45	-15	-15	∞
$P_{k,p}$ (person)	2	2	2	2
P_b (person)	50	50	50	50

Note that the right-turn lane is not under control. Accordingly, the values of G_5 and R_5 are set to be infinite, and TTR_5 to be zero.

6.4.2 Results

In the example, the following indices are estimated and compared under the control and non-control environments: (1) vehicular travel time of each lane; (2) sum of vehicular travel time of all lanes; (3) person travel time of each lane; (4) total person travel time of all lanes; (5) vehicular idling time of each lane; and (6) total vehicular idling time of all lanes. These indices are illustrated from Figs. 6.10 to 6.12.

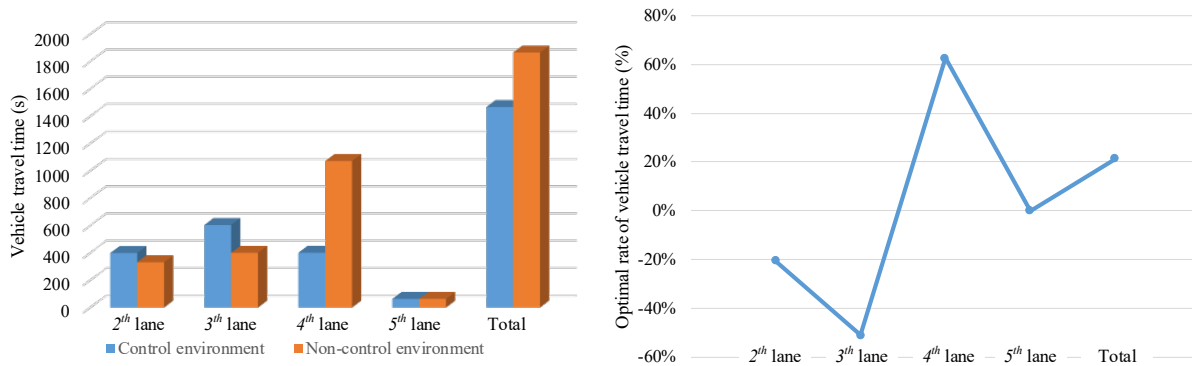


Figure 6.10 Comparison of the vehicular travel time under control and non-control

environments.

Fig. 6.10 compares the vehicular travel time under the control and no-control environments, where the bins in the left part of the figure represent the travel time, while in the right part they are the optimal rates. It can be found that although the sum of vehicular travel time of all lanes under the control environment is shorter than the one under the non-control environment, the improvement is not significant. Furthermore, the outcomes of the 2th and 3th lanes indicate the control environment performs even worse, which could also be illustrated by the negative bins of the 2th and 3th lanes in the right part of the figure. For the 5th lane, the results are identical since no vehicle needs to change the status. Finally, only the 4th lane under the control environment shows significant improvement.

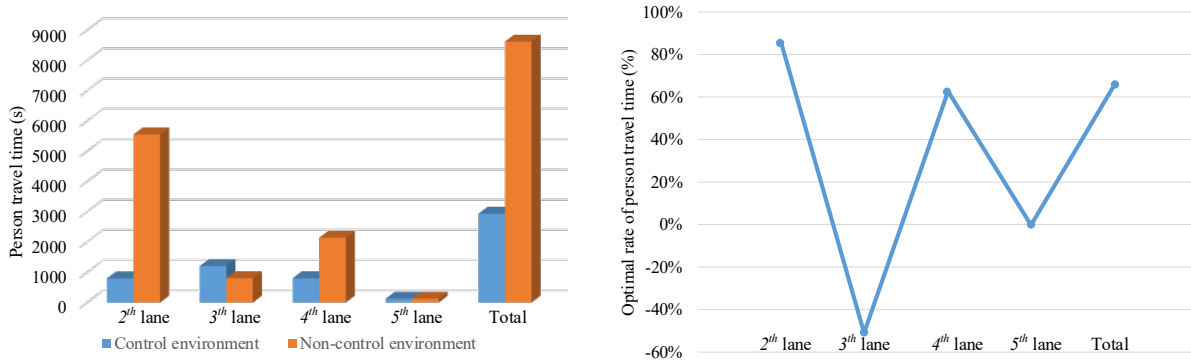


Figure 6.11 Comparison of vehicular time under control and non-control environments.

Fig. 6.11 compares the person travel time of each lane. It can be found that considering the passenger number, the control effectiveness toward the bus shows significant improvement on the destination lane. Furthermore, the sum of person travel time of all lanes is extremely shorter under the control environment. In the comparison, the person travel time of bus is categorized to the 2th lane since the bus needs traverse the 4th and 3th lanes and finally passes the intersection through the 2th lane. Therefore, the comparison result of the 2th lane regarding person travel time is contrary

to the one regarding vehicular travel time.

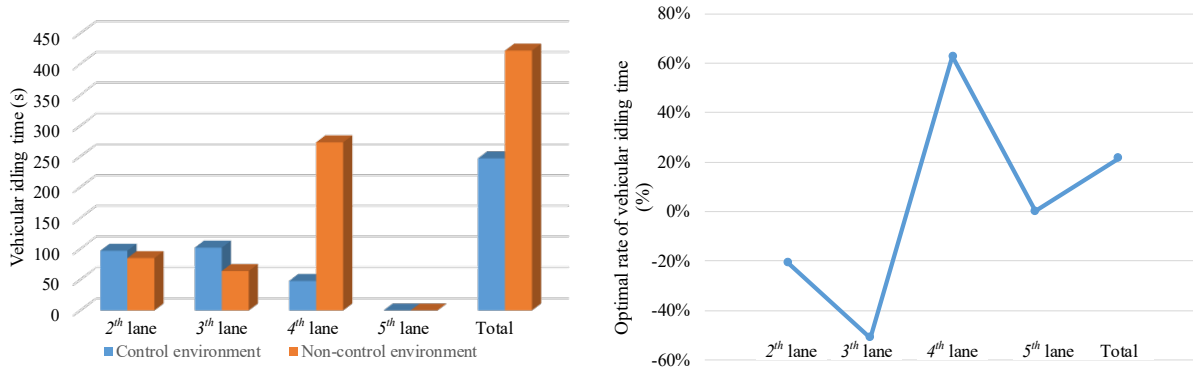


Figure 6.12 Comparison of person travel time under control and non-control environments.

Fig. 6.12 compares the vehicular idling time under the control and no-control environments, whose results are similar to those of the vehicular travel time. It can be found that the sum of vehicular idling time of all lanes under the control environment is shorter than the one under the non-control environment. While regarding the individual lane, the result of the 2th and 3th lanes under the control environment is even worse. For the 5th lane, the idling time is zero since there's no signal control for this lane.

Studying the vehicular trajectories can help in explaining the aforementioned outcomes. The trajectories of bus and its potential weaving cars in each lane (from the 5th to the 2th) are illustrated in Figs. 6.13 to 6.16.

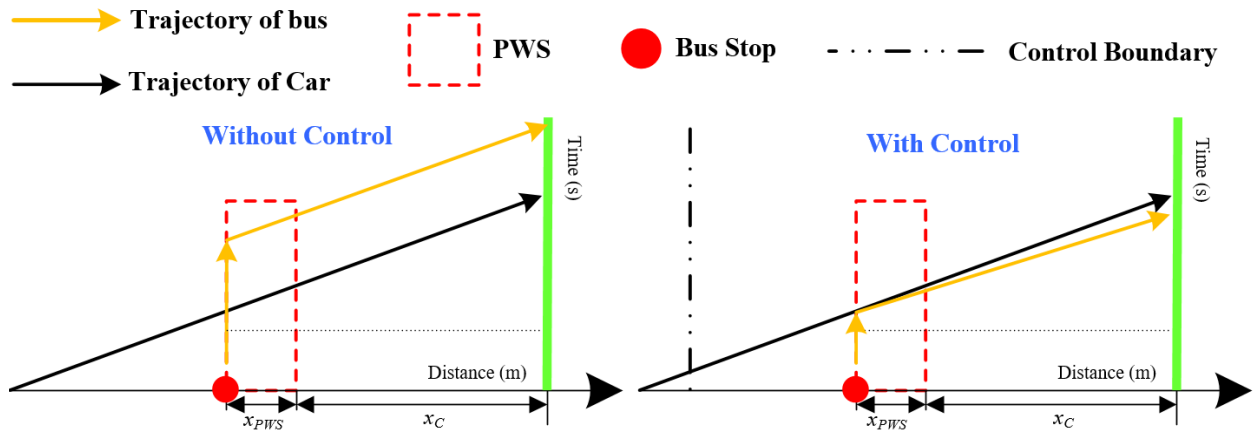


Figure 6.13 Trajectories of the last car and bus on the 5th lane, under the control and non-control environment.

Fig. 6.13 depicts the trajectories of bus and its nearest downstream car on the curb side lane (the 5th lane). Since on this lane all vehicles are not under signal control, the trajectories of cars with and without control are identical, and only the trajectories of bus under the two environments differ, due to the weaving with cars on the adjacent lane.

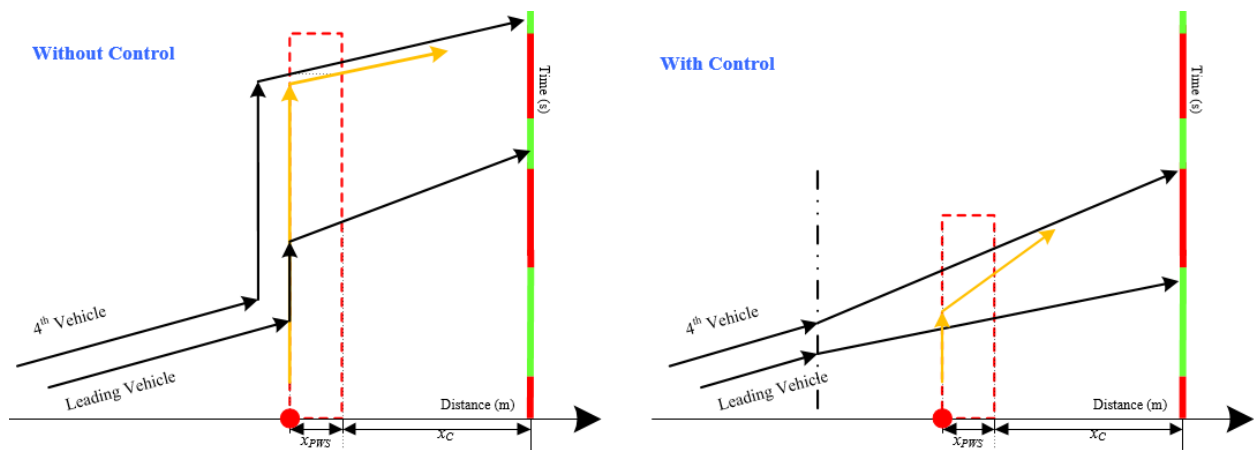


Figure 6.14 Trajectories of the cars and bus on the 4th lane under the control and non-control environment.

Fig. 6.14 depicts the trajectories of the bus, the leading and the fourth cars downstream of the PWS on the 4th lane. Selecting the leading and the fourth cars is because under the control

environment, the leading car accelerates and pass the PWS prior to the bus, while the fourth car decelerates and passes the PWS behind the bus. It causes that the car platoon is divided into two sub-platoons. When under the non-control environment, the cars and bus block each other until one more cycle passes, resulting huge delay for all vehicles.

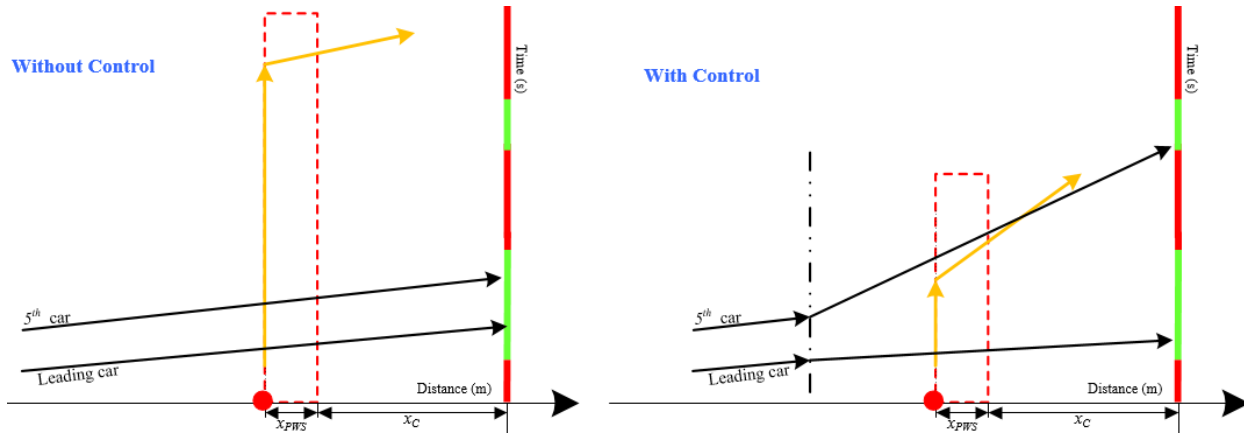


Figure 6.15 Trajectories of the cars and bus on the 3th lane under the control and non-control environment.

Fig. 6.15 depicts the leading and the fifth cars downstream of the PWS on the 3th lane. It can be noted that under the control environment, the leading car accelerates and pass the PWS prior to the bus, while the fifth vehicle decelerates and passes the PWS behind the bus. It also results in the division of car platoon. While under the non-control environment, these cars do not weave the bus, since the bus are still blocked by cars on the 4th lane, which illustrates why on this lane, both the vehicular and person travel time under the control environment are lower than under the non-control environment.

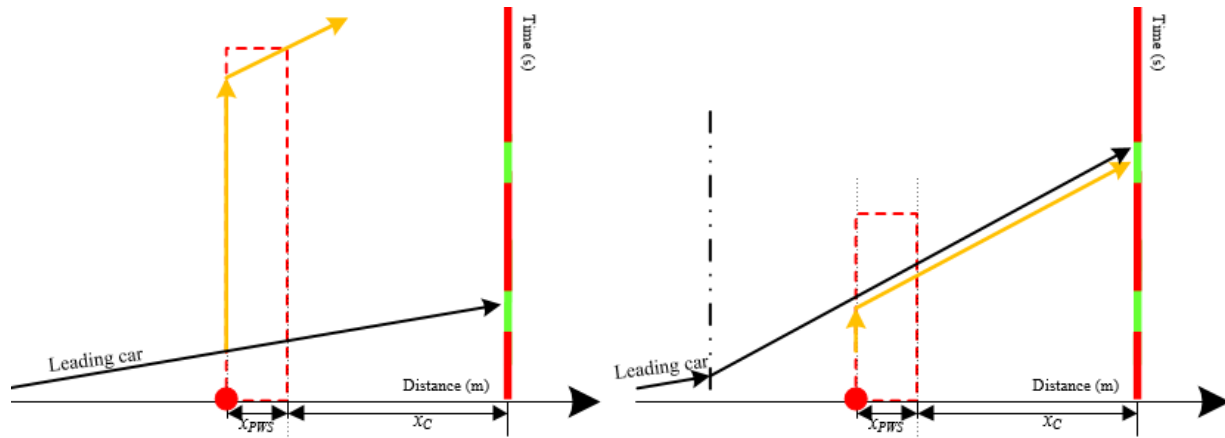


Figure 6.16 Trajectories of the car and bus on the destination lane, under the control and non-control environment.

Fig. 6.16 depicts the trajectories of bus and the leading car downstream of the PWS, on the destination (2th) lane. It can be illustrated that under the control environment, the car decelerates and pass the PWS behind the bus. While under the non-control environment, the car is not affected by the bus as well, which also explains the phenomenon demonstrated in Fig. 6.13. Although no improvement of vehicular travel time, the person travel time is much lower under the control environment, as person travel time of bus is categorized to this lane.

In summary, it can be demonstrated from Figs. 6.13 to 6.16 that since the bus doesn't weave cars on all the lanes, the improvement in terms of vehicular travel time under the control environment has no significance. While considering the effectiveness of passenger number, the control model presents remarkable advantages.

6.4.3 Sensitivity analysis

Ratio

One of the objectives in the control model is to minimize the total person travel time. Therefore, the ratio of bus passenger number over car passenger number may affect the control strategy and

outcomes. In this section, fixing the car passenger number, the study selects the various bus passenger numbers to explore the sensitivity of optimal rates of the total vehicular travel time and total person travel time under the control environment.

The passenger number in each car is fixed as 2. The optimal rates under various bus person number are shown in Fig. 6.17.

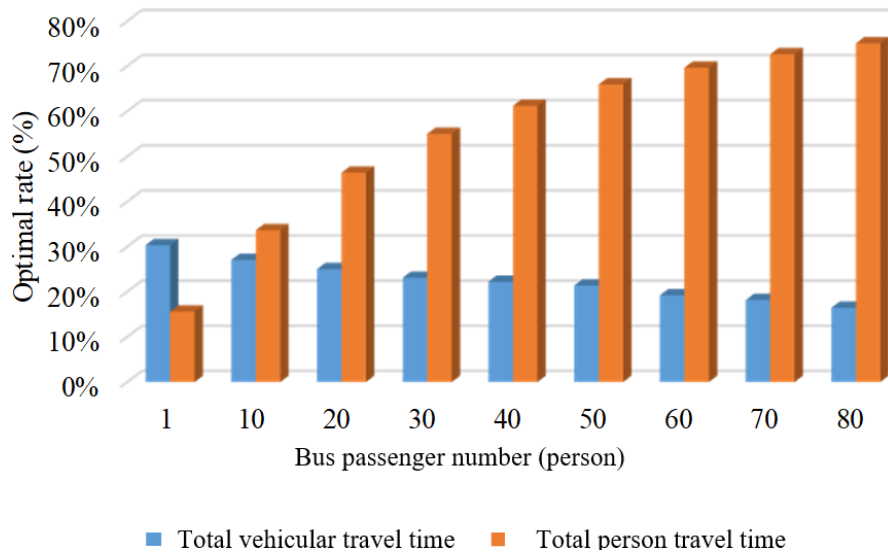


Figure 6.17 Comparison of optimal rates of vehicular and person travel time under the control environment.

It could be found in Fig. 6.17 that with the increase of bus passenger number, the optimal ratio of the total vehicular travel time declines. This is because when the bus passenger person number rises, the priority of bus becomes even higher, resulting in that more cars decelerate and pass the PWS behind the bus, which causes huge delay of cars. While for the total person travel time, the situation is rather different. Since the priority of bus becomes higher, the bus could pass the intersection faster. Therefore, multiplied by passenger number, the improvement of travel time under the control environment becomes more and more significant.

Demand

Another index affecting the model is the traffic demand around the intersection. In this section, we set the traffic demand from 500 vph to 4500 vph with the increasing step of 500 vph.

The optimal rates under various travel demand are shown in Fig. 6.18.

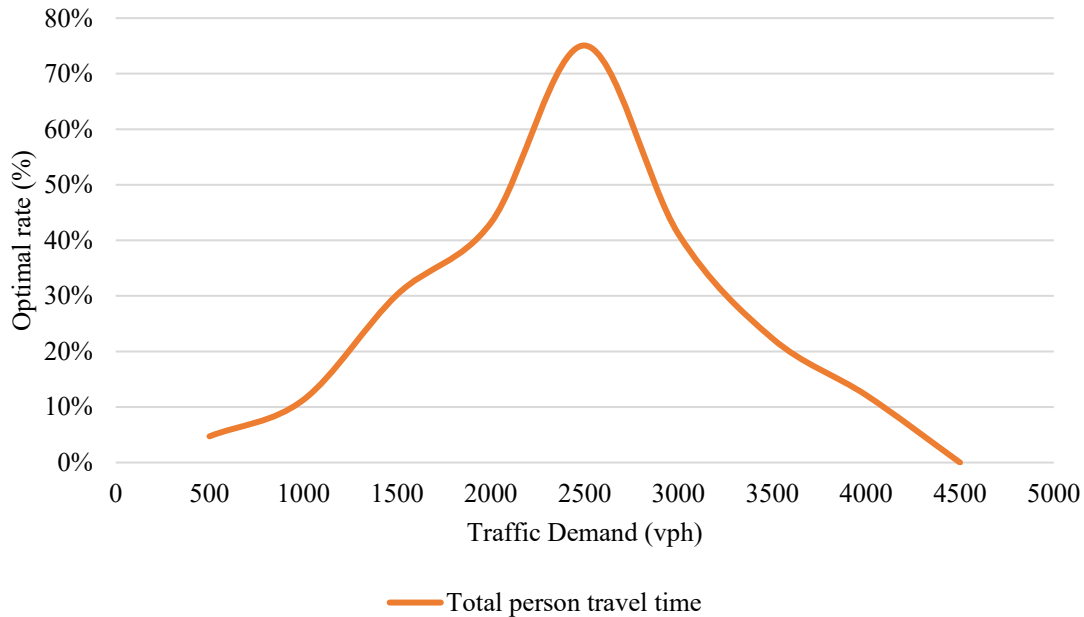


Figure 6.18 Comparison of optimal rates of person travel time under various traffic demand.

It could be found in Fig. 6.18 that the traffic demand and the optimal ratio of the total person travel time are parabolic correlated, with the vertex at demand of 2500 vph. When the traffic demand is significantly low or high, it seems the control model hardly bring improvement. It is because when demand is extremely low, the bus and cars are not likely to weave each other, therefore, it is not necessary to control the trajectories of those vehicles. Nevertheless, if the traffic demand is nearly oversaturated, there seems no space to create to avoid weaving, causing uselessness of the control model under this situation.

Station distance

The distance between the bus station and stop line could potentially affect the effectiveness

of the control model. In this section, we set traffic demand as moderate (2500 vph), and distance from 20 to 400 meters (without considering the DSRC working scope), with the increasing step of 20 meters. The optimal rates under various travel demand are shown in Fig. 6.19.

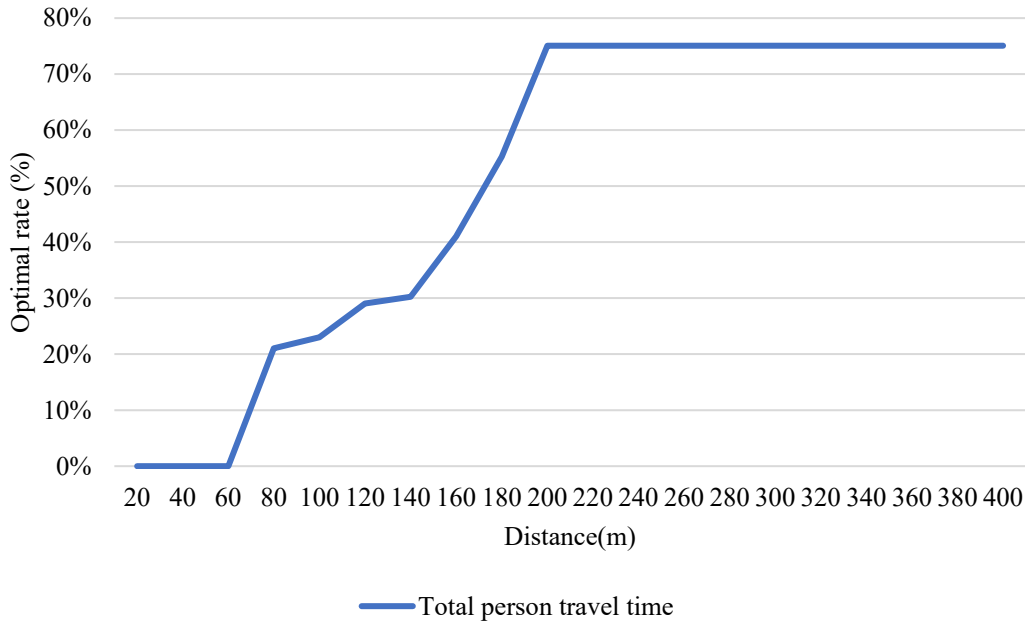


Figure 6.19 Comparison of optimal rates of person travel time under various distance.

It could be found in Fig. 6.19 that with the increase of traffic distance, the optimal ratio of the total person travel time remains 0% until the distance exceeds 60m. After that it keeps increasing and remains the same after the distance is greater than 200 meters. This is because when the station is too close to the stop line, there’s little space for optimizing the trajectories. While when the distance is too long, it becomes less significant and has little impact on the control result.

6.5 Conclusions

This chapter proposes a cooperative bus-car trajectory optimization model to eliminate weaving bottleneck around the near-side bus station. The contribution of the method is to develop a two-phase model, where the minimization of total person travel time and weaving elimination are fulfilled in Phase I model, while the minimization of total vehicular idling time is conducted in

Phase II model, conditioning on the output of Phase I. The rolling-based NLP and MILP models are applied in the Phases I and II, respectively.

The study provides an example to validate the proposed model. Firstly, the it compares the vehicular travel time under the control and non-control environments. Results show that only the lane adjacent to the curb side lane reflects significant improvement under control. Then, considering the person travel time, the study explores that not only the result of the lane adjacent to the curb side lane, but of all lanes shows remarkable benefits of the control model. After that, the vehicular idling time is compared under the control and no-control environments. The result shows similarity to the vehicular travel time. Finally, the study analyzed vehicular trajectories on each lane, indicating that without control, the bus just weaves the cars on the lane adjacent to the curb side lane, while the cars in other lanes are not impacted. This finding also explains some “contradictory” conclusions in comparison of the vehicular travel time, person travel time and vehicular idling time.

This study also conducts the sensitivity analysis towards the ratio of bus passenger number over car passenger number. The result illustrates that with the increase of bus passenger number, the optimal rate of the total vehicular time declines, while of the total person time rises.

Analysis results indicate the validity and effectiveness of the proposed speed control framework. On-going work of this study is to test the proposed model in real-world and evaluate its effectiveness with continuous arrival of bus at the station.

Chapter 7 DILEMMA ZONE PROTECTION FOR SAFETY IMPROVEMENT AT AN ISOLATED SIGNALIZED INTERSECTION

This chapter develops a dynamic speed guiding method towards dilemma zone protection through a high-speed signalized intersection. A two-stage control model is proposed where the DZ protection and travel time minimization are fulfilled in Stage I. Conditioning on the output of the Stage I, the optimization of speed trajectory is completed in Stage II. The Dynamic Programming and Multi-objective Mixed Integer Linear Programming algorithms are used to solve the models. An illustrative example is provided to validate the proposed model. Results indicate that the model is effective to achieve DZ protection while minimizing travel time, idling time and speed fluctuation. Sensitivity analysis is conducted and it implies that for the travel time, there's little impact towards higher speed while the travel time with lower speed rises with the increase of guiding scope. For the speed fluctuation, with higher speed, it declines with the rise of travel scope, while no impact shows under the lower speed.

7.1 Introduction

Improving traffic safety is almost the overriding responsibility of transportation departments at all levels, especially for reducing the risks at those hazardous intersections with deadly accidents. A report from the United States shows in 2013 there were 2,524,000 crashes happened at signalized intersections, where approximately 4470 crashes were fatal. Dilemma zone (DZ), a segment in the approach of the intersection, is one of the most contributing factors towards those crashes, since motorists can neither pass the intersection before the onset of the red phase, causing side-angle crashes; nor stop the car safely, resulting in rear-end collision. The idea of DZ was initially proposed by Gazis, who developed a model, "Type-I Model", defining DZ as a space range, where

the vehicle can neither clear the intersection safely nor slow down to stop smoothly during the yellow phase. Beside the “Type-I Model”, a concept of the “Type-II Model” was also raised, expressed as a probability of motorists’ decision for stop. Field observation or graph processing are usually adopted to study DZ boundaries or the motorists’ reaction facing DZ. A common sense is that DZ range depends on the motorist’s behaviors and the types of vehicles. Other literatures also show a boundaries range of between 2 to 6 seconds for DZ. In studying with the motorists’ behaviors, Van der Horst and Wilmlink illustrated that they depend on some objective and subjective factors, such as motorist’s emotion, personality, and vehicular speed, et. They developed a decision-making process model and some parameters in that model are adopted by some later.

The traditional studies towards DZ protection are mainly divided into two categories: one belongs to the motorist side, trying to alert the motorists in advance; the other belongs to infrastructure, extending the green time to insure the vehicles pass before the onset of the red phase. Over the motorist ride, Moon et al. developed an integrated system for assessing a DZ warning system for signalized intersections by a serial of field tests. Results from the tests indicated that the system can be implemented at signalized intersections to avoid the DZ, and to reduce red-light violations and intersection collisions. Martin et al. considered the two-advanced warning (AWS) systems presently used in Utah. It found that the setup and performance of the two systems were different. The Texas Transportation Institute has developed a new system named the Advanced Warning for End of Green System (AWEGS) for application of DZ. The system was implemented at two sites in Waco and Brenham, Texas. The result indicated that AWEGS consistently improved the DZ protection at intersections and reduced red light running by approximately 40%. Another system is called the Pre-signal Indication System (PSIS) which uses a flashing green or yellow signal at the last of the green phase.

Over the infrastructure side, Ma et al. presents an extensive investigation regarding the impacts of green signal countdown devices (GSCD) on the intersection safety, based on field observation of critical motorist and vehicle related parameters at two similar intersections (one with GSCD and the other without GSCD) in Shanghai. Also, some studies combined those two categories together.

Recently, several preliminary studies have been investigated towards applying the real-time communication theory for DZ protection. Sharma et al. developed a prototype Yellow Onset Motorist Assistance (YODA) system, consisting of a pole-mounted unit (StreetWave) and an in-vehicle unit (MobiWave), to advise the motorists on whether it is safe to proceed through the intersection. Hsu et al. developed an on-board system which can alert the motorists to slow down to avoid DZ according to the real time driving status, such as speed and position. Dong et al. presents a dilemma-zone (DZ) avoidance-guiding system for vehicles approaching an intersection. The purpose of the system is to assist motorists in determining the driving behavior and to prevent vehicles from being caught in DZ. Machiania et al. proposed a new measure, called safety surrogate histogram, to capture the degree and frequency of dilemma zone related conflicts at signalized intersection approaches

Abu-Lebdeh proposed an algorithm to study the benefits of the Intellidrive technology in terms of vehicular delay. Guler et al. proposed an algorithm to enumerate various vehicle discharging patterns before the stop line and minimize vehicular delay using the connected-vehicle technology. Wan et al. proposed a Speed Advisory System (SAS) for pre-timed traffic signals and obtained the fuel minimal driving strategy as an analytical solution to a fuel consumption minimization problem. Canadan et al. proposed a connected vehicle signal control (CVSC) strategy for an isolated intersection with significantly reduced travel time delays and average

number of stops per vehicle compared with the adaptive control strategy. Lioris et al. found that platoons of connected vehicles can double throughput in urban roads. Wei et al. developed a set of integer programming and dynamic programming models for scheduling longitudinal trajectories with both system-wide safety and throughput requirements taken into consideration.

Although the literature findings illustrate that it is possible to apply CV for DZ protection, there may have some issues which need to be addressed. For example, existing methods are not able to optimize the speed trajectories, which may result in some negative effects, such as: (1) aggressive deceleration may be harmful to the vehicular engine, while sudden acceleration may generate unnecessary fuel consumption or emissions; (2) unoptimized speed profile may increase idling time; and (3) frequent speed fluctuation may cause the motorists to feel uncomfortable.

Therefore, this chapter makes contributions to developing a dynamic speed control method that can effectively prevent vehicles from dropping in the DZ (see Fig. 7.1) while minimizing travel time and trajectory through the high-signalized intersections.

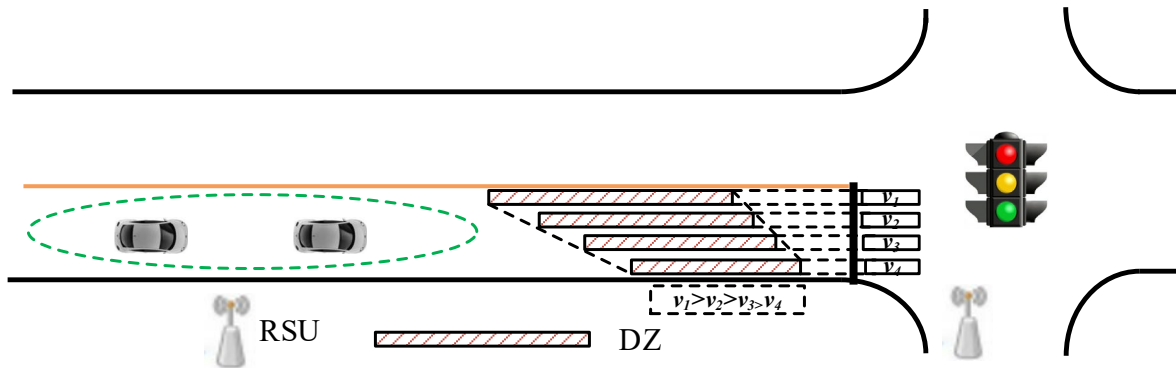


Figure 7.1 Speed guidance for DZ protection.

The proposed guiding model applies when a vehicle is detected to drop in the DZ given the speed, occupancy, location and signal timing information. The proposed model enables vehicle-signal cooperation through a two-stage optimization. A Dynamic Programming (DP) algorithm is developed in Stage I to search trajectories that eliminate the DZ issue and minimize the total travel

time; while Stage II features a Multi-objectives Mixed Integer Linear Programming (MOMILP) model to minimize speed fluctuation and idling time if multiple solutions are obtained in Stage I.

7.2 Methodology

7.2.1 Computation of DZ

As mentioned above, the DZs are divided into two categories: Type I DZ and Type II DZ. Fig. 7.2 depicts the layout of the two types, where the Type I illustrates a situation when a yellow signal is displayed, a motorist, approaching the stop line of an intersection, is unable to safely pass the intersection or stop his/her vehicle smoothly before the stop line. For the Type II, an abstract concept is demonstrated that the DZ is located between 5.5 s and 2.5 s of the travel time for hitting the stop line.

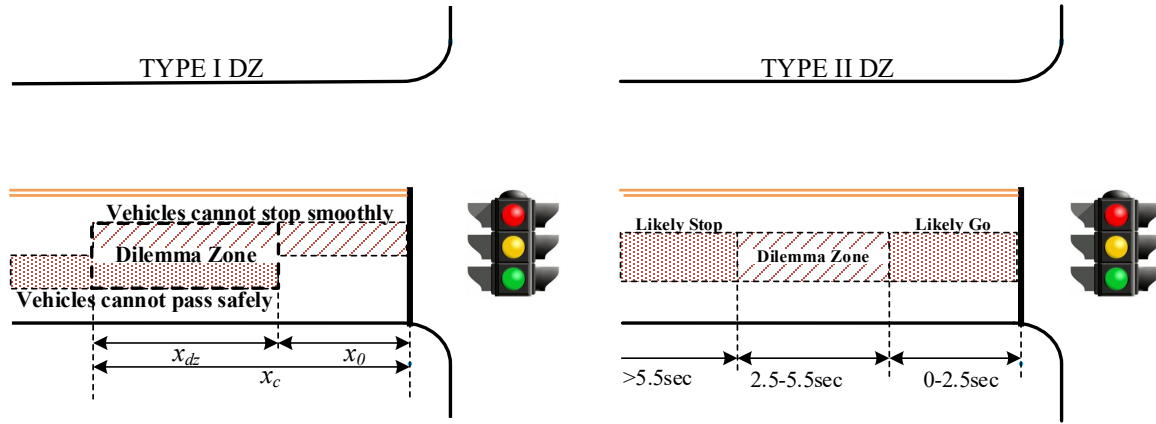


Figure 7.2 Layout of Type I and Type II DZs.

The location and length of the Type I DZ can be estimated with:

$$x_{dz1} = |x_c - x_0| = \left| \left(v\delta_2 + \frac{v^2}{2d^*} \right) - [v\tau - (w + L) + \frac{1}{2}a^*(\tau - \delta_1)^2] \right| \quad (1)$$

It can be found in Eq. (1) that if x_{dz1} is greater than 0, the Type I DZ exists.

The location and length of the Type II DZ depend on the current vehicular speed, which can be estimated with:

$$x_{dz2} = x_{stop} - x_{go} = 5.5v - 2.5v \quad (2)$$

7.2.2 Logic of guidance

The study provides a depiction of the dynamic speed guiding logic, whose architecture are depicted by a flow chart. The logic has three main components: (1) DZ detection; (2) dynamic speed guiding model; (3) guidance execution and status tracking.

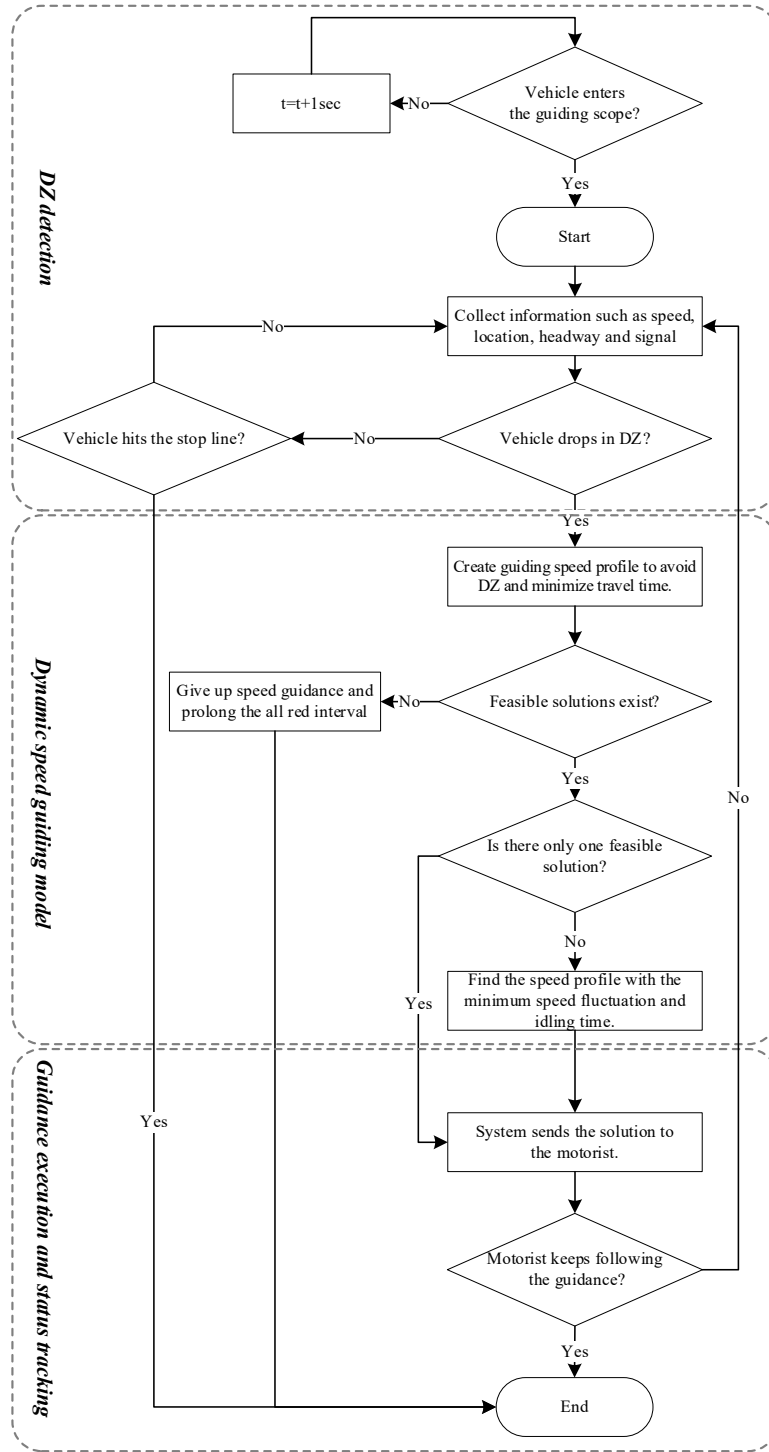


Figure 7.3 Logic of the proposed dynamic speed guiding method.

7.2.3 DZ detection

DZ detection is the first step of the speed guidance. When a vehicle enters the guiding scope, the

system shall collect information including speed, headway, location and signal timing etc., with which whether the vehicle will drop in the DZ can be detected.

The control scope should be initially determined, since an over short scope cannot provide enough space for the motorist to decelerate, and in an overlong scope the motorist cannot keep an identical driving status. Therefore, the guiding scope should obey the following constraints: (1) the motorist with the maximum speed limit has enough space to stop the vehicle, and then accelerate back to the original speed; and, (2) without any congestion, the travel time of vehicle with the median speed for hitting the stop line is no more than the green interval. One can express the constraints by:

$$-\frac{1}{2a^*} \cdot v_{max}^2 + \frac{1}{2a^*} \cdot v_{max}^2 \leq x_{scope} \quad (1)$$

$$g \cdot v_{med} \geq x_{scope} \quad (2)$$

The method for DZ detection is to estimate if the trajectory of vehicle would touch the DZ area, calculated by the current speed, during the yellow interval (See Fig. 7.4 and Eqs. (4) and (5)).

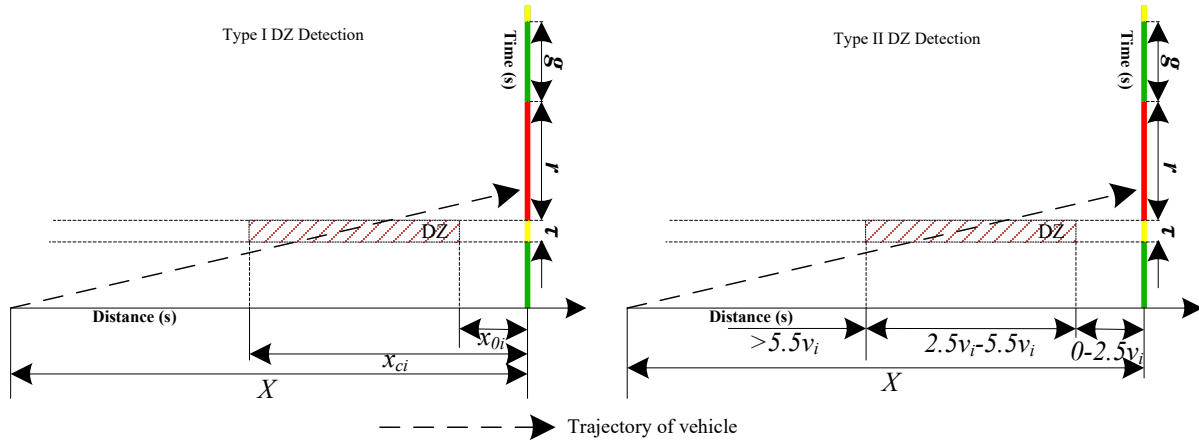


Figure 7.4 Idea for DZ detection.

$$\begin{cases} \frac{x_{scope} - \max(x_c, x_0)}{v} - TTY \leq \tau + z \cdot C \\ \frac{x_{scope} - \min(x_c, x_0)}{v} - TTY \geq \tau + z \cdot C \end{cases} \quad z = 0 \text{ or } 1 \quad (4)$$

$$\begin{cases} \frac{x_{scope}}{v} - 5.5 - TTY \leq \tau + z \cdot C \\ \frac{x_{scope}}{v} - 2.5 - TTY \geq \tau + z \cdot C \end{cases} \quad z = 0 \text{ or } 1 \quad (5)$$

The dynamic speed guiding model will be activated only if DZ is detected. Otherwise, the system will keep tracking the vehicle status until DZ is detected or the vehicle passes the stop line.

7.2.4 Determination of guiding scope

The guiding scope should be determined, since an over short scope cannot provide enough space for the motorist to decelerate, and in an overlong scope the motorist cannot keep an identical driving status. Therefore, the guiding scope should obey the following constraints: (1) the motorist with the maximum speed limit has enough space to stop the vehicle, and then accelerate back to the original speed; and, (2) without any congestion, the travel time of vehicle with the median speed for hitting the stop line is no more than the green interval. One can express the constraints by:

$$-\frac{1}{2a^*} \cdot v_{max}^2 + \frac{1}{2a^*} \cdot v_{max}^2 \leq x_{scope} \quad (6)$$

$$g \cdot v_{med} \geq x_{scope} \quad (7)$$

7.2.5 Dynamic speed guiding model

The dynamic speed guiding model proposed in this study consists of two critical modules: (1) DZ protection and travel time minimization; (2) Minimization of speed fluctuation and idling time. The two modules are processed in a two-stage model, whose architecture is illustrated in Fig. 7.5.

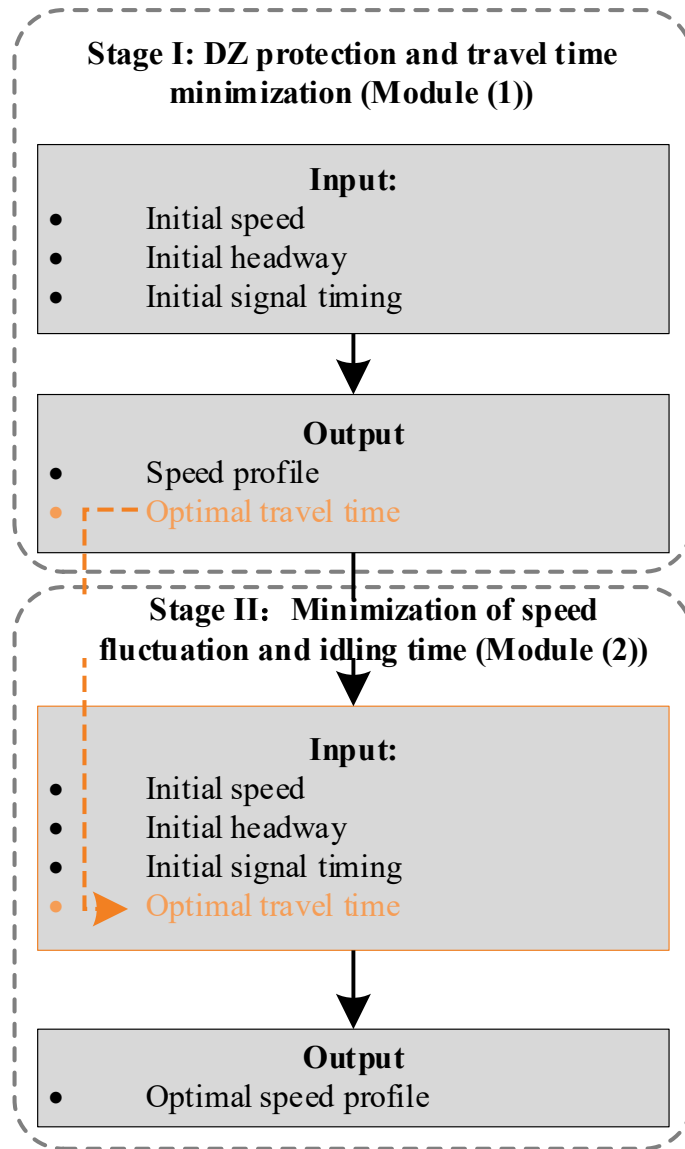


Figure 7.5 Architecture of the two-stage model.

As Fig. 7.5 depicts, the DP algorithm is introduced in the Stage I to process the first module, where the DZ protection is set as one of its constraints and travel time minimization as the objective function. The inputs include the initial speed, location, headway and signal timing etc., recorded when the vehicle just enters the guiding scope. The outputs are the vehicular speed profile and travel time.

The Module (2) is processed in the Stage II by the MOMILP algorithm, conditioning on

the output (optimal travel time) of the Stage I. The objective functions are the minimization of speed fluctuation and idling time. The inputs of the Stage II are those in the Stage I plus the optimal travel time, and the output is the optimal speed profile.

7.3 Solution Algorithm

7.3.1 Control of vehicular status - a multi-stage decision process

The optimizer usually provides a speed profile for the travel time minimization where each time point corresponds to a speed value. Therefore, the vehicle can change its status at every time point. Based on this operational feature, the travel time minimization can be modeled as a multiple-stage decision problem. As DP is one of the most efficient methods for solving multiple-stage decision problems, in this study the DP algorithm is formulated to fulfill the DZ protection and travel time minimization. Fig. 7.6 depicts an example of the DP model with i stages. Starting from the 0th stage, each stage corresponds to a time point, and between two successive stages is a second interval.

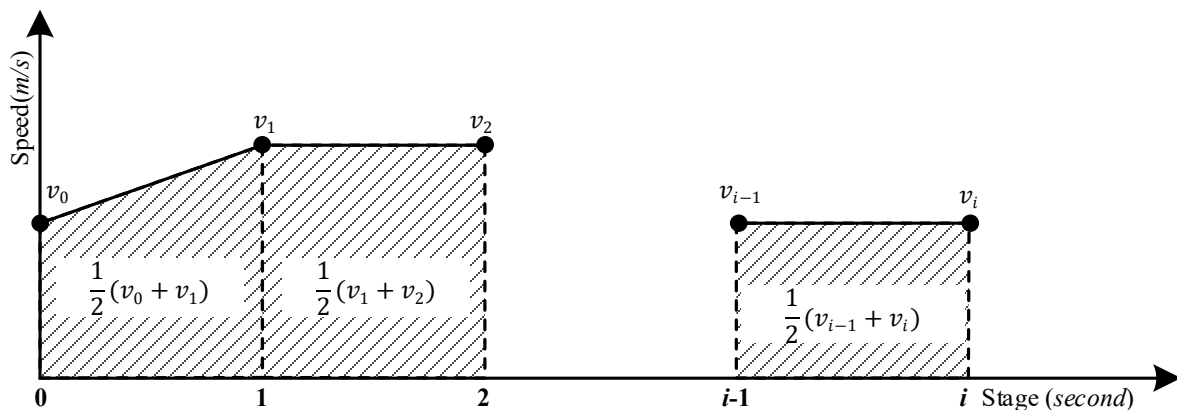


Figure 7.6 Sample DP model with i stages.

It can be illustrated from Fig.7.6 that if the speed at the current stage is determined, the travel distance can be acquired, equaling to the shaded area during the time interval between the current and previous stages. Therefore, the DP method can be used to determine the vehicular speed stage by stage so that the number of stages (travel time) can be minimized for passing the intersection.

7.3.2 Decision variable of DP

The vehicular speed at each stage is the decision variable of the DP algorithm. Assuming the acceleration and deceleration rates are constant, set as 1 m/s^2 and -1 m/s^2 respectively, the speed at the i th stage can be updated with the following equation:

$$v_i - v_{i-1} = \begin{cases} 1, v_i > v_{i-1} \\ 0, v_i = v_{i-1} \\ -1, v_i < v_{i-1} \end{cases} \quad i = 1, 2, \dots \quad (8)$$

where,

v_i = vehicular speed at the i^{th} stage (m/s) (v_0 is the initial speed).

7.3.3 State transfer functions of DP

Update travel distance

The travel distance of the vehicle at the i th stage can be updated with the following equation:

$$D_i = D_{i-1} + \frac{1}{2}(v_i + v_{i-1}), \quad i = 1, 2, \dots \quad (9)$$

where,

D_i = travel distance at the i^{th} stage (m) ($D_0 = 0$).

Update travel time

The state transfer function of travel time can be expressed with:

$$T(D_i) = T(D_{i-1}) + 1, i = 1, 2, \dots \quad (10)$$

where,

$T(D_i)$ = travel time at the i^{th} stage ($T(D_0) = 0$).

7.3.4 Objective function of DP

Given the state transfer function of vehicular speed, travel distance and travel time, the objective function of the DP algorithm can be expressed as:

$$\min T(D_i) \quad (11)$$

7.3.5 Constraints of DP

The constraints of the DP algorithm are listed as follows.

- (1) Vehicular speed cannot be higher than the maximum speed limit, or lower than 0. It can be expressed with:

$$v_{min} \leq v_i \leq v_{max}, i = 0, 1, 2, \dots \quad (12)$$

- (2) Vehicle should ultimately pass the stop line. To avoid the situation of idling before the stop line, a minor distance, set as 0.1, is added to the distance between the stop line and vehicle.

One can express the constraint by:

$$D_i \geq x + 0.1 \quad (13)$$

- (3) Vehicle needs to avoid bumping. Therefore, a safe distance should always be maintained.

To express this constraint linearly, the “Three-second rule” (Chen et al., 2016) is adopted.

One can express this constraint by:

$$x - h_i - \frac{1}{2} \sum_{k=0}^{i-1} v_k + v_{k+1} \geq 3v_i, i = 1, 2, \dots \quad (14)$$

where,

h_i = space headway between the vehicle and its downstream vehicle at the i^{th} stage (m).

(4) Vehicle should never pass the stop line when the signal light displays red. It can be expressed with:

$$x - \frac{1}{2} \sum_{k=0}^{j-1} v_k + v_{k+1} \geq 0, \forall j \in J \quad (15)$$

As Fig. 7.7 shows, when the algorithm is activated, the initial signal information may be various. Therefore, the range of J can be expressed with:

$$J = \begin{cases} [\tau + TTY, \tau + TTY + r + zC], & TTY \leq 0 \text{ or } 0 < TTY \leq g \\ [0, TTY - g + zC] \cup [\tau + TTY, \tau + TTY + r + zC], & TTY > g \end{cases} \quad (16)$$

where,

z = number of cycles ($\{0,1\}$).

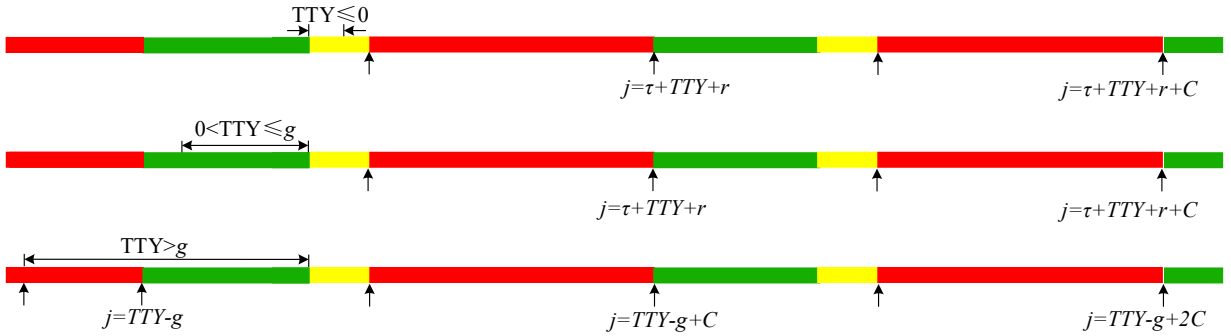


Figure 7.7 Various initial signal information.

(5) DZ protection, illustrated as the trajectory should avoid touching the shadow area, varying based upon the real-time speed, during the yellow interval. One can express the constraints by:

$$x - \frac{1}{2} \sum_{k=0}^{s-1} v_k + v_{k+1} \geq \max(x_{c,s}, x_{0,s}) \cup 0 \leq x - \frac{1}{2} \sum_{k=0}^{s-1} v_k + v_{k+1} \leq \min(x_{c,s}, x_{0,s}) \quad (17)$$

$$x - \frac{1}{2} \sum_{k=0}^{s-1} v_k + v_{k+1} \geq 5.5v_s \cup 0 \leq x - \frac{1}{2} \sum_{k=0}^{s-1} v_k + v_{k+1} \leq 2.5v_s \quad (18)$$

where,

$x_{c,s}$ = length of the area where vehicles cannot stop smoothly, based upon the speed of the s^{th} stage (m); and,

$x_{0,s}$ = length of the area where the vehicle can pass the intersection with the maximum acceleration rate, based upon the speed of the s^{th} stage (m).

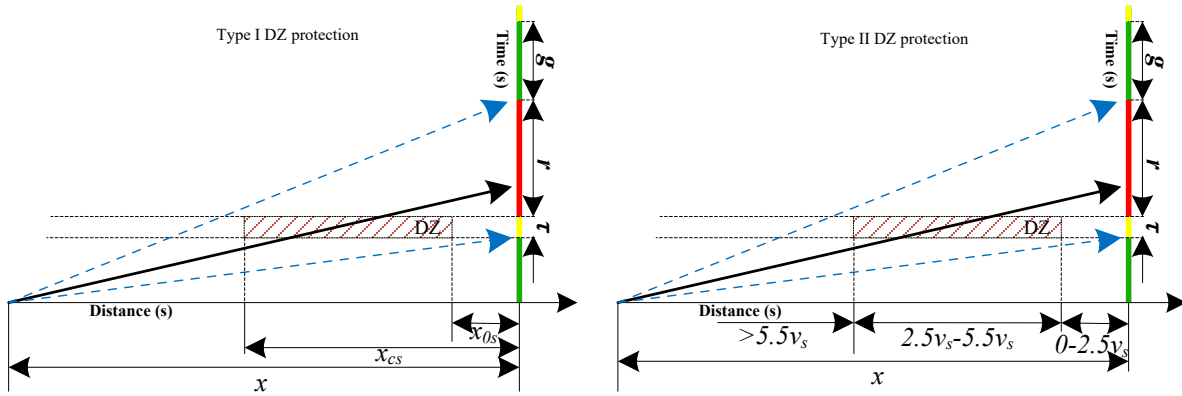


Figure 7.8 Trajectories avoid touching the DZ.

Based upon the initial signal information, the range of s can be estimated with:

$$s = \begin{cases} [0, \tau + TTY] \cup [TTY + zC, \tau + TTY + zC], & TTY \leq 0 \\ [TTY + zC, \tau + TTY + zC], & TTY > g \end{cases} \quad (16)$$

(6) Frequent speed fluctuation should be avoided, defined as the continuous switch between the acceleration modes (See Fig. 7.9). One can express the constraint with

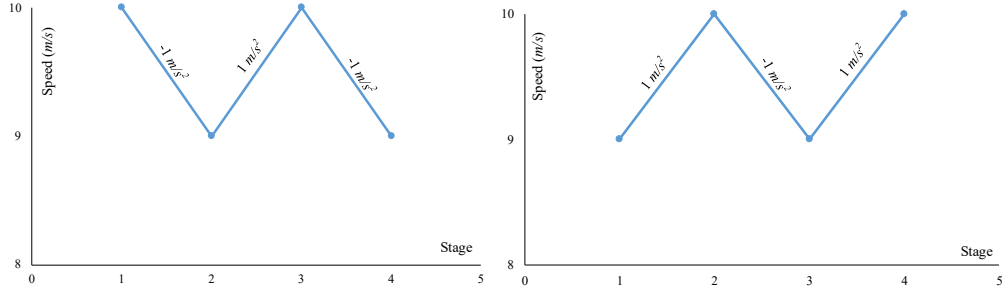


Figure 7.9 Frequent speed fluctuation.

$$-3 \leq [(v_{i+2} - v_{i+1}) - (v_{i+1} - v_i)] - [(v_{i+1} - v_i) - (v_i - v_{i-1})] \leq 3, i = 1, 2, \dots \quad (17)$$

7.4 Multi-objective Mixed Integer Linear Programming algorithm

The MOMILP algorithm is used in the Stage II to find the speed profile with minimal speed fluctuation and idling time, if multiple speed profiles are found by the DP algorithm. Conditioning on the optimal travel time (denoted as n) generated in the Stage I, the number of elements in the speed profile is known as $n+1$. The structure of the MOMILP problem is depicted as follows.

7.4.1 Decision variables of the MOMILP problem

The set of decision variables are shown as follows.

(1) Continuous variables:

v_i = vehicular speed at the i^{th} time point (m/s), $\forall i \in [0, n]$;

(2) Integer variables:

p_i = index variable of idling at the i^{th} second interval, expressed by:

$$p_i = \begin{cases} 0, & v_i = 0 \cap v_{i-1} = 0 \\ 1, & \text{o.w.} \end{cases}, \forall i \in [1, n] \quad (18)$$

q_i = index variable of speed fluctuation at the i^{th} second interval, expressed by:

$$q_i = \begin{cases} 0, & v_i - v_{i-1} = 0 \\ 1, & \text{o.w.} \end{cases}, \forall i \in [1, n]; \quad (19)$$

φ_i, ω_i = control variables for constant acceleration/deceleration;

α_i, β_i = control variables for DZ protection;

δ_i, ε_i = variables for acquiring the value range of q_i at the i^{th} second interval, $i \in [1, n]$.

7.4.2 Objective function of MOMILP

The objective function of MOMILP algorithm is expressed as:

$$\min[f_1, f_2]^T \quad (20)$$

where,

$$f_1 = n - \sum_{i=1}^n p_i \quad (21)$$

$$f_2 = \sum_{k=1}^n q_k \quad (22)$$

From Formulas (20) to (22), f_1 is for idling time minimization, which is prior to the minimization of speed fluctuation, denoted as f_2 .

7.4.3 Constraints of MOMILP

Some constraints of the MOMILP algorithm are identical to those of the DP algorithm, while they should be converted to the standard form of the linear integer programming herein. Furthermore, several additional constraints should be added.

The converted constraints are listed as follows.

$$v_i \leq v_{max}, \forall i \in [0, n] \quad (23)$$

$$v_i - v_{i-1} + \varphi_i - \omega_i = 0, \forall i \in [1, n] \quad (24)$$

$$-3v_i + \frac{1}{2} \sum_{k=0}^{i-1} v_k + v_{k+1} \leq h_i - x, \forall i \in [1, n] \quad (25)$$

$$\frac{1}{2} \sum_{k=0}^{j-1} v_k + v_{k+1} \leq x, \forall j \in J \cap [1, n] \quad (26)$$

$$\frac{1}{2} \sum_{k=0}^{i-1} v_k + v_{k+1} \leq x - x_{cs} + M \cdot \alpha_i, \forall i \in s \cap [1, n] \quad (27)$$

$$\frac{1}{2} \sum_{k=0}^{i-1} v_k + v_{k+1} \leq x - x_{os} + M \cdot \alpha_i, \forall i \in s \cap [1, n] \quad (28)$$

$$-\frac{1}{2} \sum_{k=0}^{i-1} v_k + v_{k+1} \leq x_{0s} - x + M \cdot (1 - \alpha_i), \forall i \in s \cap [1, n] \quad (29)$$

$$-\frac{1}{2} \sum_{k=0}^{i-1} v_k + v_{k+1} \leq x_{cs} - x + M \cdot (1 - \alpha_i), \forall i \in s \cap [1, n] \quad (30)$$

$$5.5v_i + \frac{1}{2} \sum_{k=0}^{i-1} v_k + v_{k+1} \leq x + M \cdot \beta_i, \forall i \in s \cap [1, n] \quad (31)$$

$$-2.5v_i - \frac{1}{2} \sum_{k=0}^{i-1} v_k + v_{k+1} \leq -x + M \cdot (1 - \beta_i), \forall i \in s \cap [1, n] \quad (32)$$

$$(v_{i+2} - v_{i+1}) - 2(v_{i+1} - v_i) + (v_i - v_{i-1}) \leq 3, \forall i \in [0, n-2] \quad (33)$$

$$-(v_{i+2} - v_{i+1}) + 2(v_{i+1} - v_i) - (v_i - v_{i-1}) \leq 3, \forall i \in [0, n-2] \quad (34)$$

$$-v_n \leq -1 \quad (35)$$

$$-\frac{1}{2} \sum_{k=0}^{i-1} v_k + v_{k+1} \leq -x - 0.1, \forall i \in [1, n] \quad (36)$$

where,

M = a large positive penalty constant.

The additional constraints are shown as follows:

The expression of p_i (Eq. (18)) should be converted to the standard form of the linear programming, which can be expressed by:

$$p_i - M(v_i + v_{i-1}) \leq 0, \forall i \in [1, n] \quad (37)$$

$$v_i + v_{i-1} - Mp_i \leq 0, \forall i \in [1, n] \quad (38)$$

$$0 \leq p_i \leq 1, \forall i \in [1, n] \quad (39)$$

(1) The expression of q_i (Eq. (20)) should be converted to the standard form for the linear programming. Combined with Eq. (25), one can express the constraints by:

$$0 \leq q_i \leq 1, \forall i \in [1, n] \quad (40)$$

$$q_i - M(v_i - v_{i-1}) \leq 0, \forall i \in [1, n] \quad (41)$$

$$v_i - v_{i-1} - Mq_i \leq 0, \forall i \in [1, n] \quad (42)$$

$$-v_i + v_{i-1} - Mq_i \leq 0, \forall i \in [1, n] \quad (43)$$

(2) All decision variables are non-negative. One can express the constraint by:

$$v_i \geq 0, \forall i \in [0, n] \quad (44)$$

7.5 Case Study

7.5.1 The study site

This study selects the intersection of US 40 (Pulaski Hwy) and Red Toad Road as the study site. US 40 is a two-lane, median-divided arterial with a posted speed limit of 55 mph (approximated 24 m/s) and isolated intersection control. Along the US 40, the spacing between intersections is long enough (1.5 kilometer) and the traffic speed is relatively high, which makes the arterial subject to risk of the DZ issue. Its aerial view is shown in Fig. 7.10.

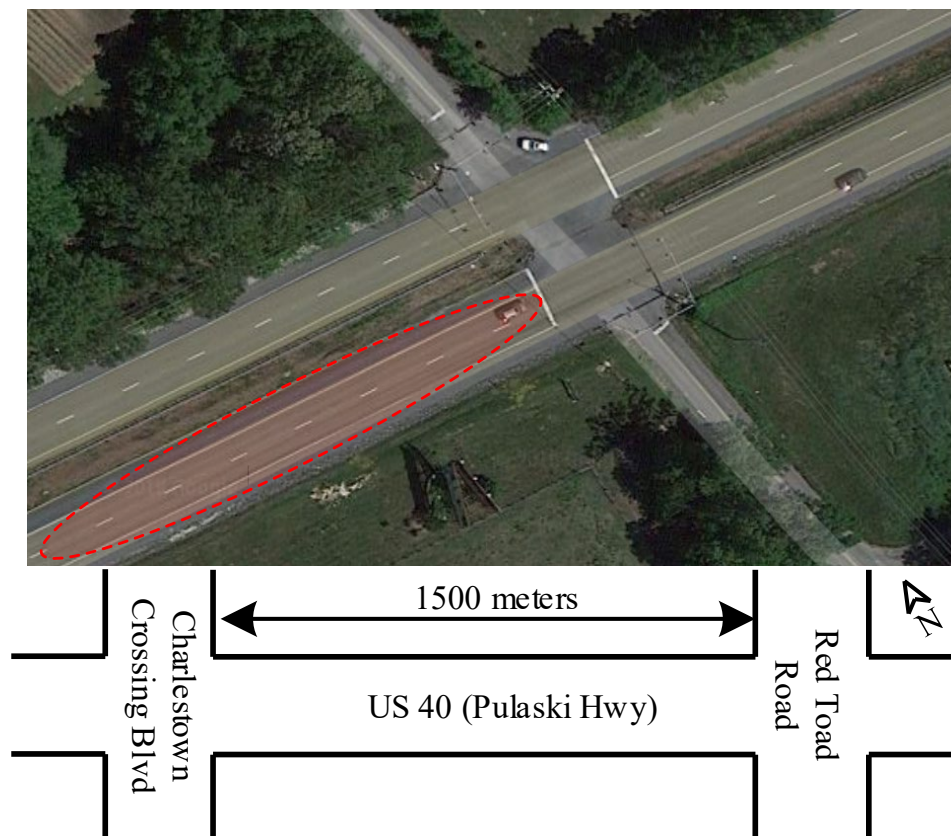


Figure 7.10 Aerial view of the US 40 and Red Toad Road intersection.

The traffic control plan at the target intersection is a semi-actuated two-phase system. The green interval for the US 40 is maintained until a call is received on the Red Toad Road. When the

Red Toad Road receives a call, the minimum green time for the US 40 is 25 seconds, and the maximum green time is 60 seconds with the gap-out logic. The yellow interval for the US 40 is 5 seconds, and for the Red Toad Road is 3 seconds. The green interval for the Red Toad Road is 8 seconds. Besides, there's a fixed all-red interval of 3 seconds. Traditionally, the DZ protection is provided by extending the all-red interval by up to an additional 2.5 seconds.

The algorithm selects the eastbound movement as the study object. Table 7.1 illustrates the pre-design survey findings of the study object (from (Liu et al. 2007)). The unit of the observed data is mile per hour, and needs to be converted to meter per second.

Table 7.1 Pre-design survey findings of the eastbound movement.

Speed Parameter	Unit of mph	Unit of m/s (Integer)
Mean Speed	49.2	22
Median Speed	49.9	22
Standard Deviation	12.3	5
Minimum Speed	19.6	9
Top Speed	86.7	39
85% Speed	62.4	28

Other parameter values are as follow: $w = 21\text{m}$; $L = 5\text{m}$; $\delta_1 = 1\text{s}$; $\delta_2 = 1\text{s}$; $a^* = 5\text{m/s}^2$; and $d^* = 7\text{m/s}^2$.

7.5.2 Test design

The DZ guiding scope of the study site is determined by Formulas (2) and (3). Using the minimum green interval, the DZ guiding scope is between 350 meters and 432 meters, and accordingly set as 400 meters.

The pre-design findings show the 85% speed is 62.4 mph and the top speed is 86.7 mph, greater than 55 mph, which means a quite number of vehicles are overspeed. Therefore, an additional guiding area is set upstream to warn the motorists to slow down, insuring the vehicles are not overspeed when entering the DZ guiding area. The scope of the additional guiding area is

estimated with:

$$x_d = \left[-\frac{1}{2d} (v_{max} + v_{top}) \cdot (v_{max} - v_{top}) \right] \quad (45)$$

where,

x_d = scope of the additional guiding area; and,

v_{top} = top speed from the pre-design findings.

Using Eq. (45), the additional guiding scope is set as 480 meters. Thus, the layout of the guiding area can be depicted by Fig. 7.11.

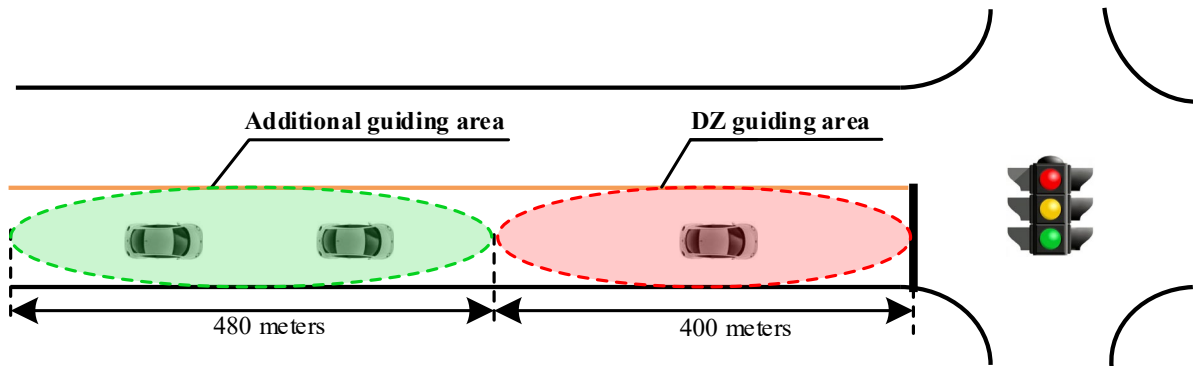


Figure 7.11 Layout of the guiding area.

7.5.3 Evaluation analysis & result

The research selects four types of speed, maximum speed (24 m/s), median speed (22 m/s), half of the maximum speed (12 m/s), and minimum speed (9 m/s), as the initial speed. Considering the situation with or without downstream vehicles, the analytic results are illustrated as follows.

Without downstream vehicles

Without considering the impact from downstream vehicles, the DZ protection method and travel time of any speed profile generated in the Stage I are compared with those without guidance.

The rests are summarized in Tab. 7.2.

Table 7.2 Comparison of DZ protection method and travel time with and without guidance.

Scenarios	TTY (s)	DZ Protection Strategy		Travel Time (s)	
		With Guidance	Without Guidance	With Guidance	Without Guidance
Scenario 1 (Maximum Speed)	10	Deceleration	All-red Extension	30	17
Scenario 2 (Median speed)	10	Deceleration	All-red Extension	30	19
Scenario 3 (50% Max Speed)	26	Acceleration	All-red Extension	20	34
Scenario 4 (Minimum Speed)	38	Acceleration	All-red Extension	22	45

It can be found in Tab. 7.2 that without speed guidance, all-red extension needs to be implemented to ensure DZ protection, while with the guidance, the vehicle can avoid DZ without all-red extension. In addition, for Scenarios 3 and 4, the travel time with guidance is shorter than without guidance, as the vehicle can accelerate to pass the stop line. While for Scenarios 1 and 2, the travel time with guidance is longer, since the vehicle with guidance needs to slow down and pass the intersection at the beginning of the next green interval, while all-red extension is used under the non-guiding environment, which allows the vehicle to pass the stop line by hitting the red.

The idling time and speed profile of the best speed profile generated in the Stage II are compared with a random speed profile (rather than the best). The results illustrate that the idling time and speed fluctuation of the best speed profile are lower than the random profile.

Table 7.3 Comparison of idling time and speed fluctuation of the best and random speed profiles.

Scenarios	TTY (s)	Idling Time (s)		Speed Fluctuation Frequency	
		Best Profile	Random Profile	Best Profile	Random Profile
Scenario 1 (Maximum Speed)	10	0	8	14	22
Scenario 2 (Median speed)	10	0	12	10	16
Scenario 3 (50% Max Speed)	26	0	14	12	16

The trajectories of travel time and speed are depicted by Figs. 7.12 to 7.15.

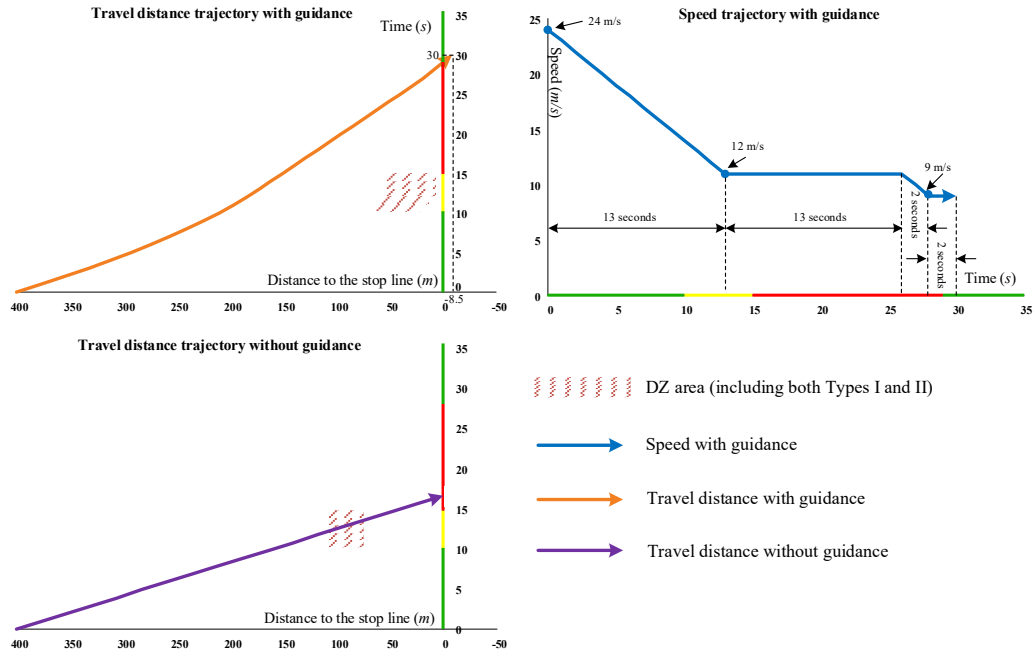


Figure 7.12 Comparison of vehicular trajectory with and without guidance in Scenario 1.

As Fig. 7.12 illustrates, without the speed guidance, the vehicle drops in the DZ at the 12th second, and should have been blocked by the red signal. While under the guiding environment, the vehicle has two deceleration parts and two cruising parts. The first deceleration part is from the 0th to 12th second, and the last is from the 26th to 28th second. The vehicle passes the stop line between the 27th and 28th second, and at the 30th second it has exceeded the stop line by 8.5 meters.

The guiding speed profile successfully prevents the vehicle from dropping in the DZ or idling. In addition, it lets the vehicle pass the stop line at the beginning of the next green interval, making the travel time minimum.

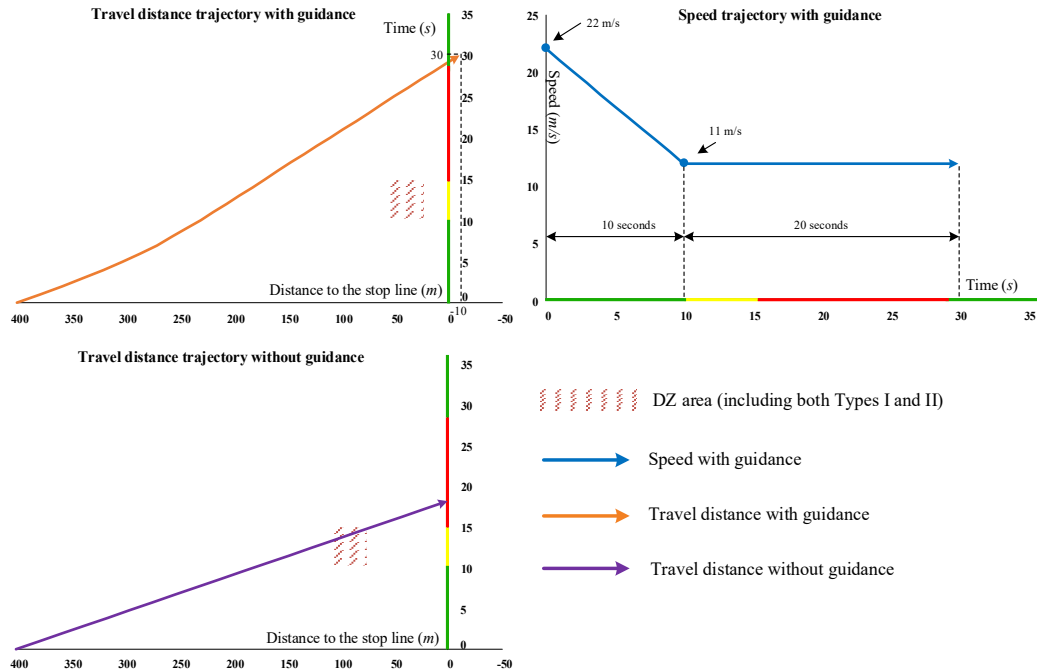


Figure 7.13 Comparison of vehicular trajectory with and without guidance in Scenario 2.

The result depicted in Fig. 7.13 is similar to the one in Fig. 7.12. It is because the median speed is extremely close to the maximum speed. Without speed guidance, the vehicle drops in the DZ at the 12th second. While with guidance, the vehicle avoids dropping in the DZ and passes the intersection, at the beginning of the next green interval. There's no idling duration through the whole process.

The vehicle has one deceleration part, from the 0th to 10th second, and one cruising part. It passes the stop line between the 29th and 30th second, and at the 30th second it has exceeded the stop line by 10 meters.

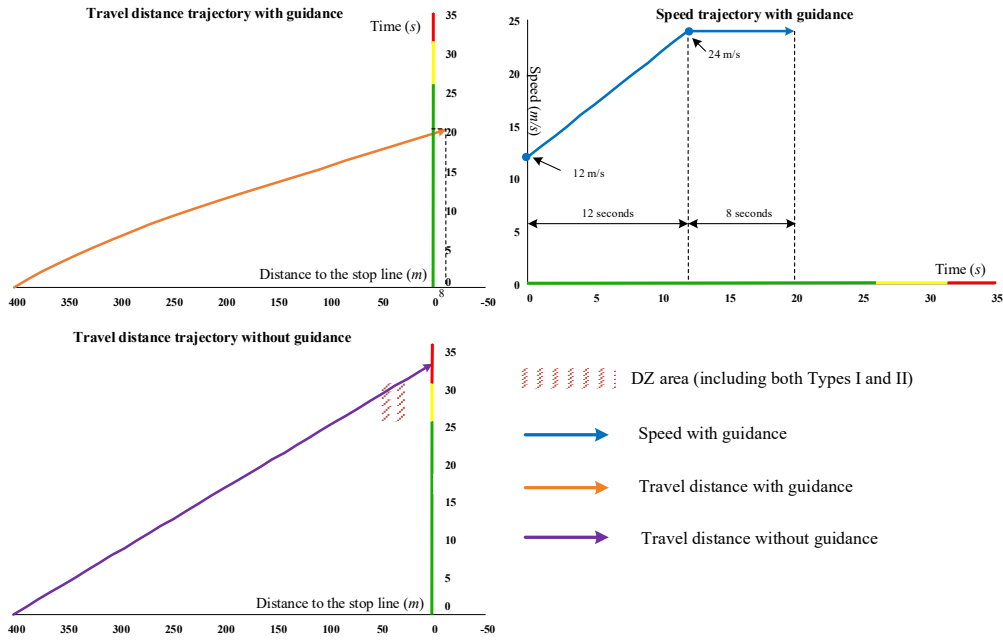


Figure 7.14 Comparison of vehicular trajectory with and without guidance in Scenario 3.

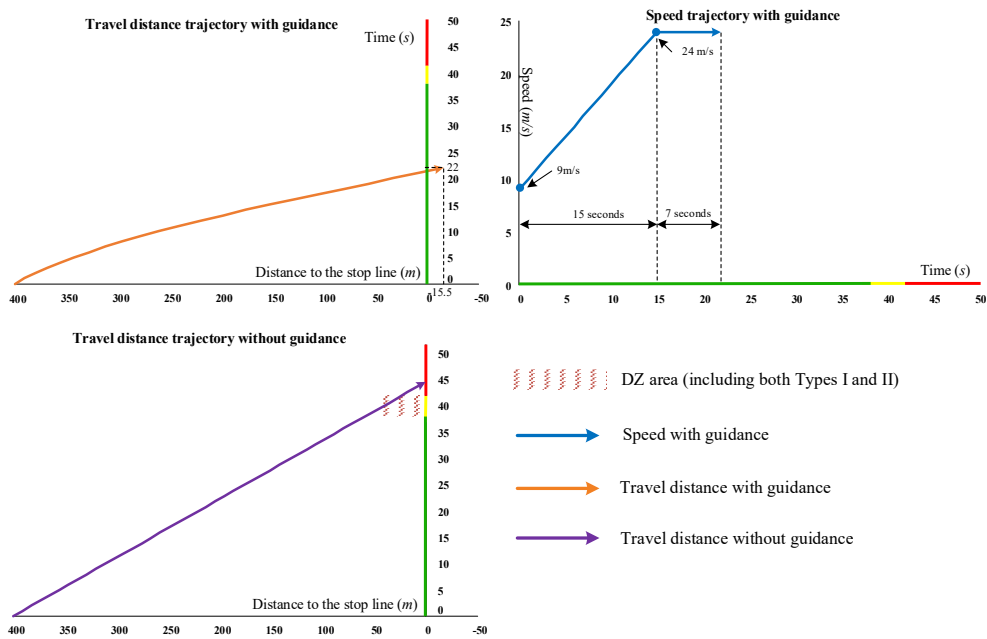


Figure 7.15 Comparison of vehicular trajectory with and without guidance in Scenario 4.

The vehicular speeds in Scenarios 3 and 4 are significantly lower than the maximum speed, which makes the DZ area shorter and closer to the stop line. This situation makes the vehicle difficult to drop in the DZ area, and furthermore provides enough space and time to the motorists

to accelerate their vehicles to pass the stop line without hitting red. As Figs. 7.14 and 7.15 illustrate, the vehicle under the guiding environment can avoid the DZ and pass the stop line in the earliest time.

With downstream vehicles

For Scenarios 1 and 2 where the vehicle avoids the DZ by deceleration, the existence of downstream vehicles has little impact, since no bumping happens if the following vehicle decelerates. While for Scenarios 3 and 4, the downstream vehicles may impose significant obstacle to the following vehicle. In this section, Scenario 4 is selected for studying, and a downstream vehicle with the same speed is added herein. The results under various space headways are depicted in Fig. 7.16.

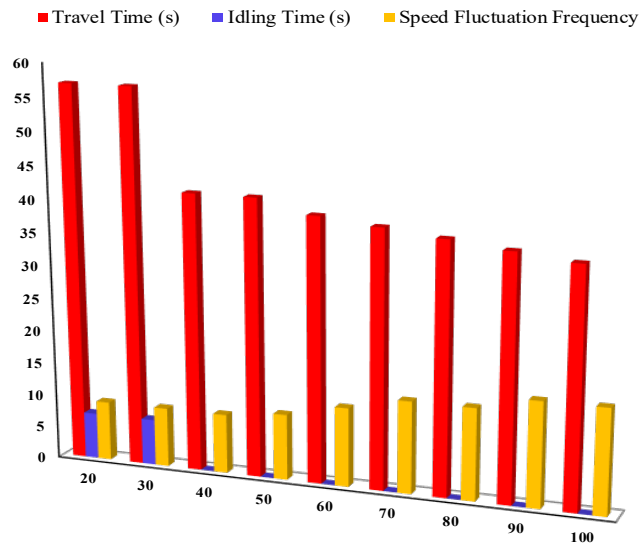


Figure 7.16 Comparison of travel time, idling time, and speed fluctuation frequency under various space headways.

It can be found in Fig. 7.16 that with the rise of space headway, the travel time and idling time declines while the speed fluctuation frequency increases. It is because when the space headway is larger, the motorist of the following (target) vehicle has more time to change the driving

status, resulting in shorter travel time, but longer speed fluctuation duration. When the space headway ≥ 40 meters, the vehicle with guidance can pass the stop line before hitting the red. On the contrary, when the space headway is less than 40 meters, the vehicle will hit the red inevitably, while the idling time can be minimized.

7.5.4 Sensitivity analysis

In this section, the study conducts the sensitivity analysis towards the dynamic speed guiding model. The DZ guiding scope is selected as the research object. Note that the impact from the downstream vehicle is eliminated to ensure that the result is not disturbed.

The impact of DZ guiding scope under various initial speed, starting from 350 meters and increased by 10 meters each time, is depicted in the Figs. 7.17 and 7.18.

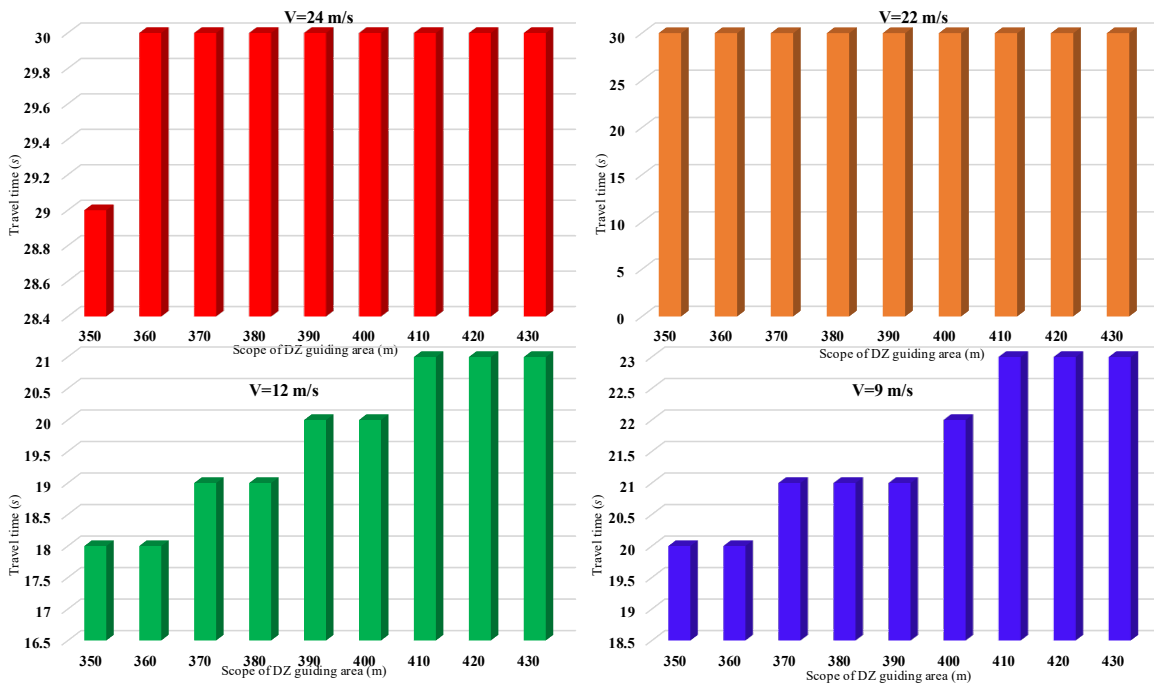


Figure 7.17 Comparison of travel time under various scope of DZ guiding area.

It can be found in Fig. 7.17 that with the initial speeds of 24 m/s and 22 m/s, the travel time

nearly maintains the same under various guiding scope. This is because under such speeds, the vehicle needs to slow down, trying to pass the stop line at the next green interval. In addition, due to the extreme short red interval, it is guaranteed that the vehicle can pass the stop line at the beginning of the next interval without idling. The only exception is the under the 350 meters of guiding scope, where the vehicle will hit the green at the stop line with the initial speed.

While for the initial speed of 12 m/s and 9 m/s, the travel time rises with the increase of guiding scope. This is because the vehicle under such speed needs to accelerate to pass the stop line, which leads to longer travel time under longer distance.

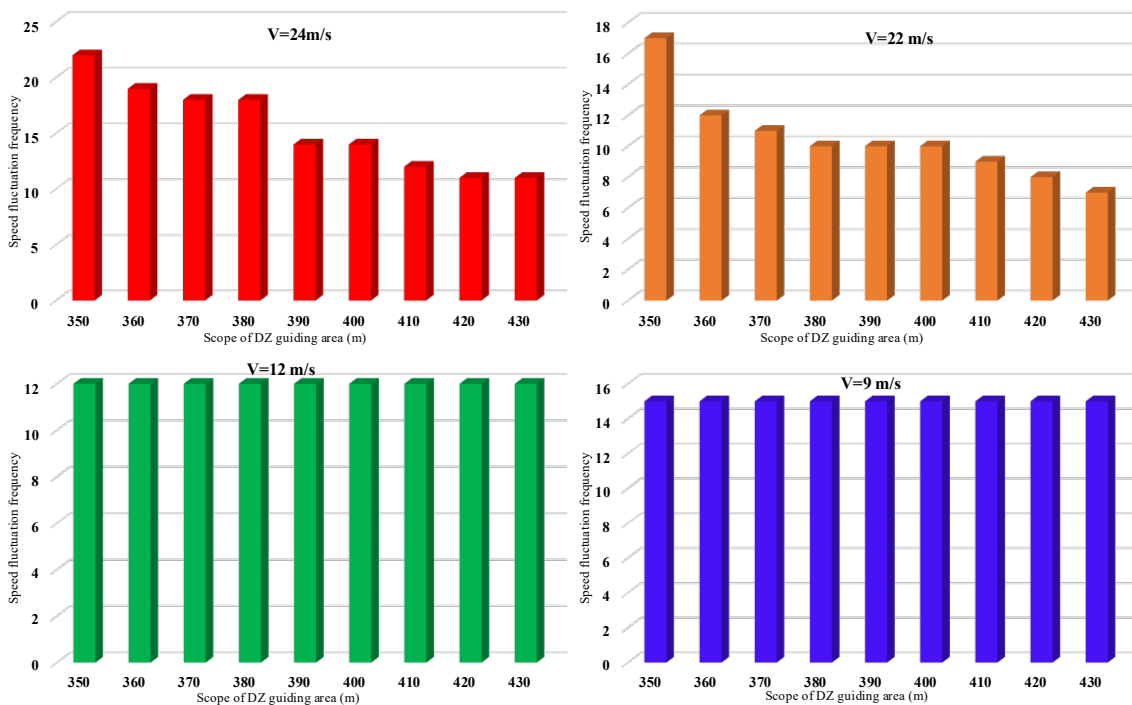


Figure 7.18 Comparison of speed fluctuation frequency under various scope of DZ guiding area.

Figure 7.18 depicts under the various guiding scope, the speed fluctuation frequency with the initial speeds of 12 m/s or 9 m/s remains the same. While for the 22 m/s and 24 m/s, the

frequency declines with the decrease of guiding scope. It is because for the lower speed, the vehicle needs longer time to accelerate to the maximum speed even under the minimum scope. Nonetheless, for the higher speed, the vehicle only needs to decelerate a target speed value to avoid the DZ and idling. In addition, if the scope is longer, the target value is higher, causing lower deceleration time.

The sensitivity analysis implies that if most vehicles have speed close to the maximum speed limit, it is appropriate to set the guiding scope longer. Otherwise, a shorter guiding scope is better.

7.6 Conclusions

This chapter proposes a dynamic speed guiding model towards the DZ protection through the high-speed signalized intersection. The contribution of the method is to develop a two-stage model, where the minimization of travel time and DZ protection are fulfilled in Stage I. Conditioning on the optimal travel time generated in Stage I, the minimization of idling time and speed fluctuation is processed in Stage II. To solve the problem, the DP and MOMILP algorithms are applied in Stages I and II, respectively.

The study provides an example at the intersection of US 40 and Red Toad Road to validate the proposed model. Four scenarios (various initial speed) are discussed. Firstly, without the impact from downstream vehicles, the DZ protection and travel time are compared under the guiding and non-guiding environments. It is illustrated that with the guidance, the vehicle can avoid DZ without all-red extension. In addition, under the guiding environment, the travel time with the initial speed, much lower than the maximum speed limit, is shorter, while with higher speed, there's no benefit of travel time under the guidance. Furthermore, the best speed profile generated in the Stage II shows advantages of idling time and speed fluctuation, compared with

other profiles.

Secondly, considering the impact of downstream vehicles, the travel time, idling time and speed fluctuation under various space headway are compared. Results indicate that with the guidance, when the space headway ≥ 40 meters, the vehicle can pass the stop line without hitting the red. Otherwise, the vehicle will hit the red inevitably while the idling time is minimal.

This study also conducts the sensitivity analysis for exploring the impact of the DZ guiding scope to the travel time and speed fluctuation. The analysis implies for the travel time, there's little impact towards higher speed while the travel time with lower speed rises with the increase of guiding scope. For the speed fluctuation, with higher speed, it declines with the rise of travel scope, while no impact shows under the lower speed.

Analysis results indicate the validity and effectiveness of the proposed speed control framework. On-going work of this study is to test the proposed algorithm in real-world.

Chapter 8 CONCLUSIONS AND FUTURE WORKS

8.1.1 Conclusions

This paper makes the following conclusions according to the research content of each chapter.

Chapter 3 develops a single vehicle-based trajectory optimization control model for CAV at a signalized intersection. The initial objective of the model is to minimize the average travel time of the platoon. Then, based on the optimal travel time, the speed trajectory of each vehicle is further optimized to minimize the average idling time and speed fluctuation in sequence. A three-phased algorithm is proposed to solve the model, where Phase I features a multi-stage-based NLP to minimize the average travel time for the platoon; Phase II develops a MILP to further minimize the average idling time, conditioned on the travel time of each vehicle determined in Phase I; and Phase III advances another MILP to ultimately minimize the average speed fluctuation of the platoon, conditioned on the outcomes of Phases I and II. This study provides several illustrative examples to validate the control model. Firstly, the study compares the travel time of each vehicle in the platoon and the resulted average travel time with and without the control. Results show that both the vehicular travel time and platoon's average travel time decrease significantly. Secondly, this study compares the fuel consumption of each vehicle and the average value of the platoon under the control and non-control environments. Results indicate that due to the lower travel time, idling time and speed fluctuation, the fuel consumption with control is significantly lower than that without control. Furthermore, the time-varying fuel consumption of the leading vehicle in the platoon with respect to control and non-control environments are compared and the fuel consumption curve under control is much smoother. Finally, this study compares the level of average travel time under different initial speeds of a platoon. Results show that when signal displays green initially, the average travel time declines

with the increase of initial speed, while no obvious relationship is found when the signal initially displays red. Such findings may help further improve the speed guidance performance by pre-adjusting vehicle speeds before they enter the control scope.

Chapter 4 proposes a dynamic speed control algorithm toward a vehicle platoon at a signalized intersection. The algorithm not only considers the running status of the target platoon but also analyzes the impact of the anterior platoon. Acceleration/deceleration rates, instead of speed, are used as the optimized target to guide the drivers to avoid idling and to hit the green light as possible as they can. Depending on the status of the platoon and signal timing, the speed control algorithms under different scenarios are discussed in details. The proposed algorithms not only work for a fully obedient platoon, but also for a mixed platoon by re-grouping vehicles into several new platoons according to their permutations. The research provides three examples provided to validate the algorithm. In the first one, considering the impact of the anterior platoons, we compare the time-varying fuel consumptions of the target platoon between the speed control mode and the free driving mode. Results indicate that the platoon under free driving will idle for some time, resulting in significantly more fuel consumption than the speed control mode using the proposed speed control algorithms. In the second example, we compare the levels of fuel consumptions under different time headways. Results show that in an acceleration scenario, a smaller headway results in less fuel consumption; while in a deceleration scenario, a smaller headway causes a little more fuel consumption. In the third example, fuel consumptions under different permutations are analyzed. The conclusion implies that if the leading vehicle is a DOV, the target platoon's fuel consumption is much larger. However, when the leading vehicle is an OV, it seems that the fuel consumption for the following vehicles in the target platoon, even for DOVs, may not increase obviously. Analysis results of the illustrative

examples indicate the validity and effectiveness of the proposed platoon-based speed control algorithm. On-going work of this study is to apply the proposed algorithm in real-world eco-driving projects and evaluate its effectiveness with calibrated fuel consumption models.

Chapter 5 proposes a dynamic speed control algorithm towards bottleneck mitigation at an unsignalized intersection. The algorithm not only considers the running status of the target vehicle but also captures the impact of downstream vehicles. Acceleration/deceleration rates, instead of speeds, are used as the control objective for speed guidance. Depending on the status of a target vehicle and gap conditions, the speed control algorithms under different scenarios are discussed in details. The proposed algorithm not only works for an “ideal” situation, but also for a realistic environment where there exist downstream vehicles and initial queue at the stop line. This study provides illustrative examples to validate the algorithm. Firstly, without considering the impact of the downstream platoons, this study compares the time-varying fuel consumption and emission of the target vehicle with respect to speed control and free driving behaviors. Results indicate that the vehicle under the proposed algorithm experience significantly lower fuel consumption and emission than that under free driving. Then, considering the impact of the downstream vehicles and queue, this study compares the level of fuel consumption of the target vehicle with and without the proposed speed control. Results demonstrate the promising application of the proposed speed control algorithm in a realistic traffic environment.

Chapter 6 proposes a cooperative bus-car trajectory optimization model to eliminate weaving bottleneck around the near-side bus station. The contribution of the method is to develop a two-phase model, where the minimization of total person travel time and weaving elimination are fulfilled in Phase I model, while the minimization of total vehicular idling time is conducted in Phase II model, conditioning on the output of Phase I. The rolling-based NLP and

MILP models are applied in the Phases I and II, respectively. The study provides an example to validate the proposed model. Firstly, it compares the vehicular travel time under the control and non-control environments. Results show that only the lane adjacent to the curb side lane reflects significant improvement under control. Then, considering the person travel time, the study explores that not only the result of the lane adjacent to the curb side lane, but of all lanes shows remarkable benefits of the control model. After that, the vehicular idling time is compared under the control and no-control environments. The result shows similarity to the vehicular travel time. Finally, the study analyzed vehicular trajectories on each lane, indicating that without control, the bus just weaves the cars on the lane adjacent to the curb side lane, while the cars in other lanes are not impacted. This finding also explains some “contradictory” conclusions in comparison of the vehicular travel time, person travel time and vehicular idling time. This study also conducts the sensitivity analysis towards the ratio of bus passenger number over car passenger number. The result illustrates that with the increase of bus passenger number, the optimal rate of the total vehicular time declines, while of the total person time rises.

Chapter 7 proposes a dynamic speed guiding model towards the DZ protection through the high-speed signalized intersection. The contribution of the method is to develop a two-stage model, where the minimization of travel time and DZ protection are fulfilled in Stage I. Conditioning on the optimal travel time generated in Stage I, the minimization of idling time and speed fluctuation is processed in Stage II. To solve the problem, the DP and MOMILP algorithms are applied in Stages I and II, respectively. The study provides an example at the intersection of US 40 and Red Toad Road to validate the proposed model. Four scenarios (various initial speed) are discussed. Firstly, without the impact from downstream vehicles, the DZ protection and travel time are compared under the guiding and non-guiding environments. It is illustrated that with the guidance,

the vehicle can avoid DZ without all-red extension. In addition, under the guiding environment, the travel time with the initial speed, much lower than the maximum speed limit, is shorter, while with higher speed, there's no benefit of travel time under the guidance. Furthermore, the best speed profile generated in the Stage II shows advantages of idling time and speed fluctuation, compared with other profiles. Secondly, considering the impact of downstream vehicles, the travel time, idling time and speed fluctuation under various space headway are compared. Results indicate that with the guidance, when the space headway ≥ 40 meters, the vehicle can pass the stop line without hitting the red. Otherwise, the vehicle will hit the red inevitably while the idling time is minimal. This study also conducts the sensitivity analysis for exploring the impact of the DZ guiding scope to the travel time and speed fluctuation. The analysis implies for the travel time, there's little impact towards higher speed while the travel time with lower speed rises with the increase of guiding scope. For the speed fluctuation, with higher speed, it declines with the rise of travel scope, while no impact shows under the lower speed.

8.1.2 Future Works

Future works of this paper is to apply the proposed algorithm in real-world projects and evaluate its effectiveness with calibrated fuel consumption models. Besides, the environment of continuous arrival of bus at the station should also be addressed.

CURRICULUM VITAE

Wenqing Chen

Education

University of Wisconsin-Milwaukee

Ph.D., Civil and Environmental Engineering, GPA: 3.67/4.00

Milwaukee, WI

Dec 2019

Tongji University

M.S., Transportation Engineering in Civil Engineering, GPA: 3.79/4.00

Thesis: Highway Safety Manual Modification on Intersection Crashes and Multivariate Model Development of Crash Types

Shanghai, China

Dec2012

Central South University

B.S., Math, GPA: 3.00/4.00

Changsha, China

Jun2008

Publications

Chen, W., Liu, Y., Yang, X., Bai, Y., Gao, Y., and Li, P. (2016). Platoon-based speed control algorithm for ecodriving at signalized intersection. *Transportation Research Record*, 248, 29–38.

Chen, W. and Yu, J., (2017). Gap-based automated vehicular speed guidance towards eco-driving at an unsignalized intersection. *Transportmetrica B: Transport Dynamics*. Retrieved from DOI: 10.1080/21680566.2017.1365661.

Chen, W., Yu, J., and Liu, Y. (2017). Automated speed guidance towards eco-driving and dilemma zone protection. *Transportation Research Board 96th Annual Meeting*, Washington, D.C.

Chen, W. and Yu, J. (2018). *Elimination of weaving bottleneck at curbside bus stops with dynamic speed guidance*. Transportation Research Board 97th Annual Meeting, Washington D.C.

Chen, W., and Yu, J. (2019). Platoon-Based Trajectory Optimization for Connected and Automated Vehicles at A Signalized Intersection. *Transportation Research Board 96th Annual Meeting*, Washington, D.C.

Chen, W., and Yu, J. (2019). Cooperative bus-car trajectory optimization to eliminate weaving bottleneck around curb side bus stations. *Computer-Aided Civil and Infrastructure Engineering*. In progress